00362

UNIVERSIDAD NACIONAL AUTONOMA
DE MEXICO

POSGRADO EN CIENCIAS FÍSICAS
FACULTAD DE CIENCIAS

"Efecto Aharonov-Bohm en estados electrónicos en cajas cilíndricas anulares"

TESIS

QUE PARA OBTENER EL GRADO DE:

MAESTRA EN CIENCIAS (FÍSICA)

PRESENTA:

GUADALUPE VILLA TORRES

DIRECTOR DE TESIS: DR. EUGENIO LEY KOO

COMITÉ TUTORAL: DRA. ROCIO JÁUREGUI RENAUD
DR. CARLOS FEDERICO BUNGE MOLINA

pcf
posgrado en ciencias físicas
unam
2004

MÉXICO, D.F.

RESUMEN.

En esta tesis analicé el efecto Aharonov-Bohm en situaciones especiales, para ilustrar el papel que juega el potencial vectorial magnético $\vec{A}$ sobre los estados de energía del electrón.

Analicé el efecto Aharonov-Bohm sobre los estados ligados del electrón dentro de una caja cilíndrica anular, al comparar dos problemas: a) en ausencia de campo de inducción magnética o campo de potencial magnético; y b) en presencia de campo uniforme, axial, centrado y confinado sólo en la perforación. Obtuve que las eigenfunciones tienen en común las funciones angular y axial; y las funciones radiales que son funciones de Bessel, son diferentes en su orden m y $m+\nu$, respectivamente, donde ν es el flujo magnético en la perforación. Para obtener las soluciones, utilicé un programa diseñado en "Numerical Recipes in C". El cambio en el espectro de energía, conforme cambia el flujo magnético, muestra la influencia del potencial sobre los estados. El espectro muestra periodicidad con período 1, y simetría con respecto a los valores medios del flujo magnético.

Análogamente analicé el efecto Aharonov-Bohm sobre los Estados de Landau del electrón en la caja cilíndrica anular, comparando dos problemas: c) en presencia de campo uniforme y axial en la caja y en la perforación; y d) considerando un campo en la caja diferente del campo en la perforación. Las funciones radiales, que son funciones Hipergeométricas Confluentes, son diferentes en términos de m y de $m+\mu$, donde μ es el cambio de flujo magnético en la perforación. Para obtener las soluciones, utilicé un programa diseñado en "Mathematica". La influencia del potencial vectorial sobre los estados se manifiesta en el cambio del espectro, al variar el cambio de flujo magnético en la perforación. Sin embargo, el espectro de energía para los Estados de Landau, aunque también muestra periodicidad 1, no es simétrico.

INDICE

Capítulo 1. INTRODUCCION.

En esta tesis se analiza el efecto Aharonov-Bohm sobre los estados ligados del electrón en una caja cilíndrica anular mediante el estudio de la dependencia de las eigenfunciones y los eigenvalores de la energía con respecto al flujo magnético a través de la perforación de la caja, en dos situaciones comparativas: a) cuando no hay campo magnético, y b) en presencia de campo magnético uniforme y axial en la perforación.

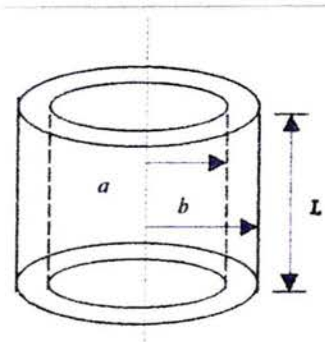

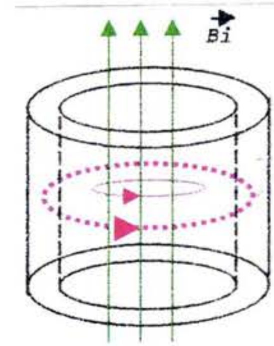

Análogamente, se analiza el mismo efecto sobre los estados de Landau del electrón en la caja, a través del estudio de la dependencia de las eigenfunciones y los eigenvalores de la energía con respecto a la diferencia de flujos magnéticos a través de la perforación, en dos situaciones comparativas: c) cuando un mismo campo magnético axial está presente tanto en la caja como en la perforación, y d) cuando la magnitud del campo en la perforación es diferente del campo en la caja.

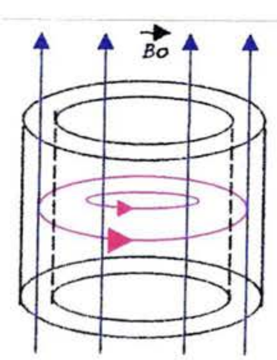

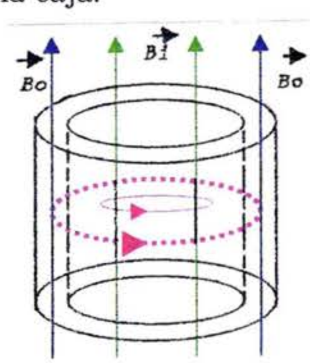

El resultado de este estudio ilustra el papel que juega el potencial vectorial magnético $\vec{A}$ en la Mecánica Cuántica.

En 1959 Aharonov y Bohm[1] analizaron las propiedades de los potenciales electromagnéticos en la Teoría Cuántica. Sugirieron que existen efectos observables de estos potenciales sobre partículas cargadas, aún en las regiones donde todos los campos (e incluso las fuerzas sobre las partículas) se anulan. Para probar tal conclusión, estudiaron posibles experimentos. Aharonov y Bohm predijeron que el patrón de franjas en un experimento de interferencia de haces de electrones debe cambiar al alterar la cantidad de flujo magnético que pasa entre dos haces, aunque los haces pasen a través de regiones libres de campo de inducción magnética $\vec{B}$.

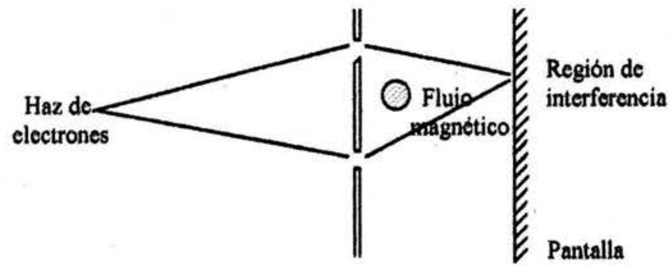

En el experimento propuesto, la diferencia de fase en las trayectorias ópticas del electrón está relacionada con el flujo magnético en la perforación como

$\oint \frac{\vec{p}_{int} \cdot d\vec{r}}{\hbar} = \frac{e}{\hbar c} \oint_c \vec{A} \cdot d\vec{r} = \frac{e}{\hbar c} \Phi_B$, donde $\vec{p}_{int}$ es el potencial de interacción entre el electrón y el campo de potencial vectorial $\vec{A}$. Tal teoría predice un cambio de ν franjas para un flujo encerrado $\nu hc/e$, donde la unidad natural de flujo o fluxón $\frac{hc}{e} = 4.135 \text{ x } 10^{-7} \text{gauss} \cdot \text{cm}^2$ está determinada por h la constante de Planck, c la velocidad de la luz, y e la carga del electrón. Aharonov y Bohm concluyeron que los electrones son influenciados por el potencial vectorial $\vec{A}$, aún cuando los electrones están fuera de las regiones con campo de inducción magnética $\vec{B}$. Un año más tarde, Chambers[2] realizó el experimento propuesto por Aharonov y Bohm. y reportó los cambios esperados del patrón de interferencia electrónico, con los correspondientes flujos magnéticos; incluyendo situaciones en las que el patrón aparece sin cambio debido a su asociación con flujos magnéticos de un número entero de fluxones.

Es conveniente analizar el momentum involucrado en los casos en que la partícula está inmersa en un campo electromagnético. Es bien sabido que cualquier sistema dinámico puede ser descrito en términos de fuerza o de energía y momentum. En la ecuación de movimiento de la partícula inmersa en un campo electromagnético (Ley de fuerza de Lorentz), $\vec{F} = q\left[\vec{E}(\vec{r},t) + \frac{\vec{v}}{c} \times \vec{B}(\vec{r},t)\right]$, al sustituir los campos de fuerza ($\vec{E}, \vec{B}$) por sus representaciones en términos de los campos de potencial ($\phi, \vec{A}$), a través de las ecuaciones de Maxwell $\vec{E}(\vec{r},t) = -\vec{\nabla}\phi(\vec{r}) - \frac{1}{c}\frac{\partial \vec{A}(\vec{r},t)}{\partial t}$ y $\vec{B}(\vec{r},t) = \vec{\nabla} \times \vec{A}(\vec{r},t)$ y después de algunos arreglos, es posible reconocer que en presencia de campo de potencial magnético $\vec{A}$ (Feynman[3]) habrá un momento de interacción adicional $\vec{p}_{\text{int}} = \frac{q}{c}\vec{A}(\vec{r},t)$, y por tanto, un cambio en el momento del sistema $\vec{p}_{\text{mec}} \longrightarrow \left(\vec{p}_{\text{mec}} + \frac{e}{c}\vec{A}(\vec{r},t)\right)$, que se conoce como prescripción de "acoplamiento mínimo". En este desarrollo se identifica también a la energía de interacción de la partícula con el campo electromagnético $U_{int} = q\left[\phi(\vec{r}) - \frac{\vec{v}}{c} \cdot \vec{A}(\vec{r},t)\right]$. Y surge así, la descripción en términos de los campos de potencial ($\phi, \vec{A}$).

Entonces, es claro que existen dos descripciones alternativas y complementarias de cualquier campo electromagnético. Es decir, tal campo electromagnético puede describirse en términos de los campos de fuerza ($\vec{E}, \vec{B}$) que representan fuerza por unidad de carga y fuerza por unidad de carga y unidad de velocidad; o bien, puede describirse en términos de los campos de potencial ($\phi, \vec{A}$), que representan energía por unidad de carga y energía por unidad de carga y unidad de velocidad, o momento de interacción por unidad de carga (Konopinski[4]).

Con base precisamente a este cambio en la cantidad de movimiento cuando la partícula se encuentra en presencia del potencial vectorial magnético $\vec{A}$, debe analizarse la influencia que tendrá tal potencial en el cambio de estados y niveles de energía en la descripción cuántica.

En la literatura se han discutido otras versiones del efecto Aharonov-Bohm sobre los estados ligados (Peshkin[5], 1989; Ballentine[6], 1990). En el libro especializado de Peshkin y Tonomura, el primer autor ilustró el efecto para el rotor con carga en un plano y puntualizó que no hay cambios importantes, si se permite que el movimiento sea tridimensional dentro del toro. En el libro de Ballentine se utiliza la partícula confinada en el interior de un toro de sección transversal rectangular, para reconocer que la energía de los estados estacionarios debe depender del flujo magnético en la perforación. Sin embargo, Peshkin y Ballentine consideraron que el análisis detallado y cuantitativo del problema no era necesario para sus propósitos.

En 1930 Landau[7] resuelve el problema del moviemiento del electrón en un campo de inducción magnética uniforme en la conocida norma de Landau; y 50 años más tarde Laughlin[8] resuelve la ecuación de Schrödinger en la norma simétrica. Fung y Wang[9] revisan el problema de Landau, obteniendo las correspondientes funciones de onda en la norma simétrica en la reprentación donde se diagonalizan el momento angular total y el cuadrado del vector de translación magnético. Así logran expresar la función de onda del trabajo original de Landau como una superposición lineal de las funciones de onda de los estados coherentes. En el presente trabajo se utiliza la norma circular, que es congruente con las condiciones de frontera y se resuelve el problema de Landau en forma exacta.

En esta tesis se presentan situaciones especiales del efecto Aharonov-Bohm, en las que se definen los campos de inducción y de potencial magnético, y con ello, el momento y el Hamiltoniano correspondiente, y se resuelven los problemas de eigenvalores. Se muestra así mismo, el efecto del potencial vectorial magnético $\vec{A}$ sobre los eigenvalores.

Contenido de la Tesis.

En el Capítulo 2 se resuelve el problema de eigenvalores para el electrón en una caja cilíndrica anular en ausencia de campos de inducción magnética o campos de potencial que interactúen con el electrón. Se muestra que las soluciones en la componente radial (en términos de las funciones de Bessel y Neumann) del sistema confinado, dependen de las dimensiones de la caja y del número cuántico magnético m .

En el Capítulo 3 se resuelve el problema de eigenvalores para el caso que involucra un campo de inducción magnética $\vec{B}_i$ uniforme, axial, centrado y confinado en la perforación, y su potencial vectorial magnético $\vec{A}$ asociado en la caja. Se muestra la influencia de este potencial (en términos del flujo magnético en la perforación $\vec{B}_i$) sobre los estados ligados, los cuales dependen de la suma $m+\nu$ y su combinación de valores, en la que ν es el flujo magnético en la perforación. En la comparación de los casos resueltos en los Capítulos 2 y 3, se ilustra el efecto Aharonov-Bohm sobre los estados ligados del sistema confinado. Se presentan los resultados cuantitativos y gráficos que ilustran las soluciones de los problemas de eigenvalores formulados en los Capítulos 2 y 3, es decir, para $\nu = 0$ y $\nu \neq 0$.

En el Capítulo 4 se resuelve el problema de eigenvalores para el electrón en presencia de campo de inducción magnética $\vec{B}_o$ uniforme, axial y de la misma magnitud en la caja y en la perforación. Se deduce que sus estados dependen del primer parámetro de las funciones Hipergeométricas Confluentes en la solución radial, para valores predeterminados del campo de inducción magnética $\vec{B}_o$, de las dimensiones de la caja y de $|m|$.

En el Capítulo 5 se resuelve el problema de eigenvalores que considera el mismo campo de inducción magnética $\vec{B}_o$ del caso anterior, pero alterando el campo en la perforación. Se muestra la influencia del nuevo potencial vectorial magnético $\vec{A}$ (en términos de la diferencia de flujos magnéticos en la perforación ($\vec{B}_i - \vec{B}_o$)) sobre los estados, los cuales ahora no sólo dependen del primer parámetro de las funciones Hipergeométricas para valores predeterminados del campo de inducción magnética $\vec{B}_o$ y las dimensiones de la caja, sino de la suma $|m+\mu|$, donde μ es la diferencia de flujos magnéticos en la perforación. En la comparación de los casos resueltos en los Capítulos 4 y 5, se ilustra el efecto Aharonov-Bohm sobre los Estados de Landau del sistema confinado. Se presentan los resultados cuantitativos y gráficos que ilustran las soluciones de los problemas de eigenvalores formulados en los Capítulos 4 y 5, es decir, para $\mu = 0$ y $\mu \neq 0$.

En el Capítulo 6 se presentan la discusión y conclusiones generales.

Capítulo 2. EL ELECTRON DENTRO DE UNA CAJA CILINDRICA ANULAR.

En este capítulo se resueve el problema de eigenvalores para el electrón en el interior de una caja cilíndrica anular, en ausencia de cualquier campo de inducción magnética o campo de potencial magnético, tanto en la caja como en la perforación. Se resueve la ecuación de Schrödinger para este problema, proponiendo una solución separable cuyos factores respectivos permiten obtener ecuaciones diferenciales ordinarias en la coordenada angular, axial y radial. Las soluciones de la ecuación para la coordenada angular, son eigenfunciones de la componente z del momento angular; y las soluciones de la ecuación para la coordenada axial, son eigenfunciones de la segunda derivada de la componente longitudinal de la cantidad de movimiento. La ecuación radial se reconoce como la ecuación de Bessel, cuya solución general es la combinación lineal de la función de Bessel ordinaria y la función de Neumann, que debe cumplir las condiciones de frontera en la coordenada correspondiente. La ecuación transcendental del determinante de tal sistema, se resuelve numéricamente para obtener el número de onda transversal, que es proporcional a las soluciones que determinan los eigenvalores de la energía y las eigenfunciones normalizadas correspondientes. Las eigenfunciones y los eigenvalores de la energía, quedan definidos en términos del número cuántico magnético entero m , y las dimensiones de la caja.

2.1 Solución del problema de eigenvalores.

Considérese un electrón de carga $-e$ confinado por las paredes impenetrables de una caja cilíndrica anular y en situación estacionaria, es decir, $V(r) = e\phi(r) = 0$ en la región donde se encuentra el electrón ($a \leq \rho \leq b$, φ , $0 \leq z \leq L$) , y $V(r) = \infty$ en ($\rho \leq a$, φ , $L \leq z$) y ($b \leq \rho$, φ , $L \leq z$) , donde a y b son los radios interno y externo respectivamente, y L la altura de la caja. Ver Fig. (a).

En este capítulo se formula y resuelve el problema de eigenvalores para el electrón en el interior de la caja cilíndrica anular ($a \leq \rho \leq b, 0 \leq \varphi \leq 2\pi, 0 \leq z \leq L$) en ausencia de cualquier campo de inducción magnética o campo de potencial magnético, tanto en la caja como en la perforación. Considérese el sistema descrito por la Fig. (a).

Fig. (a)

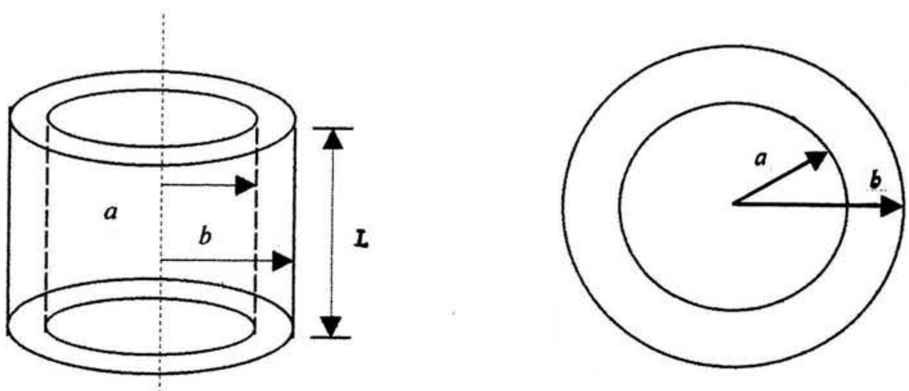

$$\vec{B}(0 \leq \rho \leq \infty, \varphi, z) = 0 \ , \ \vec{A}(0 \leq \rho \leq \infty, \varphi, z) = 0 \tag{2.1}$$

Este caso servirá de referencia para ilustrar el efecto Aharonov-Bohm en los estados ligados del electrón, al comparar con el caso que se plantea en el Capítulo 3, en el cual se aplica un campo de inducción magnética en la perforación.

Entonces el Hamiltoniano para el electrón dentro de la caja anular en coordenadas cilíndricas, es

$$\hat{H} = \frac{\vec{p}^2}{2m_e} = \frac{-\hbar^2}{2m_e}\nabla^2 = \frac{-\hbar^2}{2m_e}\Big[\frac{1}{\rho}\frac{\partial}{\partial\rho}\rho\frac{\partial}{\partial\rho} + \frac{1}{\rho^2}\frac{\partial^2}{\partial\varphi^2} + \frac{\partial^2}{\partial z^2}\Big] \tag{2.2}$$

La ecuación de Schrödinger

$$\frac{-\hbar^2}{2m_e}\Big[\frac{1}{\rho}\,\frac{\partial}{\partial\rho}\rho\frac{\partial}{\partial\rho}+\frac{1}{\rho^2}\frac{\partial^2}{\partial\varphi^2}+\frac{\partial^2}{\partial z^2}\Big]\psi(\rho,\varphi,z) \;=\; E\psi(\rho,\varphi,z) \qquad (2.3)$$

debe resolverse sujetándose a la condición de frontera de que la función de onda se anule en las posiciones de las paredes de la caja y de periodicidad en la coordenada angular

$$\psi(\rho=a,\varphi,z) \;=\; \psi(\rho=b,\varphi,z) \;=\; 0 \qquad (2.4)$$

$$\psi(\rho,\varphi,z=0) \;=\; \psi(\rho,\varphi,z=L) \;=\; 0 \qquad (2.5)$$

$$\psi(\rho,\varphi,z) \;=\; \psi(\rho,\varphi+2\pi,z) \qquad (2.6)$$

Se sabe que la ecuación (2.3) admite soluciones separables

$$\psi(\rho,\varphi,z) \;=\; R(\rho)\;\Phi(\varphi)\;Z(z) \qquad (2.7)$$

en la que los factores respectivos satisfacen las ecuaciones diferenciales ordinarias

$$\frac{-\hbar^2}{2m_e}\,\frac{d^2Z(z)}{dz^2} \;=\; E^L\;Z(z) \qquad (2.8)$$

$$-i\hbar\,\frac{d\Phi(\varphi)}{d\varphi} \;=\; m\hbar\;\Phi(\varphi) \qquad (2.9)$$

$$\Big[\frac{1}{\rho}\,\frac{d}{d\rho}\rho\frac{d}{d\rho}-\frac{m^2}{\rho^2}\Big]R(\rho) \;=\; E^T\;R(\rho) \qquad (2.10)$$

y el eigenvalor de la energía es la suma de las contribuciones transversal y longitudinal

$$E = \frac{\hbar^2}{2m_e}(k_{\text{T}}^2 + k_{\text{L}}^2) \tag{2.11}$$

donde k_{T}^2 es el número de onda asociado al movimiento transversal del electrón y k_{L}^2 es el número de onda asociado al movimiento longitudinal.

2.2 Dependencia de los estados del sistema confinado, con respecto a los parámetros de la caja y el número cuántico magnético.

Las soluciones de la ecuación (2.8) en la coordenada axial, sujetas a las condiciones de frontera de la ecuación (2.5), son

$$Z_n(z) = \sqrt{\frac{2}{L}}\ sen\Big(\frac{n\pi z}{L}\Big) \quad , \quad n = 1, 2, 3, ... \tag{2.12}$$

Las soluciones de la ecuación (2.9) en la componente angular, son las eigenfunciones de la componente z del momento angular orbital

$$\Phi(\varphi) = \frac{e^{im\varphi}}{\sqrt{2\pi}} \quad , \quad m = 0, \pm 1, \pm 2, ... \tag{2.13}$$

donde los eigenvalores enteros $m = 0, \pm 1, \pm 2, ...$ surgen de la condición de periodicidad de la ecuación (2.6) .

La ecuación (2.10) se reconoce como la ecuación de Bessel y su solución general es la combinación lineal de la función de Bessel ordinaria y la función de Neumann (Abramowitz[10])

$$R_m(\rho) \;=\; \mathcal{A}_m J_m(k_{\mathrm{T}}\,\rho) \;+\; \mathcal{B}_m Y_m(k_{\mathrm{T}}\,\rho) \tag{2.14}$$

donde m es el orden de las funciones correspondientes y es entero, ecuación (2.13). Las condiciones de frontera de las ecuación (2.4) en esta solución se expresan como

$$\mathcal{A}_m J_m(k_{\mathrm{T}}\,a) \;+\; \mathcal{B}_m Y_m(k_{\mathrm{T}}\,a) \;=\; 0 \tag{2.15}$$

$$\mathcal{A}_m J_m(k_{\mathrm{T}}\,b) \;+\; \mathcal{B}_m Y_m(k_{\mathrm{T}}\,b) \;=\; 0 \tag{2.16}$$

Este es un conjunto de dos ecuaciones lineales homogéneas algebraicas para los coeficientes desconocidos $\mathcal{A}_m$ y $\mathcal{B}_m$, que admite soluciones no triviales sólo si su determinante se anula, i.e.

$$J_m(k_{\mathrm{T}}\,a)Y_m(k_{\mathrm{T}}\,b) \;-\; J_m(k_{\mathrm{T}}\,b)Y_m(k_{\mathrm{T}}\,a) \;=\; 0 \tag{2.17}$$

Esta ecuación trascendental debe ser resuelta numéricamente para obtener el número de onda transversal k_{T} . La tarea se lleva a cabo utilizando las subrutinas inc.h, in.h y otras del programa de software "Numerical Recipes in C"[11]. Sean $k_{\mathrm{T}}a = x_{ms}$ las soluciones sucesivas $s = 1, 2, 3, ...$ para valores dados de a y b . Los eigenvalores de la energía de la ecuación (2.11) con los valores específicos de los números de onda de las ecuaciones (2.11 y 2.17) están dados por

$$E_{msn} \;=\; \frac{\hbar^2}{2m_e}\Big(\frac{x_{ms}^2}{a^2} + \frac{n^2\pi^2}{L^2}\Big) \tag{2.18}$$

La razón de los coeficientes $\mathcal{A}_m$ y $\mathcal{B}_m$ se sigue de las ecuaciones (2.15 2.16), y permite escribir la eigenfunción radial normalizada, ecuación (2.14), como

$$R_{ms}(\rho) = \frac{1}{\sqrt{\mathcal{N}_{ms}}}\left[Y_m\left(\frac{x_{ms}b}{a}\right)J_m\left(\frac{x_{ms}\rho}{a}\right) - J_m\left(\frac{x_{ms}b}{a}\right)Y_m\left(\frac{x_{ms}\rho}{a}\right)\right] \tag{2.19}$$

donde la constante de normalización es

$$\mathcal{N}_{ms} = \int_a^b \left[Y_m\left(\frac{x_{ms}b}{a}\right)J_m\left(\frac{x_{ms}\rho}{a}\right) - J_m\left(\frac{x_{ms}b}{a}\right)Y_m\left(\frac{x_{ms}\rho}{a}\right)\right]^2 \rho \mathrm{d}\rho \tag{2.20}$$

Debe notarse que las eigenfunciones, ecuación (2.19), así como los eigenvalores de la energía, ecuación (2.18), quedan definidos en términos del número cuántico magnético entero m y las dimensiones de la caja.

Para efectos de comparación, los resultados de este problema se presentan en el Capítulo 3.

El problema de este capítulo también ha sido estudiado en literatura de investigación en el diseño de estructuras artificiales, al analizar cómo la topología afecta sus estados electrónicos (Kumagai[12]).

Capítulo 3. EFECTO AHARONOV-BOHM SOBRE LOS ESTADOS DEL ELECTRON LIBRE EN UNA CAJA CILINDRICA ANULAR.

El efecto Aharonov-Bohm clásico se manifiesta como el desplazamiento de las franjas de interferencia de la partícula-onda, causado por la interacción con el potencial vectorial magnético $\vec{A}$. Aún cuando la partícula no pase por la región donde hay campo de inducción magnética $\vec{B}$, los estados dependen del flujo magnético encerrado en la perforación.

Así, un experimento en el cual una partícula se encuentra en interacción con un potencial vectorial magnético $\vec{A}$, cuyo campo de inducción magnética $\vec{B}$ se anula localmente, y en el cual el cambio de energía de los estados es causado por el flujo magnético encerrado en la perforación, se identifica como efecto Aharonov-Bohm. Para analizar este efecto, es necesario considerar la interacción de la partícula cuántica con el potencial vectorial magnético.

En este capítulo se formula y resuelve el problema Aharonov-Bohm para el electrón, que involucra un campo de inducción magnética uniforme, axial, centrado y confinado en la perforación, y el potencial vectorial magnético asociado dentro de la caja. Ver Fig. (b).

3.1 Solución del problema de eigenvalores.

Considérese el sistema descrito por la Fig. (b), donde las dimensiones de la caja cilíndrica anular y las condiciones de confinamiento quedaron definidas en el Capítulo 2.

Fig. (b)

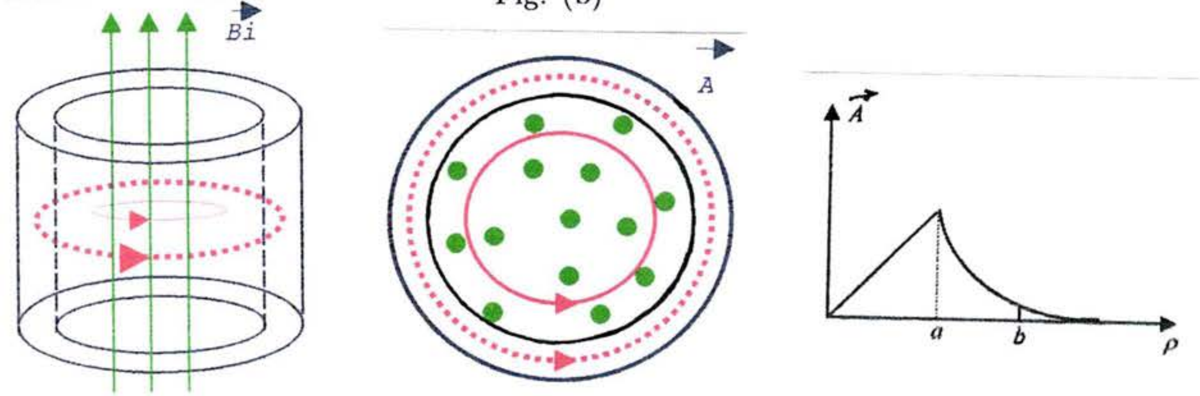

$$\vec{B}(0 \leq \rho \leq a, \varphi, z) \;=\; \hat{k} B_{\mathrm{i}} \quad , \quad \vec{A}(0 \leq \rho \leq a, \varphi, z) \;=\; \hat{\varphi}\, \frac{B_{\mathrm{i}}\rho}{2} \tag{3.1}$$

$$\vec{B}(a \leq \rho \leq \infty, \varphi, z) \;=\; 0 \quad , \quad \vec{A}(a \leq \rho \leq \infty, \varphi, z) \;=\; \hat{\varphi}\, \frac{B_{\mathrm{i}}a^2}{2\rho} \tag{3.2}$$

El Hamiltoniano asociado a este sistema está dado por la prescripción de acoplamiento mínimo (Landau[18]), considerando al electrón de carga $-e$

$$\hat{H} \;=\; \frac{(\hat{\vec{p}} + \frac{e}{c}\vec{A})^2}{2m_e} \tag{3.3}$$

donde $\quad \hat{\vec{p}} \;=\; \hat{\vec{p}}_\rho + \hat{\vec{p}}_\varphi + \hat{\vec{p}}_z \;=\; -i\hbar\left(\hat{\rho}\frac{\partial}{\partial\rho} + \hat{\varphi}\frac{1}{\rho}\frac{\partial}{\partial\varphi} + \hat{k}\frac{\partial}{\partial z}\right)$

Al separar la componente angular del momento canónico, y sustituir el potencial vectorial magnético asociado en el interior de la caja, se tiene

$$\hat{H} \;=\; \frac{\hat{\vec{p}}_\rho^{\,2}}{2m_e} \;+\; \frac{1}{2m_e}\left[\hat{\vec{p}}_\varphi + \frac{e}{c}\frac{B_{\mathrm{i}}a^2}{2\rho}\right]^2 \;+\; \frac{\hat{\vec{p}}_z^{\,2}}{2m_e}$$

o bien

$$\hat{H} \;=\; -\frac{\hbar^2}{2m_e}\frac{1}{\rho}\frac{\partial}{\partial\rho}\rho\frac{\partial}{\partial\rho} + \frac{\left(\hat{\ell}_z + \frac{eB_{\rm i}a^2}{2c}\right)^2}{2m_e\rho^2} - \frac{\hbar^2}{2m_e}\frac{\partial^2}{\partial z^2} \tag{3.4}$$

utilizando la representación diferencial asociada a los operadores de cantidad de movimiento. Y entonces la ecuación de Schrödinger es

$$\left\{-\frac{\hbar^2}{2m_e}\frac{1}{\rho}\frac{\partial}{\partial\rho}\rho\frac{\partial}{\partial\rho} + \frac{\left(\hat{\ell}_z + \frac{eB_{\rm i}a^2}{2c}\right)^2}{2m_e\rho^2} - \frac{\hbar^2}{2m_e}\frac{\partial^2}{\partial z^2}\right\}\psi(\rho,\varphi,z) \;=\; E\psi(\rho,\varphi,z) \tag{3.5}$$

donde se reconoce al segundo término, como el término centrífugo o de energía rotacional.

La comparación de la ecuación (3.5) y la ecuación (2.3), muestra que comparten las mismas contribuciones radial y logitudinal a la energía cinética, y la diferencia entre ellos reside en el término extra que surge del potencial vectorial magnético y que se suma a la componente z del momento angular. Tal término extra se identifica con el flujo magnético, como

$$\frac{eB_{\rm i}\pi a^2}{2\pi c} \;=\; \hbar\nu \tag{3.6}$$

donde ν es la magnitud del flujo magnético en la perforación en las unidades ch/e.

3.2 Dependencia de los estados ligados del sistema confinado, con respecto a la suma del número cuántico magnético y el flujo magnético en la perforación.

La ecuación (3.5) también admite una solución separable de la misma forma que la ecuación (2.7). Las ecuaciones (2.8) y (2.12) para las eigenfunciones longitudinales siguen siendo válidas. Las eigenfunciones de la componente z del momento angular de la ecuación (2.13) son también eigenfunciones del operador angular de la ecuación (3.5)

$$(\hat{\ell}_z + \hbar\nu)\ \Phi_m(\varphi) \ = \ \hbar(m+\nu)\ \Phi_m(\varphi) \tag{3.7}$$

Entonces la parte radial de la ecuación (3.5) se convierte en

$$\left[\frac{1}{\rho}\ \frac{d}{d\rho}\rho\frac{d}{d\rho} - \frac{(m+\nu)^2}{\rho^2}\right]R(\rho) \ = \ E_{\mathrm{T}}\ R(\rho) \tag{3.8}$$

La comparación de las ecuaciones radiales (2.10) y (3.8) muestra que son del mismo tipo, con la diferencia en sus parámetros

$$m \longrightarrow M \ = \ m+\nu \tag{3.9}$$

Y por tanto, la solución general de la ecuación radial (3.8), en analogía con ecuación (2.14), es

$$R_M(\rho) \ = \ \mathcal{A}_M J_M(k_{\mathrm{T}}\ \rho) \ + \ \mathcal{B}_M Y_M(k_{\mathrm{T}}\ \rho) \tag{3.10}$$

Por consiguiente, los eigenvalores de la energía, con dicho cambio en ecuación (2.18), son

$$E_{Msn} \;=\; \frac{\hbar^2}{2m_e}\Big(\frac{x_{Ms}^2}{a^2}+\frac{n^2\pi^2}{L^2}\Big) \tag{3.11}$$

3.3. Resultados numéricos y gráficos.

En esta sección se presentan algunos resultados cuantitativos que ilustran las soluciones de los problemas de eigenvalores formulados en los Capítulos 2 y 3. Se hace énfasis en la contribución transversal a los eigenvalores de la energía y las eigenfunciones radiales asociadas. Los resultados numéricos están contenidos en tablas y figuras para ambos casos $\nu = 0$ y $\nu \neq 0$.

La Figura 1 es una gráfica del determinante que aparece en la ecuación (2.17)

$$D_M(x) \;=\; J_M(x)\, Y_M\Big(\frac{bx}{a}\Big) \;-\; Y_M(x)\, J_M\Big(\frac{bx}{a}\Big) \tag{3.12}$$

como una función de $x = k_{\mathrm{T}}a$ para diferentes valores del parámetro M , ecuación (3.9), y para el caso específico de $b = 2a$. Sus ceros x_{Ms} , determinados a través del correspondiente programa que utiliza las subrutinas inc.h e in.h y otras del programa de software "Numerical Recipes in C"[11], están contenidos en la Tabla 1.

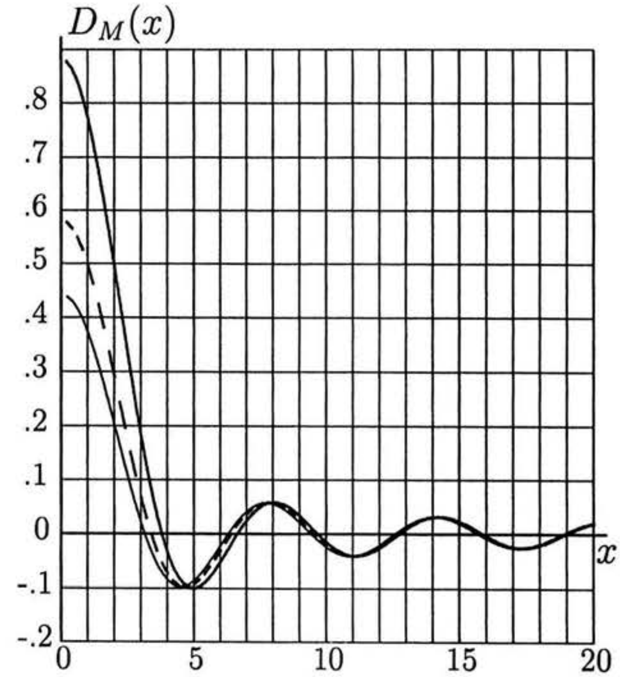

FIGURA 1. Gráfica del determinante $D_M(x)$ de ecuación (3.14), para $M = 9$ (línea fina), 1.9 (línea discontinua) y 3.14 (línea sólida) con $b = 2a$. Sus ceros determinan el número de onda transveral y los eigenvalores de la energía, de acuerdo con las ecuaciones (2.17 y 2.18).

TABLA 1. Ceros x_{Ms} para $b = 2a$ y diferentes valores de M y s . El cuadrado de sus valores, corresponde a los eigenvalores de la energía transversal, ecuación (3.11) .

$s =$	1	2	3	4
M				
0.0	3.12303	6.27344	9.41821	12.56142
0.2	3.12601	6.27500	9.41926	12.56221
0.4	3.13492	6.27968	9.42241	12.56459
0.6	3.14972	6.28747	9.42767	12.56855
0.8	3.17031	6.29837	9.43502	12.57408
1.0	3.19658	6.31235	9.44447	12.58120
1.2	3.22836	6.32940	9.45600	12.58990
1.4	3.26550	6.34950	9.46961	12.60017
1.6	3.30778	6.37261	9.48530	12.61201
1.8	3.35500	6.39871	9.50305	12.62541
2.0	3.40692	6.42777	9.52285	12.64038
2.2	3.46332	6.45974	9.54470	12.65691
2.4	3.52396	6.49458	9.56857	12.67499
2.6	3.58859	6.53226	9.59447	12.69461
2.8	3.65697	6.57272	9.62236	12.71578
3.0	3.72887	6.61592	9.65225	12.73848
3.2	3.80406	6.66181	9.68410	12.76271
3.4	3.88231	6.71033	9.71791	12.78846
3.6	3.96342	6.76144	9.75365	12.81572
3.8	4.04716	6.81507	9.79131	12.84449
4.0	4.13337	6.87116	9.83086	12.87474
4.2	4.22183	6.92967	9.87230	12.90649
4.4	4.31239	6.99054	9.91559	12.93971
4.6	4.40488	7.05369	9.96072	12.97440
4.8	4.49914	7.11908	10.00766	13.01055
5.0	4.59502	7.18665	10.05639	13.04814

La Figura 2 muestra los niveles de energía de los estados con las más bajas excitaciones angulares $m = 0, \pm 1, \pm 2, ...$ y sin excitación radial $s = 1$, como función del flujo magnético ν en la perforación. De acuerdo con la ecuación (2.18) y su extensión para el caso $\nu \neq 0$, los niveles de energía corresponden a los cuadrados de los ceros de la Tabla 1, x^2_{Ms} , en unidades de $\hbar^2/2m_e a^2$. Se puede apreciar la periodicidad del espectro de energía, conforme ν cambia por una unidad, la doble degeneración de los estados para valores de ν enteros y semi-enteros, y la simetría de las curvas de energía dentro de cada intervalo unitario de ν , bajo reflexión con respecto a la línea con el correspondiente valor semi-entero de ν .

Mientras que los valores de m están restringidos a ser enteros (ecuación (2.13)), los valores de M pueden variar continuamente siguiendo las variaciones correspondientes del flujo magnético ν . La solución de la ecuación radial ecuación (3.8) se sigue de los mismos pasos de las ecuaciones (2.14-2.20) con la substitución de m por M de la ecuación (3.9).

Incluso es importante reconocer que, mientras los eigenestados de la ecuación (2.10) dados por la ecuación (2.19) son doblemente degenerados para $m = \pm 1, \pm 2, ...$, tal degeneración se remueve cuando hay flujo magnético en la perforación, dado que los parámetros correspondientes de la ecuación (3.9), $M = |m| + \nu$ y $M = -|m| + \nu$ son diferentes. Por otra parte, comenzando con los valores dados de m y ν hay un número infinito de combinaciones de valores sucesivos de tales parámetros

$$M \;=\; m + \nu \;=\; (m - N) + (\nu + N), \quad N \;=\; 0, \pm 1, \pm 2, \pm 3, ... \qquad (3.13)$$

consistentes con el mismo valor de M . Los diferentes estados para los diferentes

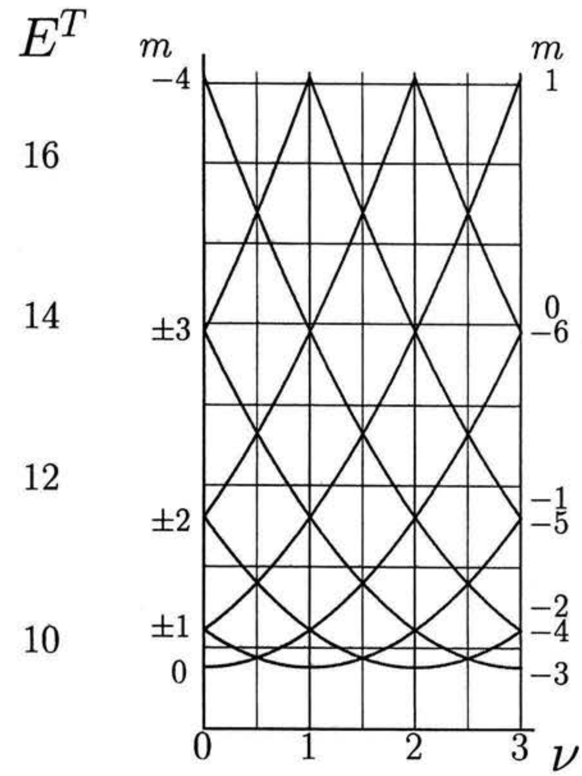

FIGURA 2. Eigenvalores de la energía transversal E^{T} en unidades $\hbar^2/2m_e a^2$, como función del flujo magnético ν en unidades hc/e , para estados con las más bajas excitaciones $m = 0, \pm1, \pm2, \ldots$, sin excitación radial $s = 1$, y $b = 2a$.

flujos magnéticos tienen las mismas energías, que se traducen en una repetición periódica del espectro de energías conforme el flujo magnético se incrementa por una unidad. En particular, el espectro de energía para $\nu = 1, 2, 3, ...$ es el mismo que para $\nu = 0$, incluyendo estados base con $m = -1, -2, -3, ...$ y estados excitados doblemente degenerados con $m = 0$ y -2, 1 y -3, 2 y -4,...; -1 y -3, 0 y -4, 1 y -5,...; -2 y -4,-1 y -5, 0 y -6,...;...; respectivamente. Al considerar el intervalo $0 < \nu < 1$, y los estados con $m = |m|$ y $-|m| - 1$, se identifica el valor común de

$$M = |m| + \nu \quad \text{y} \quad -M = -(|m| + 1) + (1 - \nu) \qquad (3.14)$$

que conduce a los mismos valores de las energías transversales. Nótese que los estados involucrados son estados vecinos en el número cuántico magnético y tienen la misma energía para valores complementarios del flujo magnético, ν y $1-\nu$. El resultado neto es que la energía del estado $|m|$ se incrementa monótonamente conforme ν cambia entre 0 y 1, mientras la energía del estado $-|m| - 1$ también se incrementa monótonamente en la misma forma que $1 - \nu$ cambia entre 0 y 1. En otras palabras, ésta última decrece monótonamente conforme ν cambia entre 0 y 1. Para $\nu = 0.5$ ambos estados tienen la misma energía para un valor común del flujo magnético, produciendo otra situación de doble degeneración. Las correspondientes curvas de energía son simétricas con respecto a la línea $\nu = 0.5$.

La Tabla 2 presenta un ejemplo de los coeficientes $\mathcal{A}_M$ y $\mathcal{B}_M$ de la función radial de la ecuación (3.10), es decir, para $\nu \neq 0$, normalizadas de acuerdo a las ecuaciones (2.19 y 2.20), con $M = m + \nu$. Las Tablas 3.1, 3.2 y 3.3 muestran las primeras seis soluciones x_{Ms} para los casos $b = 2a, 5a$ y $10a$, respectivamente.

TABLA 2. Número de onda transversal $k_{\mathrm{T}} = \frac{x_{Ms}}{a}$ y los coeficientes $\mathcal{A}_{Ms}$ $\mathcal{B}_{Ms}$ de la función radial ecuación (3.10), es decir para $\nu \neq 0$, normalizada de acuerdo a las ecuaciones (2.19 y 2.20) con el cambio $m \to M = m + \nu$, para $b = 2a$ y diferentes valores de M y s .

M	s	x_{Ms}	$\mathcal{A}_{Ms}$	$\mathcal{B}_{Ms}$
0	1	3.123039	1.18538	1.37124
	2	6.273439	1.73003	1.89366
	3	9.418211	2.14125	2.29878
	4	12.561424	2.48549	2.64229
	5	15.704000	2.78759	2.94595
	6	18.846249	3.06003	3.22109
1.9	1	3.380384	-1.80494	0.17472
	2	6.412872	-2.48722	-0.60375
	3	9.512694	-2.93332	-1.11832
	4	12.632701	-3.29758	-1.50910
	5	15.761176	-3.61801	-1.83150
	6	18.893965	-3.90917	-2.11052
3.14	1	3.781170	-1.42795	-1.10560
	2	6.647763	-0.21997	-2.55717
	3	9.674336	0.79896	-3.03178
	4	12.755284	1.54066	-3.28064
	5	15.859745	2.11991	-3.45593
	6	18.976334	2.59959	-3.60214

TABLA 3.1 Las primeras seis (s=1...6) soluciones x_{Ms} , para el caso $b = 2a$ y diferentes valores de M .

s / M	1	2	3	4	5	6
0.0	6.24606	12.54687	18.83642	25.12284	31.40800	37.69249
0.1	6.24755	12.54765	18.83694	25.12324	31.40831	37.69276
0.2	6.25202	12.54999	18.83852	25.12443	31.40927	37.69355
0.3	6.25945	12.55389	18.84115	25.12641	31.41085	37.69488
0.4	6.26985	12.55935	18.84483	25.12918	31.41307	37.69673
0.5	6.28319	12.56637	18.84956	25.13274	31.41593	37.69911
0.6	6.29944	12.57494	18.85534	25.13709	31.41942	37.70202
0.7	6.31860	12.58506	18.86216	25.14224	31.42354	37.70546
0.8	6.34063	12.59673	18.87004	25.14817	31.42830	37.70943
0.9	6.36549	12.60995	18.87896	25.15489	31.43369	37.71392
1.0	6.39316	12.62470	18.88893	25.16241	31.43971	37.71895
1.1	6.42358	12.64099	18.89994	25.17071	31.44637	37.72451
1.2	6.45673	12.65880	18.91200	25.17979	31.45366	37.73059
1.3	6.49255	12.67814	18.92509	25.18967	31.46157	37.73720
1.4	6.53099	12.69899	18.93922	25.20033	31.47013	37.74434
1.5	6.57201	12.72136	18.95439	25.21178	31.47931	37.75200
1.6	6.61556	12.74522	18.97060	25.22401	31.48913	37.76019
1.7	6.66157	12.77058	18.98783	25.23702	31.49957	37.76891
1.8	6.70999	12.79742	19.00610	25.25082	31.51065	37.77816
1.9	6.76077	12.82574	19.02539	25.26540	31.52235	37.78793
2.0	6.81384	12.85553	19.04571	25.28076	31.53469	37.79823
2.2	6.92664	12.91947	19.08940	25.31382	31.56123	37.82040
2.4	7.04792	12.98916	19.13715	25.34998	31.59029	37.84467
2.6	7.17717	13.06452	19.18894	25.38923	31.62185	37.87104
2.8	7.31394	13.14544	19.24473	25.43156	31.65590	37.89950
3.0	7.45774	13.23184	19.30449	25.47697	31.69244	37.93005
3.2	7.60812	13.32362	19.36820	25.52542	31.73145	37.96268
3.4	7.76462	13.42066	19.43581	25.57692	31.77295	37.99739
3.6	7.92683	13.52287	19.50729	25.63144	31.81690	38.03417
3.8	8.09433	13.63013	19.58261	25.68897	31.86332	38.07302
4.0	8.26673	13.74233	19.66173	25.74949	31.91217	38.11394
5.0	9.19005	14.37330	20.11278	26.09628	32.19282	38.34929
6.0	10.18893	15.10997	20.65224	26.51484	32.53304	38.63528
7.0	11.23571	15.93740	21.27418	27.00235	32.93129	38.97101
8.0	12.31131	16.84114	21.97237	27.55572	33.38584	39.35540
9.0	13.40296	17.80754	22.74051	28.17169	33.89482	39.78730
10.0	14.50237	18.82404	23.57224	28.84694	34.45625	40.26545

TABLA 3.2 Las primeras seis (s=1...6) soluciones x_{Ms} , para el caso $b = 5a$ y diferentes valores de M .

s / M	1	2	3	4	5	6
0.0	3.81596	7.78553	11.73210	15.67016	19.60421	23.53608
0.1	3.82049	7.78828	11.73406	15.67167	19.60544	23.53711
0.2	3.83403	7.79653	11.73993	15.67621	19.60913	23.54022
0.3	3.85645	7.81025	11.74972	15.68378	19.61528	23.54539
0.4	3.88753	7.82942	11.76340	15.69436	19.62389	23.55263
0.5	3.92699	7.85398	11.78097	15.70796	19.63495	23.56194
0.6	3.97446	7.88389	11.80242	15.72458	19.64848	23.57332
0.7	4.02954	7.91907	11.82773	15.74420	19.66445	23.58677
0.8	4.09177	7.95944	11.85688	15.76682	19.68287	23.60228
0.9	4.16067	8.00490	11.88984	15.79244	19.70374	23.61986
1.0	4.23575	8.05536	11.92658	15.82104	19.72705	23.63949
1.1	4.31650	8.11069	11.96708	15.85261	19.75281	23.66119
1.2	4.40242	8.17077	12.01130	15.88715	19.78100	23.68495
1.3	4.49302	8.23545	12.05921	15.92464	19.81162	23.71077
1.4	4.58783	8.30460	12.11075	15.96506	19.84466	23.73864
1.5	4.68641	8.37806	12.16588	16.00840	19.88013	23.76856
1.6	4.78831	8.45566	12.22456	16.05465	19.91800	23.80053
1.7	4.89315	8.53723	12.28674	16.10378	19.95829	23.83455
1.8	5.00056	8.62259	12.35234	16.15578	20.00097	23.87061
1.9	5.11020	8.71155	12.42132	16.21062	20.04605	23.90871
2.0	5.22177	8.80394	12.49360	16.26829	20.09351	23.94885
2.2	5.44959	8.99821	12.64779	16.39200	20.19554	24.03523
2.4	5.68211	9.20386	12.81431	16.52669	20.30699	24.12971
2.6	5.91784	9.41933	12.99247	16.67211	20.42776	24.23225
2.8	6.15563	9.64314	13.18152	16.82798	20.55774	24.34281
3.0	6.39460	9.87389	13.38065	16.99397	20.69683	24.46134
3.2	6.63411	10.11027	13.58902	17.16971	20.84486	24.58780
3.4	6.87372	10.35110	13.80573	17.35480	21.00169	24.72211
3.6	7.11309	10.59537	14.02986	17.54879	21.16713	24.86421
3.8	7.35202	10.84218	14.26052	17.75117	21.34097	25.01401
4.0	7.59038	11.09080	14.49679	17.96139	21.52298	25.17142
5.0	8.77174	12.34359	15.73444	19.10910	22.54480	26.06819
6.0	9.93614	13.59012	17.01170	20.36065	23.71630	27.13018
7.0	11.08637	14.82139	18.28916	21.65194	24.97857	28.32065
8.0	12.22509	16.03779	19.55482	22.94753	26.27929	29.59177
9.0	13.35430	17.24122	20.80709	24.23437	27.58687	30.89953
10.0	14.47550	18.43346	22.04699	25.50954	28.88808	32.21568

TABLA 3.3 Las primeras seis (s=1...6) soluciones x_{Ms} , para el caso $b = 10a$ y diferentes valores de M .

s / M	1	2	3	4	5	6
0.0	3.31394	6.85758	10.37742	13.88642	17.38963	20.88939
0.1	3.32133	6.86260	10.38123	13.88948	17.39218	20.89157
0.2	3.34334	6.87763	10.39263	13.89864	17.39983	20.89812
0.3	3.37946	6.90256	10.41160	13.91391	17.41257	20.90904
0.4	3.42890	6.93721	10.43807	13.93524	17.43039	20.92431
0.5	3.49066	6.98132	10.47198	13.96263	17.45329	20.94395
0.6	3.56354	7.03457	10.51321	13.99603	17.48126	20.96794
0.7	3.64629	7.09660	10.56163	14.03540	17.51426	20.99628
0.8	3.73760	7.16694	10.61709	14.08067	17.55229	21.02896
0.9	3.83621	7.24511	10.67941	14.13178	17.59532	21.06597
1.0	3.94094	7.33057	10.74838	14.18864	17.64331	21.10731
1.1	4.05069	7.42274	10.82375	14.25115	17.69622	21.15295
1.2	4.16449	7.52103	10.90526	14.31921	17.75401	21.20288
1.3	4.28149	7.62484	10.99261	14.39268	17.81663	21.25707
1.4	4.40096	7.73355	11.08548	14.47143	17.88401	21.31551
1.5	4.52229	7.84656	11.18354	14.55527	17.95607	21.37816
1.6	4.64498	7.96331	11.28642	14.64404	18.03275	21.44499
1.7	4.76862	8.08325	11.39374	14.73753	18.11393	21.51595
1.8	4.89289	8.20588	11.50513	14.83553	18.19951	21.59099
1.9	5.01753	8.33074	11.62019	14.93779	18.28938	21.67007
2.0	5.14235	8.45741	11.73855	15.04408	18.38339	21.75311
2.2	5.39193	8.71476	11.98364	15.26764	18.58323	21.93077
2.4	5.64083	8.97557	12.23759	15.50403	18.79770	22.12325
2.6	5.88865	9.23811	12.49790	15.75100	19.02526	22.32967
2.8	6.13521	9.50121	12.76251	16.00637	19.26421	22.54895
3.0	6.38045	9.76410	13.02979	16.26813	19.51281	22.77988
3.2	6.62439	10.02633	13.29850	16.53452	19.76930	23.02110
3.4	6.86709	10.28762	13.56776	16.80407	20.03202	23.27118
3.6	7.10860	10.54784	13.83696	17.07559	20.29946	23.52866
3.8	7.34900	10.80693	14.10571	17.34820	20.57030	23.79215
4.0	7.58835	11.06488	14.37375	17.62121	20.84345	24.06032
5.0	8.77148	12.33861	15.70025	18.98059	22.21967	25.43635
6.0	9.93611	13.58929	17.00382	20.32082	23.58625	26.82082
7.0	11.08637	14.82127	18.28758	21.64154	24.93494	28.19125
8.0	12.22509	16.03777	19.55454	22.94517	26.26682	29.54566
9.0	13.35430	17.24122	20.80705	24.23388	27.58375	30.88538
10.0	14.47550	18.43346	22.04699	25.50945	28.88738	32.21185

3.4. Discusión.

El análisis comparativo de las formulaciones y resultados de los problemas de las secciones 2.1 y 3.1 sirve para exhibir los efectos del potencial vectorial magnético en los eigenvalores de la energía y los eigenestados del electrón dentro de la caja anular, en la que no hay campo de inducción magnética. Del análisis del final de la sección 3.1 y los resultados de la sección 3.2, se pueden sacar algunas conclusiones acerca del efecto Aharonov-Bohm en los eigenvalores de la energía del electrón, como función de la magnitud del flujo magnético en la perforación. Estas conclusiones son válidas para cualesquier valores que se elijan de los números cuánticos radial y logitudinal s y n .

1) Los eigenvalores de la energía de los estados con $m = 0, 1, 2, ...$ crecen monótonamente con ν , de forma que

$$E_m(\nu + 1) \quad = \quad E_{m+1}(\nu) \tag{3.15}$$

y la correspondiente extensión iterativa

$$E_m(\nu + N) \quad = \quad E_{m+N}(\nu) \quad \text{para} \quad N = 1, 2, 3, ... \tag{3.16}$$

2) Los eigenvalores de la energía con $m = -1, -2, ...$ decrecen monótonamente al principio, de tal forma que siguen las ecuaciones (3.15 y 3.16) con los valores negativos de m , hasta que el flujo magnético toma los valores $\nu = -m$. A partir de este valor, cada uno se incrementa siguiendo las mismas ecuaciones (3.15 y 3.16) .

3) Las ecuaciones (3.15 y 3.16) describen la naturaleza periódica del espectro de energía como funciones del flujo magnético ν con período uno.

A) Para $\nu = 0$, el estado base $m = 0$ es no-degenerado y los estados excitados $m = \pm 1, \pm 2, ...$ son doblemente degenerados. Para $\nu = N$, el estado base es el estado $m = -N$ y los estados excitados doblemente degenerados corresponden a $m = -N - K$ y $-N + K$, con $K = 1, 2, 3, ...$

B) Para $\nu = 0.5$ el estado base y los estados excitados son todos doblemente degenerados correspondiendo a $m = 0$ y -1 , y K y $-K-1$, con $K = 1, 2, 3, ...$, respectivamente. Para $\nu = N + 0.5$, los estados correspondientes tienen $m = -N$ y $-N - 1$, y $-N + K$ y $-N - 1 - K$.

C) La simetría de las curvas de energía en el intervalo $0 \leq \nu \leq 1$ con respecto a la reflexión en la línea $\nu = 0.5$, se repite en cada intervalo $N \leq \nu \leq N + 1$ con respecto a la reflexión en la línea $\nu = N + 0.5$.

Es instructivo evaluar la energía de las transiciones radiativas entre dos estados transversales, que se sigue de la contraparte de la ecuación (2.18) con la substitución $m \to M$ y para el mismo número cuántico longitudinal $n\prime = n$ con el resultado

$$\Delta E(Msn \longrightarrow M's'n) \quad = \quad \frac{\hbar^2}{2m_e a^2}\left(x_{Ms}^2 - x_{M's'}^2\right) \quad \text{para} \quad m' = m \pm 1 \qquad (3.17)$$

La regla de selección para el número cuántico magnético m es la usual para transiciones dipolares dieléctricas (Sakurai[13], Sakurai[14]). El tamaño de la caja anular determina la región del espectro de las radiaciones correspondientes. En la práctica, pueden detectarse en anillos conductores microscópicos (Webb[15]), aparatos de semiconductividad mesoscópica (Timp[16]), y puntos cuánticos nanométricos (Ford[17]), que corresponden a radiación en microondas, infrarrojo lejano e infrarrojo cercano, respectivamente.

Es también ilustrativo comparar el efecto Aharonov-Bohm en la versión estandar del patrón de interferencia de los electrones, contra la versión de los estados del electrón libre de esta tesis, la cual dio origen a dos de nuestros artículos[22,23] : D. Kouznetsov, E. Ley-Koo and G. Villa-Torres, "Aharonov-Bohm effect on the bound states of an electron inside an annular cylindrical box", *Rev.Mex.Fís.* **45**(5)(1999)485, y E. Ley-Koo and G. Villa-Torres, "Clasical analysis of the Aharonov-Bohm effect", *Rev.Mex.Fís.* **47**(6)(2001)576-581. La característica común de ambas versiones es su periodicidad con período $\nu = 1$, para el patrón de interferencia y del espectro de energía, respectivamente. Ambas versiones son soluciones del mismo problema físico descrito por la ecuación de Schrödinger común, y su diferencia consiste en su correspondencia con estados de dispersión y estados ligados, respectivamente.

Capítulo 4. ESTADOS DE LANDAU DEL ELECTRON EN UNA CAJA CILINDRICA ANULAR.

En los capítulos 2 y 3 se estudió el efecto Aharonov-Bohm sobre los estados del electrón libre en la caja cilíndrica anular, comparando los casos : a) en ausencia de cualquier campo de inducción magnética o campo de potencial, y b) en presencia de un campo de inducción magnética en la perforacion. A través de los Capítulos 4 y 5 se discute otra variante del efecto Aharonov-Bohm con el hecho especial de que en la región donde se mueve el electrón hay un campo de inducción magnética. Es decir, se ilustra el efecto Aharonov-Bohm sobre los Estados de Landau del electrón, a través del estudio del espectro de energía y las eigenfunciones del electrón dentro de la caja cilíndrica anular, en dos situaciones comparativas: c) en presencia de campo de inducción magnética de la misma magnitud tanto en la caja como en la perforación, y d) cuando se modifica la magnitud del campo en la perforación .

4.1 Solución del problema de eigenvalores.

Los estados de Landau[18] corresponden a los eigenestados de un electrón bajo la acción de un campo de inducción magnética en todos los puntos del espacio. El problema de Landau se ha resuelto en la norma lineal y en la norma simétrica, y las conexiones entre los eigenestados respectivos se exhiben en Fung y Wang[9].

En este capítulo se resuelve el problema de eigenvalores del electrón en presencia de un campo de inducción magnética en una región del espacio, es decir, un campo de inducción magnética de la misma magnitud tanto en la caja anular como en la perforación, y el potencial vectorial magnético dentro de la caja. Considérese el sistema descrito por la Fig. (c), donde las dimensiones de la caja cilíndrica anular y las condiciones de confinamiento ya quedaron definidos con anterioridad.

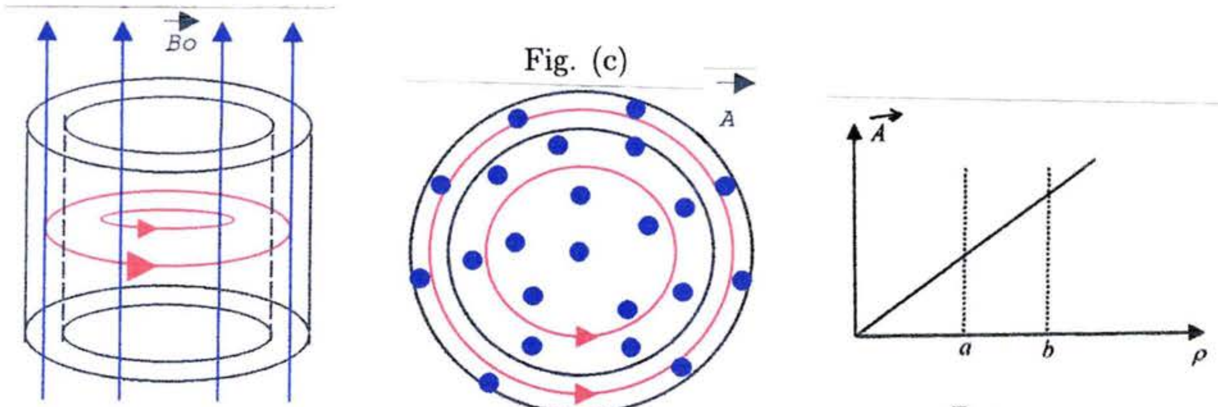

Fig. (c)

$$\vec{B}(0 \le \rho \le \infty, \varphi, z) \;=\; \hat{k} B_{\text{o}} \quad , \quad \vec{A}(0 \le \rho \le \infty, \varphi, z) \;=\; \hat{\varphi}\, \frac{B_{\text{o}}\rho}{2} \tag{4.1}$$

El Hamiltoniano para un electrón en tal campo se obtiene a partir de la prescripción de acoplamiento mínimo (Gottfried[19])

$$\begin{aligned} \hat{H} \;&=\; \frac{\left(\hat{\vec{p}} + \frac{e}{c}\vec{A}\right)^2}{2m_e} \;=\; \frac{\hat{\vec{p}}_\rho^{\,2}}{2m_e} + \frac{1}{2m_e}\left(\hat{\vec{p}}_\varphi + \frac{e}{c}\vec{A}\right)^2 + \frac{\hat{\vec{p}}_z^{\,2}}{2m_e} \\ &=\; \frac{\hat{\vec{p}}_\rho^{\,2}}{2m_e} + \frac{\left(\frac{\hat{\ell}_z}{\rho} + \frac{eB_{\text{o}}\rho}{2c}\right)^2}{2m_e} + \frac{\hat{\vec{p}}_z^{\,2}}{2m_e} \end{aligned} \tag{4.2}$$

e involucra las componentes radial $\hat{\vec{p}}_\rho$, azimutal $\frac{\hat{\ell}_z}{\rho}$ y axial $\hat{\vec{p}}_z$ del momento canónico; $\hat{\ell}_z$ es el momento angular canónico.

La ecuación de Schrödinger independiente del tiempo toma la forma

$$\left[-\frac{\hbar^2}{2m_e}\frac{1}{\rho}\frac{\partial}{\partial\rho}\rho\frac{\partial}{\partial\rho} + \frac{\hat{\ell}_z^2}{2m_e\rho^2} + \frac{eB_{\text{o}}}{2m_e c}\hat{\ell}_z + \frac{e^2B_{\text{o}}^2}{8m_e c^2}\rho^2 - \frac{\hbar^2}{2m_e}\frac{\partial^2}{\partial z^2}\right]\psi(\rho,\varphi,z) \;=\; E\psi(\rho,\varphi,z) \tag{4.3}$$

donde los tres términos que surgen del cuadrado del binomio en la ecuación (4.2) se identifican como la energía cinética rotacional, la energía diamagnética y la energía potencial de oscilador armónico con frecuencia $\omega_{\rm B} = eB_{\rm o}/2m_e c$. Esta ecuación admite solución separable, ecuación (2.7), que de nuevo son las eigenfunciones longitudinales, ecuación (2.12), y las eigenfunciones de la componente z del momento angular orbital, ecuación (2.13) . Los eigenvalores de la energía tienen contribución transversal y longitudinal $E = E^{\rm T}_{ms} + E^{\rm L}_n$.

Esta separación de variables, deja la ecuación radial

$$\Big[-\frac{\hbar^2}{2m_e}\Big(\frac{1}{\rho}\frac{d}{d\rho}\rho\frac{d}{d\rho} - \frac{m^2}{\rho^2}\Big) + \hbar\omega_{\rm B} m + \frac{1}{2}m_e\omega_{\rm B}^2\rho^2\Big]R(\rho) \quad = \quad E^{\rm T}R(\rho) \tag{4.4}$$

4.2 Dependencia de los Estados de Landau para los sistemas libre y confinado con respecto al número cuántico magnético.

4.2.1 Caso libre.

Los estados de Landau estandar corresponden al dominio $(0 \leq \rho \leq \infty)$ con las eigenfunciones del oscilador armónico (Landau[18])

$$R_{\rm n_1 m}(\rho) \quad = \quad N_{\rm n_1 m}\ \rho^{|m|}\ e^{-\frac{m_e\omega_{\rm B}\rho^2}{2\hbar}}\ M\Big(-n_1, |m|+1; \frac{m_e\omega_{\rm B}\rho^2}{\hbar}\Big) \tag{4.5}$$

donde $n_1 = 0, 1, 2, ...$ y $M({\rm a}, {\rm b}; z)$ es la función Hipergeométrica Confluente de Kummer de primera clase (Abramowitz[10]); y los eigenvalores de la energía son la suma de las energías del oscilador armónico más la energía diamagnética

$$E^{\mathrm{T}}_{\mathrm{n_1 m}}(\rho) \;=\; \hbar\omega_{\mathrm{B}}\Big[2n_1 + |m| + m + 1\Big] \tag{4.6}$$

Estos niveles de energía están igualmente espaciados con espaciamiento $2\hbar\omega_{\mathrm{B}}$. Cada nivel es infinitamente degenerado, debido a la cancelación de los términos dependientes de m, para $m = -|m|$.

4.2.2 Caso confinado.

Las condiciones de frontera en los radios interno y externo a y b, requieren la inclusión de la segunda solución de Kummer $U(\mathrm{a}, \mathrm{b}; z)$ que es singular en el origen y bien comportada al infinito

$$\begin{aligned} R_{\nu_1 m}(\rho) \;=\; & \rho^{|m|}\, e^{-\frac{m_e\omega_{\mathrm{B}}\rho^2}{2\hbar}} \Big[A\, M\Big(-\nu_1, |m|+1; \frac{m_e\omega_{\mathrm{B}}\rho^2}{\hbar}\Big) \;+ \\ & B\, U\Big(-\nu_1, |m|+1; \frac{m_e\omega_{\mathrm{B}}\rho^2}{\hbar}\Big)\Big] \end{aligned} \tag{4.7}$$

donde las funciones Hipergeométricas Confluentes de primera y segunda clase M y U están definidas por

$$M(\alpha, \beta; z) \;=\; \sum_{n=0}^{\infty} \frac{(\alpha)_n\, z^n}{(\beta)_n\, n!} \tag{4.8}$$

$$U(\alpha, \beta; z) \;=\; \frac{\pi}{\mathrm{sen}(\pi\beta)}\Big[\frac{M(\alpha, \beta; z)}{\Gamma(1+\alpha-\beta)\,\Gamma(\beta)} - z^{1-\beta}\,\frac{M(1+\alpha-\beta, 2-\beta; z)}{\Gamma(\alpha)\,\Gamma(2-\beta)}\Big] \tag{4.9}$$

donde $(\alpha)_n = (\alpha)(\alpha+1)(\alpha+2)(\alpha+3)...(\alpha+n-1)$; $(\alpha)_0 = 1$ es símbolo de Pochhammer, o bien, $(\alpha)_n = \frac{\Gamma(\alpha+1+n)}{\Gamma(\alpha+1)}$

La serie de la ecuación (4.8) es convergente para todos los valores de z y todos los valores de α y β que no sean enteros negativos. Esta serie se convierte en un polinomio de grado N cuando $\alpha = N$ es un entero negativo.

Cuando β es un entero positivo, como en el presente caso ($\beta = |m| + 1$), la ecuación (4.9) toma la forma logarítmica

$$U(\alpha, m+1; z) = \frac{(-)^{m+1}}{m!\,\Gamma(\alpha - m)} \Bigg\{ M(\alpha, m+1; z)\; ln\; z \; +$$

$$\sum_{r=0}^{\infty} \frac{(\alpha)_r\, z^r}{(m+1)_r\, r!} \Big[\psi(\alpha+r) - \psi(1+r) - \psi(1+m+r)\Big] \Bigg\} +$$

$$\frac{(m+1)!}{\Gamma(\alpha)}\, z^{-m}\;\; M(\alpha-m, 1-m, z)_m \tag{4.10}$$

para $m = 0, 1, 2, ...$, donde $\psi(x) = \frac{\Gamma'(x)}{\Gamma(x)}$ y el último factor es la suma de los m términos con el valor cero para $m = 0$. Y sus formas asintóticas para $z \to \infty$, son

$$M(\alpha, \beta; z) = \frac{\Gamma(\beta)}{\Gamma(\alpha)}\; e^z\; z^{\alpha-\beta} \Big[1 + O(|z|^{-1})\Big]$$

$$U(\alpha, \beta; z) = z^{-\alpha} \Big[1 + O(|z|^{-1})\Big]$$

De nuevo, las condiciones de frontera $R_{\nu_1 m}(a) = 0 = R_{\nu_1 m}(b)$:

$$A_m M\Big(-\nu_1, |m|+1; \frac{m_e\omega_{\rm B}}{\hbar}a^2\Big) \;+\; B_m U\Big(-\nu_1, |m|+1; \frac{m_e\omega_{\rm B}}{\hbar}a^2\Big) \;=\; 0 \quad (4.11)$$

$$A_m M\Big(-\nu_1, |m|+1; \frac{m_e\omega_{\rm B}}{\hbar}b^2\Big) \;+\; B_m U\Big(-\nu_1, |m|+1; \frac{m_e\omega_{\rm B}}{\hbar}b^2\Big) \;=\; 0 \quad (4.12)$$

proporcionan un sistema de ecuaciones lineales homogéneas algebraicas para los coeficientes desconocidos A_m B_m , que admite soluciones cero no triviales sólo si su determinante se anula, es decir

$$\begin{aligned} D_m(\nu_1) \;&=\; M\Big(-\nu_1, |m|+1; \frac{m_e\omega_{\rm B}}{\hbar}a^2\Big)\, U\Big(-\nu_1, |m|+1; \frac{m_e\omega_{\rm B}}{\hbar}b^2\Big) \;- \\ & M\Big(-\nu_1, |m|+1; \frac{m_e\omega_{\rm B}}{\hbar}b^2\Big)\, U\Big(-\nu_1, |m|+1; \frac{m_e\omega_{\rm B}}{\hbar}a^2\Big) \;=\; 0 \qquad (4.13)\end{aligned}$$

Tal ecuación trascendental debe resolverse numéricamente para obtener el parámetro ν_1 , que determina la energía para $a, b, \omega_{\rm B}$ y m predeterminados. Sus soluciones se obtienen utilizando un programa diseñado en "Mathematica" [19].

Los eigenvalores de la energía transversal son

$$E^{\rm T}_{\nu_1 m} \;=\; \hbar\omega_{\rm B}\Big[2\nu_1 + |m| + m + 1\Big] \qquad (4.14)$$

y los eigenvalores de la energía total son

$$E \;=\; \hbar\omega_{\rm B}\Big[2\nu_1 + |m| + m + 1\Big] + \frac{\hbar^2}{2m_e}\Big(\frac{n\pi}{L}\Big)^2 \qquad (4.15)$$

Y la solución radial normalizada, es

$$R_{\nu_1 m}(\rho) = \frac{1}{\sqrt{N_m}}\Big[U\Big(-\nu_1, |m|+1; \frac{m_e\omega_B}{\hbar}\Big(\frac{a}{b}\Big)^2\Big)\, M\Big(-\nu_1, |m|+1; \frac{m_e\omega_B}{\hbar}\Big(\frac{\rho}{b}\Big)^2\Big) -$$
$$M\Big(-\nu_1, |m|+1; \frac{m_e\omega_B}{\hbar}\Big(\frac{a}{b}\Big)^2\Big)\, U\Big(-\nu_1, |m|+1; \frac{m_e\omega_B}{\hbar}\Big(\frac{\rho}{b}\Big)^2\Big)\Big] \tag{4.16}$$

donde la constante de Normalización, es:

$$N_m(\rho) = \int_a^b \rho \mathrm{d}\rho \Big[U\Big(-\nu_1, |m|+1; \frac{m_e\omega_B}{\hbar}\Big(\frac{a}{b}\Big)^2\Big) M\Big(-\nu_1, |m|+1; \frac{m_e\omega_B}{\hbar}\Big(\frac{\rho}{b}\Big)^2\Big) -$$
$$M\Big(-\nu_1, |m|+1; \frac{m_e\omega_B}{\hbar}\Big(\frac{a}{b}\Big)^2\Big) U\Big(-\nu_1, |m|+1; \frac{m_e\omega_B}{\hbar}\Big(\frac{\rho}{b}\Big)^2\Big)\Big] \tag{4.17}$$

4.3 Discusión.

El problema estandar de Landau, en el que el electrón puede estar en cualquier punto en el rango $0 \leq \rho \leq \infty$, corresponde al caso particular de $a = 0$ y $b = \infty$. La función Hipergeométrica U es singular en $\rho = 0$, por lo que para el caso estandar ésta se elimina de la ecuación (4.7), tomando $B = 0$. Por otra parte, M diverge conforme $\rho \to \infty$, y la forma de hacer que la ecuación (4.7) siga siendo útil, es tomar ν_1 como entero no-negativo N , para el que M se convierte en un polinomio de grado $2N$. De la misma manera, los niveles de energía de Landau de la ecuación (4.14) se convierten en el espectro de enteros impares en unidades $\hbar\omega_{\rm B}$, siendo cada nivel infinitamente degenerado, como consecuencia de la cancelación de las contribuciones rotacional y diamagnética $|m| + m$ para $m = -|m|$.

Los ceros de ν_1 en la ecuación (4.15), que en general no son enteros, dependen de los valores de los otros parámetros de M y U, es decir, de $|m|$, $\frac{m_e\omega_{\rm B}a^2}{\hbar}$ y $\frac{m_e\omega_{\rm B}b^2}{\hbar}$. El confinamiento del electrón dentro de la caja cilíndrica anular remueve la degeneración infinita de los niveles de energía estandar de Landau descritos anteriormente.

Para efectos de comparación, los resultados de este problema se presentan en el capítulo 5.

Capítulo 5. EFECTO AHARONOV-BOHM SOBRE LOS ESTADOS DE LANDAU DEL ELECTRON EN UNA CAJA CILINDRICA ANULAR.

En este capítulo se discute otra variante del efecto Aharonov-Bohm con la característica especial de que en la región donde se mueve el electrón hay un campo de inducción magnética. Es decir, se ilustra el efecto Aharonov-Bohm sobre los Estados de Landau del electrón dentro de una caja cilíndrica anular, comparando la situación descrita en el capítulo 4 y la situación descrita en este capítulo, en la que la magnitud del campo de inducción magnética en la perforación es diferente de la del campo en la caja anular.

5.1 Solución del problema de eigenvalores.

En este capítulo se formula y resuelve el problema Aharonov-Bohm para el electrón, que involucra un campo de inducción magnética en la caja y un campo diferente en la perforación. Considérese el sistema descrito por la Fig. (d).

Fig. (d)

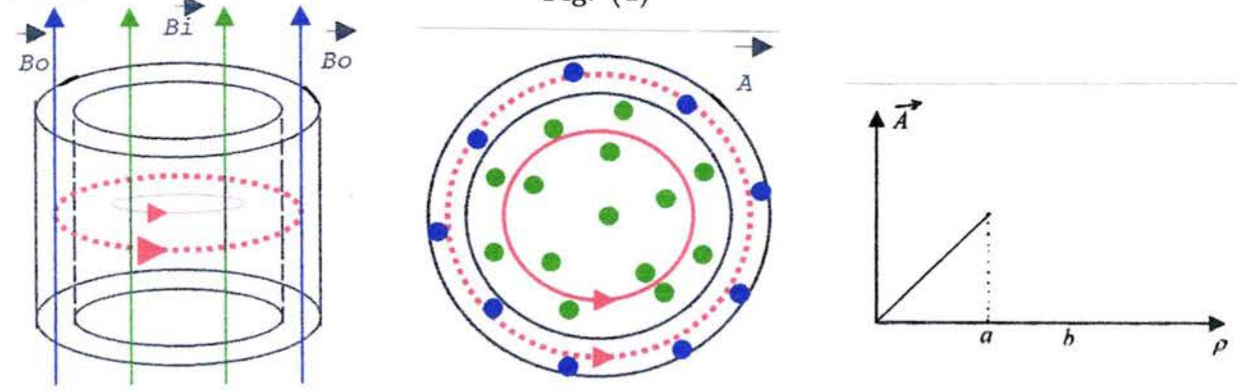

$$\vec{B}(0 \leq \rho \leq a, \varphi, z) = \hat{k} B_{\mathrm{i}} \quad , \quad \vec{A}(0 \leq \rho \leq a, \varphi, z) = \hat{\varphi}\, \frac{B_{\mathrm{i}}\rho}{2} \tag{5.1}$$

$$\vec{B}(a \leq \rho \leq b, \varphi, z) = \hat{k} B_{\mathrm{o}} \quad , \quad \vec{A}(a \leq \rho \leq b, \varphi, z) = \hat{\varphi} \left(\frac{B_{\mathrm{o}}\rho}{2} + \frac{(B_{\mathrm{i}} - B_{\mathrm{o}})a^2}{2\rho} \right) \tag{5.2}$$

El Hamiltoniano para la nueva situación se construye a partir del potencial vectorial magnético de la ecuación (5.2)

$$\hat{H} \;=\; \frac{\vec{p}_\rho^{\,2}}{2m_e} + \frac{\left[\frac{\hat{\ell}_z\, +\, (B_\mathrm{i}-B_\mathrm{o})a^2e/2c}{\rho} + \frac{eB_\mathrm{o}\rho}{2c}\right]^2}{2m_e} + \frac{\vec{p}_z^{\,2}}{2m_e} \tag{5.3}$$

La diferencia de campo de inducción magnética en la perforación, ecuación (5.1), comparado con el de la caja, ecuación (5.2), se traduce en la diferencia del potencial vectorial magnético de la ecuación (5.2) comparado con el de la ecuación (4.1), y correspondientemente a la diferencia entre el Hamiltoniano de la ecuación (5.3) comparado con el de la ecuación (4.2). Tal diferencia consiste en el reemplazo $\hat{\ell}_z \rightarrow \hat{\ell}_z + \frac{e\,(B_\mathrm{i}-B_\mathrm{o})\,a^2}{2c}$ al ir de ecuación (4.2) a la ecuación (5.3), en los términos inversamente proporcionales a la coordenada radial ρ .

La ecuación de Schrödinger

$$\left\{ -\frac{\hbar^2}{2m_e}\frac{1}{\rho}\frac{\partial}{\partial\rho}\rho\frac{\partial}{\partial\rho} + \frac{\left[\hat{\ell}_z + \frac{e(B_\mathrm{i}-B_\mathrm{o})a^2}{2c}\right]^2}{2m_e\rho^2} + \frac{eB_\mathrm{o}}{2m_e c}\left[\hat{\ell}_z + \frac{e(B_\mathrm{i}-B_\mathrm{o})a^2}{2c}\right] + \right.$$

$$\left. \frac{e^2B_\mathrm{o}^2}{8m_e c^2}\,\rho^2 - \frac{\hbar^2}{2m_e}\frac{\partial^2}{\partial z^2}\right\} \psi(\rho,\varphi,z) \;=\; E\psi(\rho,\varphi,z) \tag{5.4}$$

admite soluciones separables, ecuación (2.7) $\psi(\rho,\varphi,z) = R(\rho)\Phi(\varphi)Z(z)$, donde las soluciones axial y angular, son las mismas ecuaciones (2.12 y 2.13) .

La ecuación radial es

$$-\frac{\hbar^2}{2m_e}\left\{\frac{1}{\rho}\frac{d}{d\rho}\rho\frac{d}{d\rho} + \frac{\hbar^2(m+\mu)^2}{2m_e\rho^2} + \hbar\omega_\mathrm{B}(m+\mu) + \frac{1}{2}m_e\omega_\mathrm{B}^2\rho^2\right\}R(\rho) \;=\; E^\mathrm{T}R(\rho) \tag{5.5}$$

donde $\omega_{\mathrm{B}} = \frac{eB_{\mathrm{o}}}{2m_e c}$, donde se reconoce a los términos centrífugo, diamagnético y de oscilador armónico, y donde

$$\frac{(B_{\mathrm{i}} - B_{\mathrm{o}})a^2 e}{2c\hbar} = \frac{(B_{\mathrm{i}} - B_{\mathrm{o}})\pi a^2}{hc/e} = \mu \tag{5.6}$$

es el cambio en el flujo magnético en la perforación en unidades de hc/e entre las situaciones (5.1 y 4.1).

5.2 Dependencia de los Estados de Landau para el sistema confinado con respecto a la suma del número cuántico magnético y el cambio en el flujo magnético en la perforación.

La comparación de las ecuaciones (5.5 y 4.4) muestra que tienen la misma forma con el reemplazo

$$m \rightarrow \mathcal{M} = m + \mu \tag{5.7}$$

Las eigenfunciones radiales correspondientes para el electrón en la caja anular se obtienen a partir de la ecuación (4.7) con este reemplazo

$$\begin{aligned} R_{\nu_1 \mathcal{M}}(\rho) &= \rho^{|\mathcal{M}|}\, e^{-\frac{m_e \omega_{\mathrm{B}} \rho^2}{2\hbar}} \Big[A\, M\Big(-\nu_1, |\mathcal{M}|+1; \frac{m_e \omega_{\mathrm{B}} \rho^2}{\hbar} \Big) + \\ & \qquad B\, U\Big(-\nu_1, |\mathcal{M}|+1; \frac{m_e \omega_{\mathrm{B}} \rho^2}{\hbar} \Big) \Big] \end{aligned} \tag{5.8}$$

Las condiciones de frontera $R_{\nu_1\mathcal{M}}(a) = 0 = R_{\nu_1\mathcal{M}}(b)$ proporcionan un sistema de ecuaciones lineales homogéneas algebraicas para los coeficientes desconocidos $A_{\mathcal{M}}$ $B_{\mathcal{M}}$, y se resuelve numéricamente el determinante correspondiente (análogo a la ecuación 4.13) de tal sistema

$$\begin{aligned} D_{\mathcal{M}}(\nu_1) &= M\Big(-\nu_1, |\mathcal{M}|+1; \frac{m_e\omega_{\rm B}}{\hbar}a^2\Big)U\Big(-\nu_1, |\mathcal{M}|+1; \frac{m_e\omega_{\rm B}}{\hbar}b^2\Big) - \\ & M\Big(-\nu_1, |\mathcal{M}|+1; \frac{m_e\omega_{\rm B}}{\hbar}b^2\Big)U\Big(-\nu_1, |\mathcal{M}|+1; \frac{m_e\omega_{\rm B}}{\hbar}a^2\Big) = 0 \end{aligned} \tag{5.9}$$

para obtener el parámetro ν_1 que determina la energía, para diferentes valores del parámetro $\mathcal{M} = m+\mu$. Los ceros $\nu_{1\mathcal{M}s}$ se determinan a través del correspondiente programa diseñado en "Mathematica" [19] , y están contenidos en tablas.

Los eigenvalores de la energía transversal se obtienen a partir de la adaptación corrrespondiente de la ecuación (4.14)

$$E^{\rm T}_{\nu_1\mathcal{M}} = \hbar\omega_{\rm B}\Big[2\nu_1 + |\mathcal{M}| + \mathcal{M} + 1\Big] \tag{5.10}$$

y los eigenvalores de la energía del sistema son

$$E = \hbar\omega_{\rm B}\Big[2\nu_1 + |\mathcal{M}| + \mathcal{M} + 1\Big] + \frac{\hbar^2}{2m_e}\Big(\frac{n\pi}{L}\Big)^2 \tag{5.11}$$

Por supuesto, los valores de ν_1 serán en general diferentes de los valores previos (Capítulo 4), debido al cambio del parámetro $m \to \mathcal{M} = m + \mu$ en las funciones de Kummer.

5.3 Resultados numéricos y gráficos.

Esta sección contiene algunos resultados numéricos y gráficos que ilustran el efecto de confinamiento de la caja anular sobre los Estados de Landau y el efecto Aharonov-Bohm en los mismos estados, a partir del análisis del Capítulo 4 y de este capítulo, respectivamente. Para el primero, los ceros de la ecuación (4.13) en ν_1 se basan en la forma logarítmica de la función U , ecuación (4.10). Para el segundo, la ecuación (5.9) requiere el uso de la forma de U de la ecuación (4.9) para valores no enteros de μ . La Tabla 4 y Figuras 4a y 4b, ilustran el efecto de confinamiento; y la Tabla 5 y Figuras 5a y 5b, ilustran el efecto Aharonov-Bohm sobre los Estados de Landau, como se explica y discute a continuación.

5.3.1 Efecto de confinamiento de la caja anular sobre los Estados de Landau.

La Tabla 4 presenta los eigenvalores de la energía transversal E^{T}_{sm} para los Estados de Landau con $s = 1, 2, 3$ y $m = 0, \pm 1, \pm 2, ...$ obtenidos a partir de las ecuaciones (4.13 y 4.14), para el electrón confinado en cajas con $b = 2a$, $5a$ y $10a$, en diferentes campos de inducción magnética que producen flujos magnéticos de 1 y 15 fluxones en las secciones de corte circular de radio b . Los valores de ν_s de la solución numérica de la ecuación (4.13), cuando se duplica y se incrementa por una unidad, proporcionan los eigenvalores de la energía para los estados cero y con valores negativos de m ; para los estados positivos de m , se requiere la suma adicional de $2m$.

El efecto de confinamiento de la caja sobre los Estados de Landau del electrón se manifiesta obviamente por la desviación de los niveles de energía a partir del espectro igualmente espaciado e infinitamente degenerado $(2N+1)\hbar\omega$ con valores enteros de N . Los datos de la Tabla 4 indican que tal efecto es dominante para el primer conjunto de tres pequeñas cajas, y decrece para el conjunto de cajas más grandes; adicionalmente, dentro de cada conjunto, el efecto es más notable para cajas con perforaciones más grandes. Las Figuras 4a y 4b ilustran el cambio del efecto de confinamiento, así como los efectos del campo magnético en el espectro de energía del electrón para las cajas de las columnas primera y última, respectivamente. Para la caja chica con $b=1$ en la unidad de longitud $(\hbar/m_e\omega)^{1/2}$ y con amplia perforación $a=0.5$, el efecto de confinamiento es grande, como se ilustra por los valores numéricos de las eigenenergías de los estados $m=0$ en la caja expresadas en términos de las correspondientes eigenenergías estandar de Landau, $E^{\mathrm{T}}_{10}=19.79178\ E^{\mathrm{L}}_{10}$, $E^{\mathrm{T}}_{20}=26.33333\ E^{\mathrm{L}}_{20}$, $E^{\mathrm{T}}_{30}=35.53925\ E^{\mathrm{L}}_{30}$,una situación extensiva a los otros estados E^{T}_{sm} . Puede notarse las diferentes regiones en la escala de energía en la Fig. 4a para los niveles de energía $s=1$ y 2 debidas a la amplia magnitud del efecto de confinamiento; la inclusión de los niveles de energía $s=3$ requerirían brincar a la región con $E^{\mathrm{T}}_{sm}\geq 170$. La degeneración de los niveles de energía $(s,m\geq 0)$ y $(s,-m-1)$ se hace muy evidente, y puede entenderse como el resultado de la combinación del efecto de confinamiento y los efectos magnéticos asociados con los Estados de Landau, incluyendo el notable comportamiento de los estados $m>0$ y $m<0$ debidos a la energía diamagnética. Por otra parte, la Fig. 4b para una caja grande con $b=\sqrt{15}$ y una pequeña perforación $a=\sqrt{15}/10$, la escala de energía es la misma que la de los Estados de Landau normales, porque el efecto de confinamiento se reduce apreciablemente. Sin embargo, se conserva presente definitivamente como indica la comparación $E^{\mathrm{T}}_{10}=1.91268\ E^{\mathrm{L}}_{10}$, $E^{\mathrm{T}}_{20}=1.38849\ E^{\mathrm{L}}_{20}$, $E^{\mathrm{T}}_{30}=1.21120\ E^{\mathrm{L}}_{30}$. En este caso, todos los niveles de energía con $s=1,2$ y 3 se pueden dibujar juntos. El espaciamiento de los niveles de energía para cada valor de s y los valores positivos sucesivos de m , no está lejos de 2, el espaciamiento de los niveles de energía de Landau normal. Por otra parte, la tendencia a la degeneración de los niveles de energía, para cada valor de s y los valores negativos sucesivos de $m = -1, -2, -3, ...$, en las posiciones de los niveles de energía de Landau normal $1, 3, 5, ...$ es explícitamente aparente. El espectro de energía del electrón en las cajas de las columnas 2-5 en la Tabla 4 ilustran su comportamiento intermedio entre las dos situaciones explícitamente discutidas en conexión con las Figs. 4a y 4b.

5.3.2 Efecto Aharonov-Bohm sobre los Estados de Landau.

La Tabla 5 presenta los eigenvalores de la energía transversal E^{T}_{sm} para los Estados de Landau con $s = 1$ y $m = 0, 1, 2, ...$ para un electrón en cajas con $b = 1$ y $a = 0.5$, 0.2 y 0.1 , cuando los campos de inducción magnética en la perforación y en la caja son diferentes de acuerdo a las ecuaciones (5.6 y 5.10). Los valores de ν_s son soluciones numéricas de la ecuación(5.9) y dependen del valor de $|m+\mu|$. Los eigenvalores de la energía mismos también dependen del valor y signo de $m+\mu$, como se distingue en las columnas correspondientes. La primer columna proporciona los valores de $|m + \mu|$ interpolando entre los valores enteros de m ya considerados en la Tabla 4. De nuevo los valores de ν_s cuando se duplican y se incrementan por una unidad proporciona las entradas para las energías en la primera, tercera y quinta columnas para los estados con $(m + \mu) < 0$, en las que la energía rotacional y diamagnética se cancelan mutuamente, ecuación (5.10). Las energías para las siguientes columnas se obtienen por la nueva adición de $2|m + \mu|$ y corresponden a los estados con $(m + \mu) > 0$, ecuación (5.10).

Es importante entender que las entradas en cada par de columnas de la Tabla 5 son válidas para las energías $E^{\mathrm{T}}_{sm}(\mu)$ para las diferentes combinaciones de los valores de m de los estados seleccionados, y de las diferencias μ del campo de inducción magnética en la perforación con respecto al de la caja. Como ilustración, considérese el valor específico $|m+\mu| = 0.2$ común a $m+\mu = -0.2$ y $m+\mu = 0.2$. El valor negativo puede obtenerse a partir de las siguientes combinaciones (m,μ) : $(0,-0.2),(-1,.8),(1,-1.2),(-2,1.8),(2,-2.2),...$ y el valor positivo a partir de: $(0,0.2),(-1,1.2),(1,-.8),(-2,2.2),(2,-1.8),...$ Todos ellos tienen el valor común de ν_s obtenido a partir de la ecuación (5.9) con $|m+\mu| = 0.2$ y, como ya se estableció, las energías para los estados con el valor negativo de $(m+\mu)$ es la entrada en la columna impar, y la energía para los estados con valores positivos de $(m+\mu)$ es dos veces este valor de arriba. La generalización de este resultado es

$$E^{\mathrm{T}}_{sm}(m+\mu) \quad = \quad E^{\mathrm{T}}_{s,m+N}\left[(m+N) \ + \ (\mu-N)\right] \tag{5.12}$$

con $N = 0,1,2,...$ expresando la repetición periódica de los niveles de energía de Landau del electrón en la caja anular cuando el flujo magnético en la perforación cambia por un fluxón, acompañado por un cambio compensatorio de una unidad en el número cuántico de momento angular. Este comportamiento se ilustra gráficamente en las Figs. 5a y 5b para las cajas con perforaciones grandes y pequeñas.

Para $\mu = 0$, los niveles de energía coinciden con los de la Fig. 4a y la tercer columna de la Tabla 4. Conforme μ se incrementa a partir de su valor inicial, los estados con cero y valores positivos de m incrementan sus energías, mientras que los estados con valores negativos de m decrecen sus energías; los estados de energía $s=1$, $m=-1$ alcanzan su valor mínimo para $\mu \approx 0.5$ en la Fig. 5a y $\mu \approx 0.8$ en la Fig. 5b. Cuando μ alcanza el valor de 1, se lleva a cabo la primera repetición periódica de la ecuación (5.12) con $N = 1$, y continúa conforme μ se sigue incrementando. Por otra parte, conforme μ decrece desde cero, los estados con cero y valores positivos de m decrecen sus energías, y los estados con valores negativos de m incrementan sus energías; el estado $s = 1$, $m = 0$ alcanza su valor mínimo para $\mu \approx -0.5$ en la Fig. 5a y $\mu \approx -0.2$ en la Fig. 5b. Cuando μ alcanza el valor -1, se lleva a cabo la primera repetición periódica de la ecuación (5.12) con $N = -1$, y continúa conforme μ sigue decreciendo moviéndose hacia la izquierda en la gráfica. Al dibujar la curva de energía $E_{10}(\mu)$ a partir de los datos de la Tabla 5, las otras curvas para E^{T}_{sm} se obtienen a partir de las translaciones horizontales de esa curva por m unidades, hacia la derecha para m negativa y hacia la izquierda para m positiva. Aquí se ha ilustrado el efecto Aharonov-Bohm en los Estados de Landau para los niveles de energía con $s = 1$, pero en general se conserva para cualesquier estados sm , como se expresa en la ecuación (5.12).

En conclusión, esta tesis ha presentado un análisis del efecto de confinamiento en cajas cilíndricas anulares sobre los Estados de Landau, y del efecto Aharonov-Bohm sobre tales estados. Dicho análisis dio origen a uno de nuestros artículos, E. Ley-Koo, G. Villa-Torres and D. Kouznetsov, "Aharonov-Bohm effect on Landau States in Annular Cylindrical Boxes", *Chinese Journal of Physics*, Vol. 40, No 2(2002)130-141. La característica de los Estados de Landau en el primer sistema se manifiesta a través de las energías más altas de los estados con m positiva y las energías más bajas de los estados con m negativa, incluyendo la evolución de sus degeneraciones conforme las cajas se hacen más grandes. El efecto Aharonov-Bohm se manifiesta a través de la repetición periódica del espectro de energía como una función de la variación del flujo magnético en la perforación de la caja con los cambios correspondientes en el número cuántico angular de los Estados de Landau, y con un período de un fluxón.

TABLA 4. Números cuánticos radial s y de momento angular m , y eigenvalores de la energía transversal $E^{\mathrm{T}}_{s,m}$ en unidades $\hbar\omega$ para un electrón confinado en cajas con $\mathrm{b} = 2\mathrm{a}, 5\mathrm{a}$ y $10\mathrm{a}$, en campos de inducción magnética definidos por el parámetro de flujo magnético adimensional $m_e\omega \mathrm{b}^2/\hbar$.

$m_e\ \omega\ \mathrm{b}^2\ /\ \hbar$		1	1	1	15	15	15
$m_e\ \omega\ \mathrm{a}^2\ /\ \hbar$		0.25	0.04	0.01	3.75	0.6	0.15
s	m	E^{T}_{sm}	E^{T}_{sm}	E^{T}_{sm}	E^{T}_{sm}	E^{T}_{sm}	E^{T}_{sm}
1	0	19.79178	7.46920	5.65108	5.33410	2.46994	1.91268
	-1	19.72188	8.16592	6.94048	4.40352	1.76000	1.23668
	+1	21.72188	10.16592	8.94048	6.40352	3.76000	3.23668
	-2	21.50142	11.84566	11.42684	3.61104	1.29718	1.03460
	+2	25.50142	15.84566	15.42684	7.61104	5.29718	5.03460
	-3	25.09870	17.67902	17.58700	2.95458	1.09156	1.00632
	+3	31.09870	23.67902	23.58700	8.95458	7.09156	7.00632
	-4	30.46266	25.06046	25.04484			
	+4	38.46266	33.06046	33.04484			
	-5	37.52606	33.74222	33.73996			
	+5	47.52606	43.74222	43.73996			
2	0	79.00098	30.51030	23.69370	9.06064	5.06776	4.16546
	-1	78.98152	31.64624	26.04792	8.72414	4.21142	3.41790
	+1	80.98152	33.64624	28.04792	10.72414	6.21142	5.41790
	-2	80.92192	36.95496	33.94736	7.91474	3.63896	3.11796
	+2	84.92192	40.95496	37.94736	11.91474	7.63896	7.11796
	-3	84.82974	45.94932	44.86382	7.23292	3.33512	3.09164
	+3	90.82974	51.94932	50.86382	13.23292	9.33512	9.09164
3	0	177.69628	69.02626	54.02880	16.23734	7.82040	6.05602
	-1	177.78674	70.32580	56.94516	15.30200	6.95948	5.74480
	+1	179.78674	72.32580	58.94516	17.30200	8.95948	7.74480
	-2	179.66006	76.24628	67.07614	14.49612	6.38078	5.44980
	+2	183.66006	80.24628	71.07614	18.49612	10.38078	9.44980
	-3	183.62184	86.71936	82.07110	13.82010	6.09200	5.53434
	+3	189.62184	92.71936	88.07110	19.82010	12.09200	11.53434

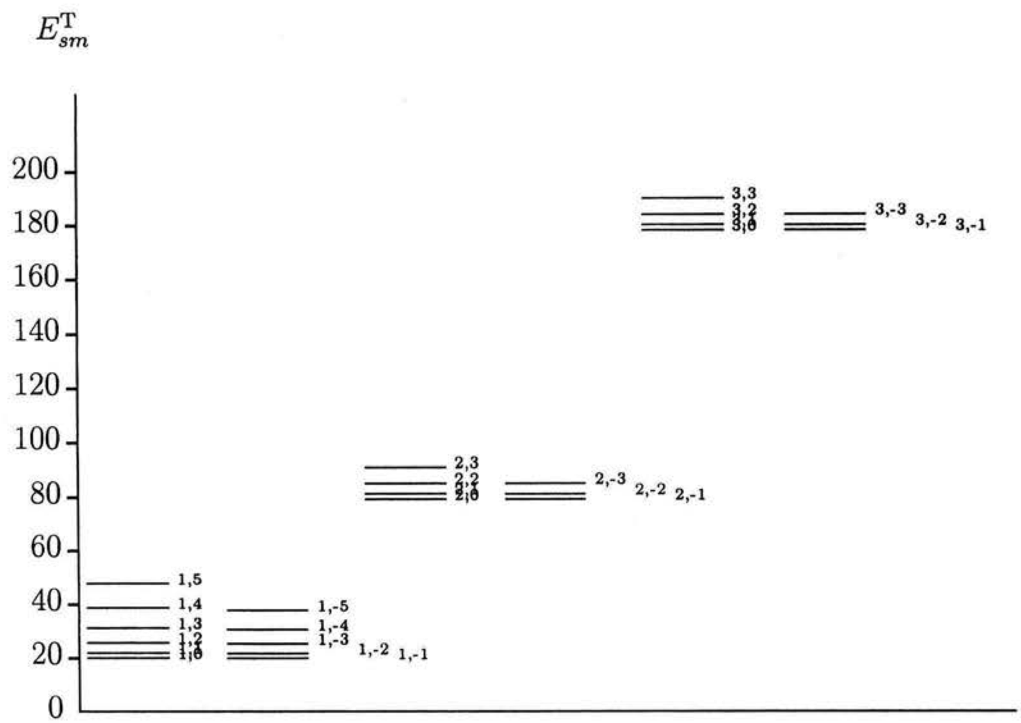

FIGURA 4a Los niveles de energía de Landau más bajos E_{sm}^{T} para un electrón confinado en una caja con $m_e\omega \mathrm{b}^2/\hbar = 1$ y $m_e\omega \mathrm{a}^2/\hbar = 0.25$

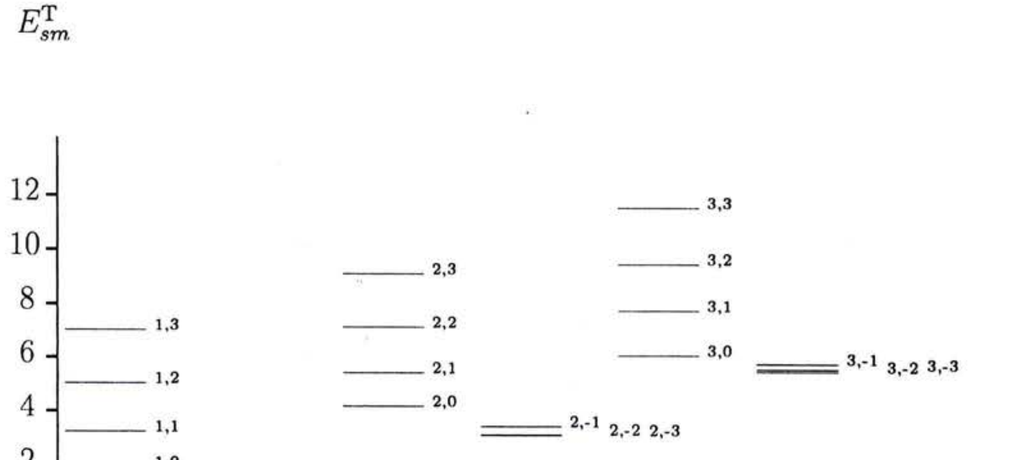

FIGURA 4b Los niveles de energía de Landau más bajos E^{T}_{sm} para un electrón confinado en una caja con

$m_e\omega \mathrm{b}^2/\hbar = 15$ y $m_e\omega \mathrm{a}^2/\hbar = 0.15$

TABLA 5. Eigenvalores de la energía transversal $E^{\mathrm{T}}_{1,m}$ como función del parámetro $m+\mu$, ecuación (5.10), para el electrón confinado en cajas con $m_e\omega \mathrm{b}^2/\hbar = 1$ y los valores indicados de $m_e\omega \mathrm{a}^2/\hbar$ y signos de $m+\mu$.

$m_e\omega \mathrm{a}^2/\hbar$	0.25		0.04		0.01	
$m+\mu$	$-$	$+$	$-$	$+$	$-$	$+$
$\lvert m+\mu\rvert$	E^{T}_{1m}	E^{T}_{1m}	E^{T}_{1m}	E^{T}_{1m}	E^{T}_{1m}	E^{T}_{1m}
0.0	19.79178	19.79178	7.46920	7.46920	5.65108	5.65108
0.2	19.62901	20.02901	7.33859	7.73859	5.54960	5.94960
0.4	19.54074	20.34074	7.34598	8.14598	5.64130	6.44130
0.6	19.52680	20.72680	7.48904	8.68904	5.91518	7.11518
0.8	19.58724	21.18724	7.76399	9.36399	6.35476	7.95476
1.0	19.72188	21.72188	8.16592	10.16592	6.94048	8.94048
1.2	19.93154	22.33154	8.68844	11.08844	7.65207	10.05207
1.4	20.21310	23.01310	9.32507	12.12507	8.47078	11.27078
1.6	20.56924	23.76924	10.06840	13.26840	9.38064	12.58064
1.8	20.99979	24.59979	10.91102	14.51102	10.36910	13.96910
2.0	21.50142	25.50142	11.84566	15.84566	11.42684	15.42684
2.2	22.09683	26.49683	12.86538	17.26538	12.54727	16.94727
2.4	22.72467	27.52467	13.96385	18.76385	13.72597	18.52597
2.6	23.44452	28.64452	15.13541	20.33541	14.95999	20.15999
2.8	24.23603	29.83603	16.37518	21.97518	15.24742	20.84742
3.0	25.09870	31.09870	17.67902	23.67902	17.58700	23.58700
3.2	26.03209	32.43209	19.04350	25.44350	18.97790	25.37790
3.4	27.03570	33.83570	20.46588	27.26588	20.41952	27.21952
3.6	28.10905	35.30905	21.94392	29.14392	21.91144	29.11144
3.8	29.25156	36.85156	23.47590	31.07590	23.45330	31.05330
4.0	30.46266	38.46266	25.06046	33.06046	25.04484	33.04484
4.2	31.74178	40.14178	26.69655	35.09655	26.76582	35.16582
4.4	33.08831	41.88831	28.38334	37.18334	28.37600	37.17600
4.6	34.50163	43.70163	30.12020	39.32020	30.11521	39.31521
4.8	35.98110	45.58110	31.90662	41.50662	31.90325	41.50325
5.0	37.52606	47.52606	33.74222	43.74222	33.73996	43.73996

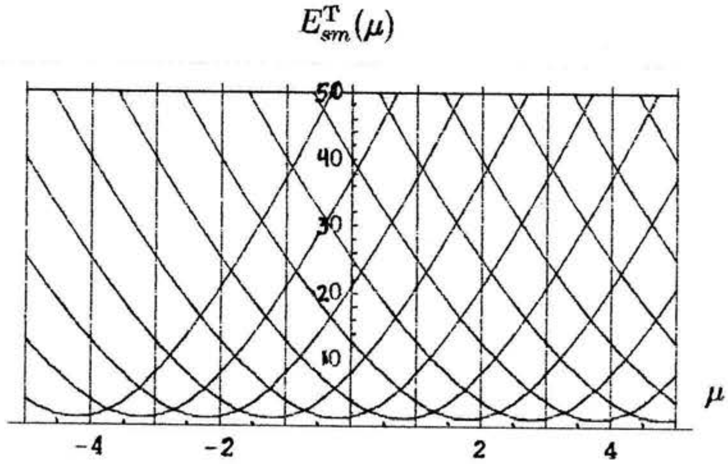

FIGURA 5a. Se ilustra el efecto Aharonov-Bohm sobre los niveles de energía de Landau $E^{\mathrm{T}}_{sm}(\mu)$ a través de su dependencia periódica en el cambio de flujo magnético μ en la perforación de una caja cilíndrica anular con $m_e\omega \mathrm{b}^2/\hbar = 1$ y $m_e\omega \mathrm{a}^2/\hbar = 0.25$

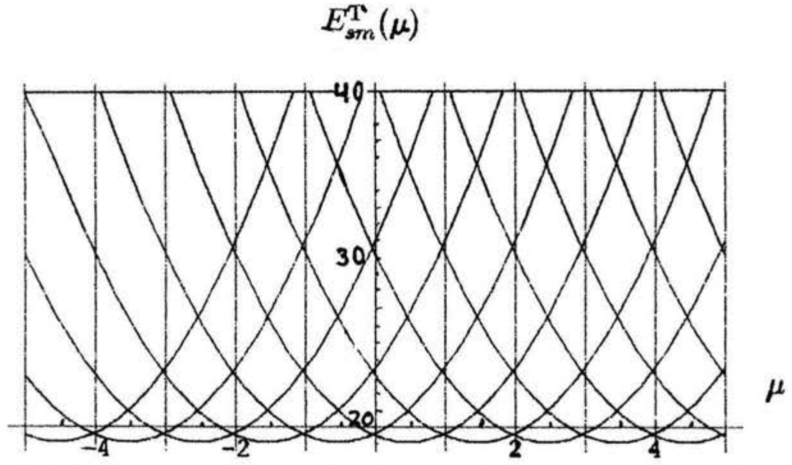

FIGURA 5b. Se ilustra el efecto Aharonov-Bohm sobre los niveles de energía de Landau $E^{T}_{sm}(\mu)$ a través de su dependencia periódica en el cambio de flujo magnético μ en la perforación de una caja cilíndrica anular con $m_e\omega b^2/\hbar = 1$ y $m_e\omega a^2/\hbar = 0.01$

Capítulo 6. DISCUSION Y CONCLUSIONES.

6.1 Discusión.

El efecto Aharonov-Bohm se manifiesta en las eigenfunciones del electrón confinado para valores definidos de la inducción magnética en la perforación, y todo se explica a partir de los cambios del potencial electromagnético en situaciones estacionarias, pero también puede analizarse desde un punto de vista dinámico. Considérese el paso de una configuración estacionaria a otra (por ejemplo, las configuraciones descritas en los capítulos 2 a 3 ó 4 a 5). El paso entre estas configuraciones se puede ver en términos del cambio en el tiempo del campo de inducción magnética, el cual implica un cambio en el tiempo del campo vectorial magnético. También el cambio en el tiempo del campo de inducción magnética en la perforación es claro que implica un cambio en el tiempo del flujo magnético en la perforación; entonces, por la ley de inducción electromagnética de Faraday, esto implica que en la región de la caja vecina al solenoide, en el paso de la situación inicial a la final, se tenga una fuerza electromotriz inducida y en consecuencia un campo de intensidad eléctrica, que a su vez es proporcional al cambio en el tiempo del potencial vectorial magnético. Así entonces, el cambio en el tiempo de la inducción magnética en la perforación, se traduce en una fuerza en la dirección azimutal sobre la carga. En conclusión, esta fuerza eléctrica es la responsable del cambio en la energía del sistema; y su efecto integrado depende exclusivamente del cambio en el potencial vectorial magnético, y es también, desde luego, el cambio en la cantidad de movimiento de interacción. Por tanto, $\vec{A}$ tiene realidad operacional y es más que un recurso matemático. El efecto Aharonov-Bohm podría ser clásicamente utilizado para medir $\vec{A}$ y definirlo operacionalmente.

6.2 Conclusiones.

En esta tesis se analiza el efecto Aharonov-Bohm sobre los estados del electrón libre dentro de una caja cilíndrica anular, al comparar los problemas planteados y resueltos en los Capítulos 2 y 3 : a) en ausencia de cualquier campo de inducción magnética o campo de potencial magnético, tanto en la caja como en la perforación; y b) en presencia de campo de inducción magnética uniforme, axial, centrado y confinado en la perforación.

En la solución de la ecuación de Schrödinger de cada problema, se obtiene que las eigenfunciones de los operadores Hamiltonianos tienen en común las funciones angular y axial; y las funciones radiales que son funciones de Bessel, son diferentes en su orden m y $m + \nu$, respectivamente, donde ν es el flujo magnético en la perforación. El cambio en el espectro de energía, conforme cambia el flujo magnético dentro de la perforación, muestra la influencia del potencial vectorial magnético $\vec{A}$ sobre los estados del electrón. El espectro de energía muestra periodicidad con período 1, y simetría con respecto a los valores semienteros de ν .

Por otra parte, se analiza también el efecto sobre los Estados de Landau del electrón en la caja, en la comparación de los problemas planteados y resueltos en los Capítulos 4 y 5: c) en presencia de campo de inducción magnética uniforme y axial de la misma magnitud en la caja y en la perforación; y d) considerando un campo de inducción magnética en la caja, pero cambiando el campo en la perforación.

Similarmente, las funciones angular y axial son comunes en la solución de la ecuación de Schrödinger de cada problema. Las funciones radiales, que son funciones Hipergeométricas Confluentes, de entrada son diferentes en términos de m y de $m+\mu$, respectivamente, donde μ es el cambio de flujo magnético en la perforación. La influencia del potencial vectorial magnético $\vec{A}$ sobre los estados del electrón, se manifiesta en el cambio del espectro de energía, al variar el cambio de flujo magnético dentro de la perforación. Sin embargo, el espectro de energía para los estados de Landau, aunque también muestra periodicidad 1, no es simétrico.

REFERENCIAS

[1] Aharonov Y. and Bohm D., *Phys. Rev.* **115**(1959)485-491.

[2] Chambers R.G., *Phys. Rev. Lett.* **5**(1960)3-5.

[3] Feynman R.P., Leighton R.B., and Sands M., The Feynman Lectures (Addison- Wesley, Palo Alto, CA, 1965), Cap. 15 Vol III, Cap 21.

[4] Konopinski E.J., *Am. J. Phys.* **46**(1978)499-502.

[5] Peshkin M. and Tonomura A., "The Aharonov-Bohm Effect". Springer-Verlag, Berlin Heidelber (1989)10.

[6] Ballentine L., "Quantum Mechanics". Prentice Hall, Englewood Cliff, N.J. (1990)222.

[7] Landau, L.D., Z. Phys. **64**(1930)629.

[8] Laughlin

[9] Fung, M.K. and Wang, Y.F., Chin. J. Phys. **37**(1999)435.

[10] Abramowitz M. and Stegun I., *Hand book of Mathematical Functions.* Dover, N.Y. (1965) Chapter 9.

[11] Press W.H., Teukolsky S.A., Vitterling W.T. and Flannery B.P., *Numerical Recipes in C. The Art of Scientific Computing.* U.P. Cambridge N.Y., U.S.A. (1992) Chapter 9.

[12] Kumagai M. and Ohno T., *Solid State Commun.* **83**(1992)837-841.

[13] Sakurai J.J., *Advanced Quantum Mechanics.* Addison-Wesley, Reading MA (1967)11,14-16 y 41-44.

[14] Sakurai J.J. and Tuan S.F., Modern Quantum Mechanics. Addison-Wesley, Reading, MA (1994)130-136 y 338.

[15] Webb R.A., Washburn S., Umbach C.P. and Leibowitz R.B., *Phys. Rev. Lett.* **83**54(1985)2696.

[16] Timp G. *et al., Phys. Rev. Lett.* **58**(1987)2814.

[17] Ford C.J.B. *et al., Phys. Rev.* **B43**(1991)7339.

[18] Landau, L.D. and Lifshitz, I.M. Quantum Mechanics.

[19] Gottfried K., Quantum Mechanics. *Benjamin/Cummings Publishing Company* (1979).

[20] Mathematica 3.0 Wolfram Research, Inc.

[21] D. Kouznetsov, E. Ley-Koo and G. Villa-Torres, "Aharonov-Bohm effect on the bound states of an electron inside an annular cylindrical box", *Rev. Mex. Fís.* **45**(1999)485.

[22] E. Ley-Koo and G. Villa-Torres, "Clasical analysis of the Aharonov-Bohm effect", *Rev. Mex. Fís.* **47**(6)(2001)576-581.

[23] E. Ley-Koo, G. Villa-Torres and D. Kouznetsov. "Aharonov-Bohm effect on Landau States in Annular Cylindrical Boxes". *Chinese Journal of Physics* Vol. 40, No 2(2002)130-141.

Aharonov-Bohm effect on the bound states of an electron inside an annular cylindrical box

D. Kouznetsov
Hopelchen 353 L13, Colonia Torres de Padierna, 14200 México, D.F. México

E. Ley-Koo and G. Villa-Torres
Instituto de Física, Universidad Nacional Autónoma de México
Apartado postal 20-364, 01000 México, D.F., Mexico

Recibido el 16 de marzo de 1999; aceptado el 1 de julio de 1999

We solve the Schröedinger equation for an electron inside an annular cylindrical box in two situations: *i)* in the absence of any fields, and *ii)* in the presence of a uniform, axial magnetic induction field confined and centered in the perforation. The Aharonov-Bohm effect on the bound states of the electron is exhibited through the analysis of the dependence of the energy eigenvalues and eigenfunctions on the enclosed magnetic flux. The results of this study serve to illustrate the roles of the magnetic vector potential and the gauge transformations in quantum mechanics.

Keywords: Magnetic vector potential in quantum mechanics

Se resuelve la ecuación de Schröedinger para un electrón en el interior de una caja anular cilíndrica en dos situaciones; *i)* en ausencia de cualquier campo, y *ii)* en presencia de un campo de inducción magnética axial y uniforme confinado y centrado en la perforación. Se exhibe el efecto Aharonov-Bohm sobre los estados ligados del electrón a través del análisis de la dependencia de los eigenvalores de la energía y las eigenfunciones con respecto al flujo magnético encerrado. Los resultados de este estudio sirven para ilustrar los papeles del potencial vectorial magnético y las transformaciones de norma en mecánica cuántica.

Descriptores: Potencial vectorial magnético en mecánica cuántica

PACS: 03.65

1. Introduction

It is almost forty years since Aharonov and Bohm analyzed the significance of the electromagnetic vector potential in quantum theory, and suggested an experiment to test for the effect of the potential in regions where there are no magnetic fields [1]. They predicted that the fringe pattern in an electron interference experiment should be shifted by altering the amount of magnetic flux passing between two beams, even though the beams themselves pass only through field-free regions. Specifically, a shift of ν fringes is associated with an enclosed flux of $\nu hc/e$, where the natural unit of flux or fluxon, $hc/e = 4.135 \times 10^{-7}$ gauss $\cdot$ cm^2, is determined by the Planck constant h, the velocity of light c, and the electron's electric charge e. Within a year, Chambers performed such an experiment reporting the expected shifts of an electron interference pattern by the corresponding magnetic fluxes, including situations in which the pattern appears unchanged due to their association with magnetic fluxes of an integer number of fluxons [2].

It is also twenty years since two didactic articles on related topics were published [3, 4]. In the first one, Konopinski discussed the explicit physical meaning and direct measurability of the electromagnetic vector potential in the classical context. And in the second one, Kobe deduced Maxwell's equations from the gauge invariance of quantum mechanics. Konopinski's book on electromagnetism [5] and Sakurai's books on quantum mechanics [6, 7] contain more detailed treatments of these topics.

Bound state versions of the Aharonov-Bohm effect have also been discussed in the literature [8, 9]. In the specialized book of Peshkin and Tonomura [8], the first author illustrated the effect for the charged rotator in a plane, and pointed out that there are no important changes if the motion is allowed to be three-dimensional inside a torus. In Ballentine's book [9] the charged particle confined to the interior of a torus of rectangular cross-section is also used to recognize that the energy of the stationary states must depend on the magnetic flux in the perforation. In both references the respective authors considered that the detailed quantitative analysis of the problem was not necessary for their purposes.

This paper presents a bound state version of the Aharonov-Bohm effect through the study of the energy spectra and eigenfunctions of an electron inside an annular cylindrical box in two comparative situations: *i)* in the absence of any fields, and *ii)* in the presence of a uniform, axial magnetic induction field confined and centered in the perforation with its associated magnetic vector potential in the interior of the box. In Sect. 2, the reference problem of situation *i)* is formulated and solved for the electron inside a box defined in cylindrical coordinates ($a \leq \rho \leq b$, φ, $0 \leq z \leq L$). Section 3 contains the formulation and solution of the Aharonov-

Bohm problem involving a magnetic induction field $\vec{B} = \hat{k}B$ confined in $(0 < \rho < \rho_0 \leq a,\ \varphi,\ z)$ and the magnetic vector potential $\vec{A} = \hat{\varphi}B\rho_0^2/2\rho$ inside the box. Section 4 presents illustrative numerical and graphical results of the solutions for the energy eigenvalues and eigenfunctions as the magnetic flux enclosed inside the perforation, $\nu = (B\pi\rho_0^2)/(hc/e)$, is changed. Section 5 contains a discussion of the Aharonov-Bohm effect on the bound states with emphasis on the symmetry and periodicity of the energy spectra as functions of ν, including the degeneraces for integer and half-integer values.

2. The electron inside an annular cylindrical box

The Schröedinger equation for the electron inside an annular cylindrical box in cylindrical coordinates,

$$-\frac{\hbar^2}{2m_e}\left[\frac{1}{\rho}\frac{\partial}{\partial\rho}\rho\frac{\partial}{\partial\rho} + \frac{1}{\rho^2}\frac{\partial^2}{\partial\varphi^2} + \frac{\partial^2}{\partial z^2}\right]\psi(\rho,\varphi,z) = E\psi(\rho,\varphi,z), \quad (1)$$

must be solved subject to the boundary condition that the wavefunction vanishes at the positions of the walls of the box:

$$\psi(\rho = a,\varphi,z) = \psi(\rho = b,\varphi,z) = 0, \quad (2a)$$

$$\psi(\rho,\varphi,z) = \psi(\rho,\varphi + 2\pi,z), \quad (2b)$$

$$\psi(\rho,\varphi,z = 0) = \psi(\rho,\varphi,z = L) = 0. \quad (2c)$$

Equation (1) is known to admit the separable solution

$$\psi(\rho,\varphi,z) = R(\rho)\Phi(\varphi)Z(z), \quad (3)$$

in which the respective factors satisfy the ordinary differential equations

$$\frac{\mathrm{d}^2 Z(z)}{\mathrm{d}z^2} = -k_L^2 Z(z), \quad (4a)$$

$$\frac{\mathrm{d}^2\Phi(\varphi)}{\mathrm{d}\varphi^2} = -m^2\Phi(\varphi), \quad (4b)$$

$$\left[\frac{1}{\rho}\frac{\mathrm{d}}{\mathrm{d}\rho}\rho\frac{\mathrm{d}}{\mathrm{d}\rho} - \frac{m^2}{\rho^2}\right]R(\rho) = -k_T^2 R(\rho), \quad (4c)$$

and the energy eigenvalue is the sum of the transverse and longitudinal contributions,

$$E = \frac{\hbar^2}{2m_e}(k_T^2 + k_L^2). \quad (5)$$

The solutions of Eq. (4a) subject to the boundary conditions of Eq. (2c) are

$$Z(z) = \sqrt{\frac{2}{L}}\sin\frac{n\pi z}{L}, \qquad n = 1,2,3,\ldots \quad (6)$$

The solutions of Eq. (4b) are the eigenfuctions of the z-component of the orbital angular momentum,

$$\Phi(\varphi) = \frac{e^{im\varphi}}{\sqrt{2\pi}}, \qquad m = 0,\pm1,\pm2,\ldots \quad (7)$$

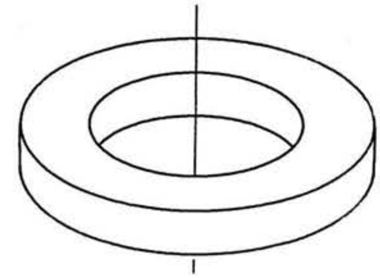

FIGURE 1. Annular cylindrical box with inner radius a, outer radius b and height L. A uniform axial magnetic induction field is applied and centered in the perforation.

Equation (4c) is recognized as the Bessel equation and its general solution is the linear combination of the ordinary Bessel function and the Neumann function [10],

$$R(\rho) = \mathcal{A}_m J_m(k_T\,\rho) + \mathcal{B}_m Y_m(k_T\,\rho), \quad (8)$$

since m is an integer, Eq. (7). The boundary conditions of Eqs. (2a) on this solution are expressed by

$$\mathcal{A}_m J_m(k_T a) + \mathcal{B}_m Y_m(k_T a) = 0, \quad (9a)$$

$$\mathcal{A}_m J_m(k_T b) + \mathcal{B}_m Y_m(k_T b) = 0. \quad (9b)$$

This is a set of two algebraic homogeneous linear equations for the unknown coefficients $\mathcal{A}_m$ and $\mathcal{B}_m$, which admits non-trivial zero solutions only if its determinant vanishes, *i.e.*,

$$J_m(k_T a)Y_m(k_T b) - J_m(k_T b)Y_m(k_T a) = 0. \quad (10)$$

This transcendental equation has to be solved numerically to obtain the transverse wave number k_T. The task is accomplished by using numerical recipes in C [11]. Let $k_T a = x_{ms}$ be the successive solutions $s = 1,2,3,\ldots$, for given values of a and b. The energy eigenvalues of Eq. (5) with the explicit values of the wavenumbers from Eqs. (5) and (10) are given by

$$E_{msn} = \frac{\hbar^2}{2m_e}\left(\frac{x_{ms}^2}{a^2} + \frac{n^2\pi^2}{L^2}\right), \quad (11)$$

in terms of the azimuthal m, radial s and axial n quantum numbers.

The ratio of the coefficients $\mathcal{A}_m$ and $\mathcal{B}_m$ follows from Eq. (9a) or Eq. (9b), and it allows to write the normalized radial eigenfuction, Eq. (8), as

$$R_{ms}(\rho) = \frac{1}{\sqrt{\mathcal{N}_{ms}}}\left[Y_m\left(\frac{x_{ms}b}{a}\right)J_m\left(\frac{x_{ms}\rho}{a}\right) - J_m\left(\frac{x_{ms}b}{a}\right)Y_m\left(\frac{x_{ms}\rho}{a}\right)\right], \quad (12)$$

where the normalization constant is

$$\mathcal{N}_{ms} = \int_a^b \left[Y_m\left(\frac{x_{ms}b}{a}\right)J_m\left(\frac{x_{ms}\rho}{a}\right) - J_m\left(\frac{x_{ms}b}{a}\right)Y_m\left(\frac{x_{ms}\rho}{a}\right)\right]^2 \rho\,\mathrm{d}\rho. \quad (13)$$

The problem of this section has also been studied in the specialized research literature [12].

3. Aharonov-Bohm effect on the bound states of the electron

In this section we formulate and solve the problem with the magnetic induction field confined in the perforation of the annular box and its associated magnetic vector potential inside the box. The Hamiltonian for the system is given by the minimal coupling prescription

$$\hat{H} = \frac{(\hat{\vec{p}} + \frac{e}{c}\vec{A})^2}{2m_e}, \tag{14}$$

in which $\hat{\vec{p}} = -i\hbar\nabla$ is the "conjugate" momentum and the second term is the negative of the "potential momentum" of the electron in the magnetic vector potential [3, 5]. Then the Schödinger equation can be written as

$$\left\{ -\frac{\hbar^2}{2m_e}\frac{1}{\rho}\frac{\partial}{\partial\rho}\rho\frac{\partial}{\partial\rho} + \frac{\left(\ell_z + \frac{eB\rho_o^2}{2c}\right)^2}{2m_e\rho^2} - \frac{\hbar^2}{2m_e}\frac{\partial^2}{\partial z^2}\right\}\psi(\rho,\varphi,z) = E\psi(\rho,\varphi,z). \tag{15}$$

Comparison of Eqs. (1) and (15) shows that they share the same radial and longitudinal contributions to the kinetic energy, and their difference resides in the extra term arising from the magnetic vector potential and added to the z-component of the angular momentum

$$\frac{eB\pi\rho_0^2}{2\pi c} = \hbar\nu, \tag{16}$$

where ν is the magnitude of the magnetic flux in the perforation in the units hc/e. Equation (15) also admits a separable solution of the same form as Eq. (3). Equations (4a) and (6) for the longitudinal eigenfunctions continue to be valid. The eigenfunctions of the z-component of the angular momentum of Eq. (7) are also eigenfunctions of the angular operator of Eq. (15):

$$(\hat{\ell}_z + \hbar\nu)\Phi_m(\varphi) = \hbar(m+\nu)\Phi_m(\varphi). \tag{17}$$

Then the radial part of Eq. (15) becomes

$$\left[\frac{1}{\rho}\frac{\mathrm{d}}{\mathrm{d}\rho}\rho\frac{\mathrm{d}}{\mathrm{d}\rho} - \frac{(m+\nu)^2}{\rho^2}\right]R(\rho) = -k_{\mathrm{T}}^2\,R(\rho). \tag{18}$$

Comparison of the radial Eqs. (4c) and (18) shows that they are of the same type with the difference in their parameters,

$$m \longrightarrow M = m + \nu. \tag{19}$$

While the values of m are restricted to be integers, Eq. (7), the values of M can vary continuously following the corresponding variations of the magnetic flux ν. The solution of the radial Eq. (18) follows the same steps of Eqs. (8)–(13) with the substitution of m by M of Eq. (19).

It is also important to recognize that while the eigenstates of Eq. (4c) given by Eq. (12) are doubly degenerate for $m = \pm 1, \pm 2, \ldots$, such a degeneracy is removed when there is magnetic flux in the perforation, since the corresponding parameters from Eq. (19), $M = |m| + \nu$ and $M = -|m| + \nu$ are different. On the other hand, starting from given values of m and ν there are an infinite number of combinations of successive values of such parameters,

$$M = m + \nu = (m - N) + (\nu + N), \qquad N = 0, \pm 1, \pm 2, \pm 3, \ldots \tag{20}$$

consistent with the same value of M. The different states for the different magnetic fluxes have the same energies, which translates into a periodic repetition of the energy spectrum as the magnetic flux increases by one unit. In particular, the energy spectra for $\nu = 1, 2, 3, \ldots$ are the same as for $\nu = 0$ including ground states with $m = -1, -2, -3, \ldots$ and excited doubly degenerate states with $m = 0$ and -2, 1 and -3, 2 and $-4, \ldots$; -1 and -3, 0 and -4, 1 and $-5, \ldots$; -2 and -4, -1 and -5, 0 and $-6, \ldots$; $\ldots$; respectively. By considering the interval $0 < \nu < 1$, and the states with $m = |m|$ and $-|m| - 1$, we identify the common value of

$$M = |m| + \nu \quad \text{and} \quad -M = -(|m| + 1) + (1 - \nu), \tag{21}$$

leading to the same values of the transverse energies. Notice that the states involved are neighbour states in the angular momentum quantum number and have the same energy for complementary values of the magnetic flux, ν and $1 - \nu$. The net result is that the energy of the $|m|$-state increases monotonically as ν changes between 0 and 1, while the energy of the $(-|m| - 1)$-state also increases monotonically in the same way as $1 - \nu$ changes between 0 and 1. In other words, the latter decreases monotonically as ν changes between 0 and 1. For $\nu = 0.5$ both states have the same energy for the common value of the magnetic flux, producing another situation of double degeneracy. The respective energy curves are symmetric relative to the line $\nu = 0.5$.

4. Illustrative numerical and graphical results

In this section we present some quantitative results illustrating the solutions of the eigenvalue problems formulated in Sects. 2 and 3. The emphasis is on the transverse contribution to the energy eigenvalues and the associated radial eigenfunctions. The numerical results are contained in tables and figures for both cases $\nu = 0$ and $\nu \neq 0$ together.

Figure 2 is a graph of the determinant appearing in Eq. (10)

$$D_M(x) = J_M(x)Y_M\left(\frac{bx}{a}\right) - Y_M(x)J_M\left(\frac{bx}{a}\right), \tag{22}$$

as a function of $x = k_{\mathrm{T}}a$ for different values of the parameter M, Eq. (19), and for the specific case of $b = 2a$. Its zeros x_{Ms}, determined through the corresponding program of [11], are contained in Table I.

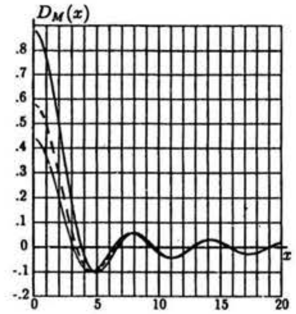

FIGURE 2. Graph of the determinant $D_M(x)$ of Eq. (22) for $M = 0$ (thin line), 1.9 (dashed line) and 3.14 (solid line), and $b = 2a$. Its zeros determine the transverse wave number and the energy eigenvalues according to Eqs. (10) and (11).

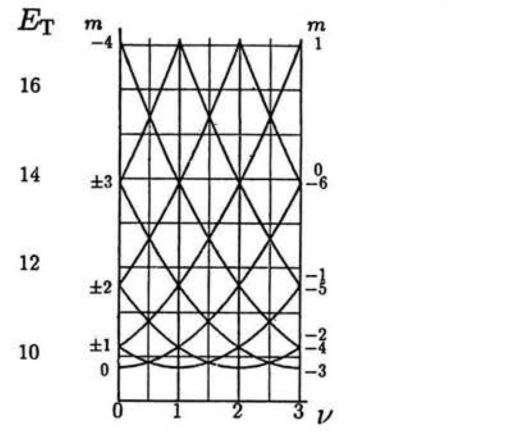

FIGURE 3. Transverse energy eigenvalues E_T in units $\hbar^2/2m_ea^2$ as functions of the magnetic flux ν in units ch/e, for states with the lowest angular excitations $m = 0, \pm1, \pm2, \ldots$ and no radial excitation $s = 1$, and $b = 2a$.

TABLE I. Zeros of Eq. (22) x_{Ms} for different values of M and s, and $b = 2a$. Their squares correspond to the transverse energy eigenvalues, Eq. (11).

$M \setminus s$	1	2	3	4
0.0	3.12303	6.27344	9.41821	12.56142
0.2	3.12601	6.27500	9.41926	12.56221
0.4	3.13492	6.27968	9.42241	12.56459
0.6	3.14972	6.28747	9.42767	12.56855
0.8	3.17031	6.29837	9.43502	12.57408
1.0	3.19658	6.31235	9.44447	12.58120
1.2	3.22836	6.32940	9.45600	12.58990
1.4	3.26550	6.34950	9.46961	12.60017
1.6	3.30778	6.37261	9.48530	12.61201
1.8	3.35500	6.39871	9.50305	12.62541
2.0	3.40692	6.42777	9.52285	12.64038
2.2	3.46332	6.45974	9.54470	12.65691
2.4	3.52396	6.49458	9.56857	12.67499
2.6	3.58859	6.53226	9.59447	12.69461
2.8	3.65697	6.57272	9.62236	12.71578
3.0	3.72887	6.61592	9.65225	12.73848
3.2	3.80406	6.66181	9.68410	12.76271
3.4	3.88231	6.71033	9.71791	12.78846
3.6	3.96342	6.76144	9.75365	12.81572
3.8	4.04716	6.81507	9.79131	12.84449
4.0	4.13337	6.87116	9.83086	12.87474
4.2	4.22183	6.92967	9.87230	12.90649
4.4	4.31239	6.99054	9.91559	12.93971
4.6	4.40488	7.05369	9.96072	12.97440
4.8	4.49914	7.11908	10.00766	13.01055
5.0	4.59502	7.18665	10.05639	13.04814

Figure 3 shows the energy levels of the states with lowest angular excitations $m = 0, \pm1, \pm2, \ldots$ and no radial excitation $s = 1$, as functions of the magnetic flux ν in the perforation. According to Eq. (11) and its extension for the case $\nu \neq 0$, the energy levels correspond to the squares of the zeros of Table I, x_{Ms}^2, in units of $\hbar^2/(2m_ea^2)$. The reader may appreciate the periodicity of the energy spectra as ν changes by one unit, the double degeneracy of the states for integer and half-integer values of ν, and the symmetry of the energy curves within each unit interval of ν under reflection with respect to the line with the corresponding half-integer value of ν.

TABLA II. Transverse wavenumbers $k_T = x_{Ms}/a$ and coefficients of normalized radial eigenfunction $\mathcal{A}_{Ms}$ and $\mathcal{B}_{Ms}$, Eqs. (8) and (12), for different values of M and s, and $b = 2a$.

M	s	x_{Ms}	$\mathcal{A}_M$	$\mathcal{B}_M$
0	1	3.123039	1.18538	1.37124
	2	6.273439	1.73003	1.89366
	3	9.418211	2.14125	2.29878
	4	12.561424	2.48549	2.64229
	5	15.704000	2.78759	2.94595
	6	18.846249	3.06003	3.22109
1.9	1	3.380384	−1.80494	0.17472
	2	6.412872	−2.48722	−0.60375
	3	9.512694	−2.93332	−1.11832
	4	12.632701	−3.29758	−1.50910
	5	15.761176	−3.61801	−1.83150
	6	18.893965	−3.90917	−2.11052
3.14	1	3.781170	−1.42795	−1.10560
	2	6.647763	−0.21997	−2.55717
	3	9.674336	0.79896	−3.03178
	4	12.755284	1.54066	−3.28064
	5	15.859745	2.11991	−3.45593
	6	18.976334	2.59959	−3.60214

Table II presents a sample of the coefficients $\mathcal{A}_M$ and $\mathcal{B}_M$ of the radial function of Eq. (8) and its extensions for $\nu \neq 0$, normalized according to Eqs. (12) and (13).

5. Discussion

The comparative analysis of the formulations and results of the problems of Sects. 2 and 3 serves to exhibit the effects of the magnetic vector potential on the energy eigenvalues and eigenstates of the electron inside the annular box, in which there is no magnetic force field. From the analysis at the end of Sect. 3 and the results of Sect. 4 some general statements about the Aharonov-Bohm effect on the electron's energy eigenvalues, as functions of the magnitude of the magnetic flux in the perforation, can be made. These statements are valid for any chosen values of the radial and longitudinal quantum numbers s and n.

1) The energy eigenvalues of the states with $m = 0, 1, 2, \ldots$ increase monotonically with ν, in such a way that

$$E_m(\nu + 1) = E_{m+1}(\nu), \tag{23a}$$

and the corresponding iterative extension

$$E_m(\nu + N) = E_{m+N}(\nu) \quad \text{for} \quad N = 1, 2, 3, \ldots \tag{23b}$$

2) The energy eigenvalues with $m = -1, -2, \ldots$ decrease monotonically at first, in such a way that they follow Eqs. (23a) and (23b) with the negative values of m, until the magnetic flux takes the values $\nu = -m$. From this value on, each one increases following the same Eqs. (23a) and (23b).

3) Equations (23a) and (23b) describe the periodic nature of the energy spectra as functions of the magnetic flux ν with period one.

A. For $\nu = 0$, the ground state $m = 0$ is nondegenerate and the excited states $m = \pm 1, \pm 2, \ldots$ are doubly degenerate. For $\nu = N$, the ground state is the $m = -N$ state and the doubly degenerate excited states correspond to $m = -N - K$ and $-N + K$, with $K = 1, 2, 3, \ldots$

B. For $\nu = 0.5$ the ground and excited states are all doubly degenerate corresponding to $m = 0$ and -1, and K and $-K - 1$, with $K = 1, 2, 3, \ldots$ respectively. For $\nu = N + 0.5$, the corresponding states have $m = -N$ and $-N - 1$, and $-N + K$ and $-N - 1 - K$.

C. The symmetry of the energy curves in the interval $0 \leq \nu \leq 1$ with respect to reflection in the line $\nu = 0.5$, is repeated in each interval $N \leq \nu \leq N + 1$ with respect to reflection in the line $\nu = N + 0.5$.

It is also instructive to evaluate the energy of the radiative transitions between two transverse states, which follows from the counterpart of Eq. (11) with the substitution $m \to M$ and for the same longitudinal quantum number $n' = n$ with the result

$$\Delta E(Msn \to M's'n) = \frac{\hbar^2}{2m_e a^2}\left(x^2_{Ms} - x^2_{M's'}\right) \quad \text{for} \quad m' = m \pm 1. \tag{24}$$

The selection rule for the angular momentum quantum number m is the usual standard one for electric dipole transitions [6, 7]. The size of the annular box determines the region of the spectrum for the corresponding radiations. In practice, they could be detected in microscopic conducting rings [13], mesoscopic semiconducting devices [14] and nanometric quantum dots [15], corresponding to microwave, far infrared and near infrared radiations, respectively. While the enclosed magnetic flux is not always quantized, the Aharonov-Bohm effect should open new possibilities in the construction of ultra-sensitive detectors.

As a conclusion of this discussion it is also enlightening to compare the Aharonov-Bohm effect in the standard version of the interference pattern of the electrons and of the electron bound-states version of this paper. The common feature of both versions is their periodicity with period $\nu = 1$, of the interference pattern and of the energy spectrum, respectively. Both versions are solutions of the same physical problem described by the common Schröedinger equation, and their difference consists in their correspondence with scattering states and bound states, respectively.

1. Y. Aharonov and D. Bohm, *Phys. Rev.* **115** (1959) 485.
2. R.G. Chambers, *Phys. Rev. Lett.* **5** (1960) 3.
3. E.J. Konopinski, *Am. J. Phys.* **46** (1978) 499.
4. D.H. Kobe, *Am. J. Phys.* **46** (1978) 342.
5. E.J. Konopinski, *Electromagnetic Fields and Relativistic Particles*, (McGraw-Hill, New York, 1981) p. 158.
6. J.J. Sakurai, *Advanced Quantum Mechanics*, (Addison-Wesley, Reading MA, 1967) p. 11, p. 14, and p. 41.
7. J. J. Sakurai and S.F. Tuan, *Modern Quantum Mechanics*, (Addison-Wesley, Reading, MA, 1994) p. 130 and p. 338.
8. M. Peshkin and A. Tonomura, *The Aharonov-Bohm Effect*, (Springer-Verlag, Berlin Heidelberg, 1989) p. 10.
9. L. Ballentine, *Quantum Mechanics*, (Prentice Hall, Englewood Cliff, N.J., 1990) p. 222.
10. M. Abramowitz and I. Stegun, *Handbook of Mathematical Functions*, (Dover, New York, 1965) Chapt. 9.
11. W.H. Press, S.A. Teukolsky, W.T. Vitterling, and B.P. Flannery, *Numerical Recipes in C. The Art of Scientific Computing*, (U.P. Cambridge New York, U.S.A., 1992) Chapt. 9.
12. M. Kumagai and T. Ohno, *Solid State Commun.* **83** (1992) 837.
13. R.A. Webb, S. Washburn, C.P. Umbach, and R.B. Leibowitz, *Phys. Rev. Lett.* **54** (1985) 2696.
14. G. Timp *et al.*, *Phys. Rev. Lett.* **58** (1987) 2814.
15. C.J.B. Ford *et al.*, *Phys. Rev.* **B43** (1991) 7339.

Classical analysis of the Aharonov-Bohm effect

E. Ley-Koo[1] and G. Villa-Torres
Instituto de Física, Universidad Nacional Autónoma de México
Apartado postal 20-364, 01000 México, D.F., México
e-mail: [1] eleykoo@fisica.unam.mx

Recibido el 30 de marzo de 2001; aceptado el 14 de septiembre 2001

This work presents an analysis of the Aharonov-Bohm effect taking into account both regions where the electron is present and where it is excluded, and also the time variations of the magnetic vector potential and the magnetic induction field as they change between two of their stationary values. This analysis allows the identification of the electrical force field induced in the region where the electron is present by the time variation of the magnetic flux in the region where the electron is excluded, thus providing a classical explanation of the changes in the stationary properties of the electron when the magnetic potential and field change from one set of stationary values to another. Some apparent contradictions in attempts to interpret the A-B effect are also discussed and clarified.

Keywords: Magnetic vector potential in quantum mechanics; particles in electromagnetic fields

En este trabajo se presenta un análisis del efecto Aharonov-Bohm, tomando en cuenta las regiones donde el elelectrón está presente y donde está excluido, y también las variaciones en el tiempo del potencial vectorial y el campo de inducción magnética cuando cambian entre dos de sus valores estacionarios. Este análisis permite la identificación del campo de fuerza eléctrica inducido en la región donde está el electrón por la variación en el tiempo del flujo magnético en la región donde el electrón está excluido, proporcionando así una explicación clásica de los cambios en las propiedades estacionarias del electrón cuando el potencial y el campo magñeticos cambian de un conjunto de valores estacionarios a otro. También se discuten y aclaran algunas contradiccciones aparentes en intentos de interpretar el efecto A-B.

Descriptores: Potencial vectorial magnético en mecánica cuántica; partículas en campos electromagnéticos

PACS: 03.65; 41.70

1. Introduction

The original Aharonov-Bohm (A-B) effect is manifested as the change in the fringe pattern in an electron interference experiment due to the change in the magnetic flux in a region between two electron beams, even though the two beams themselves pass only through a field-free region [1]. The authors were interested in the significance of the electromagnetic vector potential in quantum theory, and came up with this effect testing the potential in a region where the magnetic induction field is absent. Chambers carried out the electron interference experiments around a magnetized whisker confirming the effect predicted by Aharonov and Bohm [2].

Bound state versions of the A-B effect have also been analyzed [3, 4]. Peshkin illustrated the changes in the energy spectrum of a charged rotator in a plane and around an infinite solenoid perpendicular to the plane, due to the change in the magnetic flux inside the solenoid [3]. The A-B effect on the energy eigenvalues and eigenfunctions of the bound states of an electron inside an annular cylindrical box was quantitatively evaluated and illustrated in Ref. 4. In this work, it was also recognized that the electron bound-state and interference versions of the A-B effect are described by the same Schrödinger equation, differing their solutions by the corresponding boundary conditions, but sharing the common feature of energy spectra and interference patterns that are periodic in the magnetic flux in the region where the electrons are excluded. The period is one fluxon $hc/e = 4.135 \times 10^{-7}$ gauss cm^2, the natural unit of flux determined by Planck's constant, the speed of light and the charge of the electron. Our group has also investigated the A-B effect on Landau states of electrons in annular cylindrical boxes and in quantum antidots [5–7].

The Schrödinger equation describes the time evolution of the wave-function of a quantum system. The hamiltonian operator appearing in the equation includes the kinetic and potential energy terms. When the quantum system participates in electromagnetic interactions, the latter are incorporated via the minimal coupling prescription $\vec{p} \rightarrow \vec{p} - q/c\vec{A}$, where $\vec{p}$ is the conjugate momentum, q is the electric charge of the particle and $\vec{A}$ is the vector potential. It was in this context that Aharonov and Bohm analyzed the significance of $\vec{A}$ in quantum mechanics [1].

On the other hand, classical mechanics in the newtonian version formulates the time evolution of the system in terms of forces. Of course, in hamiltonian classical mechanics the time evolution of a system is formulated in terms of the hamiltonian function. In any case the equivalence of the newtonian and hamiltonian formulations of classical mechanics are well established. Appendix A contains some of their basic equations and connections.

Classical electrodynamics has also been formulated in terms of the force fields, electric intensity $\vec{E}(\vec{r}, t)$ and magnetic induction $\vec{B}(\vec{r}, t)$, and in terms of the potential fields, the scalar potential $\phi(\vec{r}, t)$ and the vector potential $\vec{A}(\vec{r}, t)$. Feynman [8] and Konopinski [9, 10] have explained the physical meaning of the latter in the classical context, and their works serve as a bridge to understand the quantum A-B effect. Appendix B contains the basic equations of the alternative descriptions of the electromagnetic field, and most important the connections between them.

There are several features of the A-B effect that are worth emphasizing since they contribute to make it interesting, and even mysterious, and are also at the root of some apparent contradictions in attempts to interpret it. First, the distinction between the region where the electron is present and there is no magnetic induction field, and the region where the electron is excluded and the magnetic induction field may change. Second, in both regions there is a magnetic vector potential with a different space dependence in each region, and a magnitude proportional to the magnetic induction. Third, the electron is not subject to any force as it follows from the vanishing of the fields in Eq. (29), but shares the interaction momentum with the vector potential as stated by Eq. (34). Fourth, the electron interference and bound state versions of the A-B effect correspond to stationary situations.

Different interpretations of the A-B effect have been proposed and here some of them are illustrated in order to appreciate the issues that they have raised and addressed. The original authors attributed the change in the electron interference pattern to the local physical effects of the electromagnetic vector potential [1]. Since the primary source of the effect is the change in the magnetic flux in the region where the electron is excluded, the latter's action takes place non-locally or through the local vector potential in the region where the electron is present. Boyer has investigated alternative explanations in terms of classical local electromagnetic fields [11–13]. His position is illustrated through a couple of paragraphs from Ref. 13:

> "The solenoid Aharonov-Bohm effect has attracted considerable attention, partly because the experimental effects are said to be produced without electromagnetic fields being present. Aharonov and Bohm have provided the presently accepted view that indeed electromagnetic fields are not present outside the solenoid, and the observed effects are due to local physical effects of the electromagnetic vector potential. However, this view may be wrong. We suspect that the experimental effects are actually due to electromagnetic fields acting locally and that the only new physics involves an unrecognized classical-electromagnetic-lag effect arising from electromagnetic fields of the multiparticle soleinod system."

He also questioned the work of Feynman

> "..., and a new physical role for the electromagnetic vector potential has now passed into the physics textbook literature," referring to Ref. 8.

Rubio, Getino, and Rojo, in their work "The Aharonov-Bohm effect as a classical Electromagnetic Effect Using Electromagnetic Potentials" [14], start out by recognizing the dispute about whether the force fields or the potentials are the "fundamental" quantities in electromagnetism, and conclude "we agree with Boyer in this interpretation of the AB and AC effects as due to classical lag effects, but instead of rejecting the electromagnetic potentials as something unphysical, we consider them as the fundamental entities of electromagnetism, both quantum and classical." The question of the locality or non-locality of the interaction responsible for the A-B effect, is discussed in Ref. 15.

The literature about the prediction, experimental observation and interpretations of the A-B effect is predominantly in the research area. The present contribution is written from a didactical perspective, recognizing from the outset that there are two complementary, rather than opposing, classical descriptions of the dynamical and electromagnetic phenomena, as summarized in Appendices A and B. Both descriptions are taken into account in Sec. 2 in order to analyze the A-B effect, considering

i) Both regions where the electron is present and excluded.

ii) The magnetic potential and magnetic induction in both regions.

iii) Including their time variations between two sets of their stationary values.

iv) Identifying the presence of the induced electric intensity field and evaluating its time and space integrated effects on the motions of the electron around the region where it is excluded.

The analysis based on *i*) and *ii*) is the standard one to obtain the hamiltonian of the electron. The analysis based additionally on *iii*) and *iv*) is a new one, leading to the same results as the previous one. The equivalence of both analysis, one starting from the magnetic vector potential and the other from the electric intensity field, allows a better understanding of the A-B effect and some of its interpretations as discussed in Sec. 3.

2. Analysis of the Aharonov-Bohm effect in terms of the time changes of the potential and force fields

The idealized experimental situation, on which the analysis of the A-B effect is based, involves and infinite straight solenoid with a circular cross-section of radius a. The electron moves around the solenoid, so that we can recognize the interior of the latter as the region where the electron is excluded and its exterior as the region where the electron is present. Circular cylindrical coordinates (ρ, φ, z) are appropriate for the chosen geometry. The situations to be compared are those in which

1) There is no magnetic induction field anywhere,

$$\vec{B}(0 \leq \rho < \infty, \varphi, z) = 0. \qquad (1)$$

2) There is an axial uniform magnetic induction field only in the interior of the solenoid,

$$\vec{B}(0 \le \rho \le a, \varphi, z) = \hat{k}B_0. \tag{2}$$

Then the magnetic vector potential for the respective situations can be chosen as

$$\vec{B}(a \le \rho < \infty, \varphi, z) = 0, \tag{3}$$

and

$$\begin{aligned} \vec{A}(0 \le \rho \le a, \varphi, z) &= \frac{1}{2}\hat{\varphi}B_0\rho, \\ \vec{A}(a \le \rho \le \infty, \varphi, z) &= \frac{1}{2}\hat{\varphi}\frac{B_0 a^2}{\rho}, \end{aligned} \tag{4}$$

corresponding to the circular or symmetric gauge for the latter. The reader can check that the curls of the magnetic vector potentials of Eqs. (3) and (4) lead to the respective magnetic induction fields of Eqs. (1) and (2), in agreement with Eq. (31).

Then the hamiltonian for the first situation is simply the kinetic energy term,

$$\hat{H}(\vec{r}, \vec{p}) = \frac{p^2}{2m_q} = \frac{p_\rho^2}{2m_q} + \frac{l_z^2}{2m_q\rho^2} + \frac{p_z^2}{2m_q}, \tag{5}$$

in which the radial, rotational and axial contributions to the kinetic energy can be recognized. A particle with an electric charge q and mass m_q is assumed and l_z is the axial component of the orbital angular momentum. The hamiltonian for the second situation is constructed from the minimal coupling prescription described at the end of Appendix B, by using Eqs. (5) and (4):

$$\begin{aligned} H(\vec{r}, \vec{p}) &= \frac{\left(\vec{p} - \frac{q}{c}\vec{A}\right)^2}{2m_q} \\ &= \frac{p_\rho^2}{2m_q} + \frac{\left(l_z - \frac{qBa^2}{2c}\right)^2}{2m_q\rho^2} + \frac{p_z^2}{2m_q}. \end{aligned} \tag{6}$$

Notice that the hamiltonians of Eqs. (5) and (6) have in common the radial and axial terms and differ in the numerator of the rotational term. This difference is associated with the interaction momentum of the charge q and the magnetic vector potential given by Eqs. (34) and (4).

The analysis so far has been classical, and before continuing it through the incorporation of the time variations of the magnetic induction and vector potential, it is appropriate to examine at this moment the quantum implications in the stationary situation. Actually this has been done in detail in Refs. 1 and 4, so it will be sufficient to say here that the angular momentum is quantized:

$$l_z = m\hbar = \frac{mh}{2\pi}, \qquad m = 0, \pm 1, \pm 2, \ldots \tag{7}$$

and the difference of the rotational energy contributions in Eqs. (5) and (6) corresponds for a negatively charged electron with $q = -e$ to the change

$$m \to m + \nu, \tag{8}$$

where

$$\nu = \frac{eB_0a^2}{2c\hbar} = \frac{B_0\pi a^2}{(ch/e)} \tag{9}$$

is the number of fluxons in the interior of the solenoid. At the level of the solutions of the Schrödinger equation the eigenfunctions of the hamiltonian operators of Eqs. (5) and (6) have in common the angular and axial functions; their radial functions, which are Bessel functions, differ in their orders m and $m + \nu$, respectively. This leads to the changes in the electron interference pattern analyzed in Ref. 1 and to the changes in the energy spectra and eigenfunctions analyzed in Ref. 4 as the magnetic flux inside the solenoid, Eq. (9) changes.

Now we continue the classical analysis by considering the time variations of the magnetic induction inside the solenoid. It is important to recognize that the space configuration is maintained, so that the space dependencies of the magnetic induction and vector potential remain the same as given by Eqs. (2) and (4). Therefore, the changes of B_0 are followed by proportional changes in $\vec{A}$ and ν. On the other hand, according to the Faraday-Lenz-Henry law of electromagnetic induction, the time rate of change of the magnetic flux inside the solenoid induces an electromotive force around it:

$$\mathcal{E} = -\frac{d\Phi_m}{c\,dt}. \tag{10}$$

For any circle coaxial with the solenoid and with a radius $\rho > a$, the evaluation of both sides of this equation is immediate:

$$2\pi\rho E = -\frac{dB_0}{c\,dt}\pi a^2, \tag{11}$$

since the electric field intensity $\vec{E}$ has circular lines. Consequently, the induced electric field has the explicit form

$$\vec{E} = -\hat{\varphi}\frac{a^2}{2\rho}\frac{dB_0}{c\,dt}. \tag{12}$$

From Eq. (4), it is recognized that this field is the partial time derivative of the vector potential around the solenoid, which could have been obtained directly by applying Eq. (32) to the situation under study. In any case, it is the electromagnetic induction phenomenon which accounts for the identification of the electric force $q\vec{E}$ in the region where the charge is present during the interval in which the magnetic induction field is changing.

Next, we proceed to evaluate the time and space integrated effects of such a force when the magnetic field changes from one stationary value to another. Without any loss of generality the initial value can be taken as zero and the final one as B_0. The time integration of q times Eq. (12) gives the impulse imparted to the charge,

$$\int q\vec{E}\, dt = -\frac{\hat{\varphi} q B_0 a^2}{2c\rho} = -\frac{q}{c}\vec{A}, \tag{13}$$

which, again through Eq. (4), is identified as minus q/c times the vector potential or the negative of the interaction momentum, [Eq. (34)]. The integration of q times Eq. (12) along a circle around the solenoid gives

$$\oint q\vec{E}\cdot d\vec{r} = -\frac{q}{c}\pi a^2 \frac{dB_0}{dt}, \tag{14}$$

the work done by the force on the charge, which is q times Eq. (10).

Additionally, the line integral of Eq. (13) around the circle or the time integral of Eq. (14) give the change in action due to the change in the magnetic induction:

$$S = -\frac{qB_0\pi a^2}{c} = -\frac{q}{c}\Phi_m. \tag{15}$$

In quantum mechanics, this change in action divided by $\hbar$ gives the relative phase difference for charged particles which pass around opposite sides of the solenoid due to the change in the magnetic induction inside the solenoid:

$$\frac{S}{\hbar} = -\frac{q\Phi_m}{c\hbar}\bigg|_{q=-e} = 2\pi\nu. \tag{16}$$

This result was obtained in Refs. 1 and 12–14 from different assumptions and approximations.

3. Discussion

This section includes a general and brief discussion of the alternative formulations of classical mechanics and electromagnetism and their connections, and also discussions of specific issues related to the analysis and interpretations of the A-B effect. Some of the latter are motivated by specific statements in the works of Refs. 11–15 about the roles of the electromagnetic fields and potentials in classical and quantum mechanics.

We have intentionally included Appendices A and B, making reference to them since the introduction, in recognition that there exist alternative and complementary formulations of mechanics and electromagnetism. Their equivalences in mechanics are well established: integration of the force leads to the potential energy Eq. (23) and the conservation of energy Eq. (26), and differentiation of the potential energy Eq. (25) and of the hamiltonian Eq. (28) lead to the force. Similar relations hold in electromagnetism: the integration of the Maxwell equations independent of the sources, Eqs. (30), lead to the potentials, whose derivatives give the force fields, Eqs. (31) and (32); the Lorentz force may be written in terms of the fields Eq. (29), or in terms of the potentials Eq. (33); the latter allows the identification of the interaction potential energy and interaction potential momentum Eq. (34); also Eqs. (30) correspond to the Maxwell equation in differential form, but they can also be cast into their integral forms or described phenomenologically, like for example Eqs. (14) and (10) for the electromagnetic induction.

Several elements have been used in the classical analysis of Sec. 2. The explicit expressions for the magnetic induction and vector potential inside and outside the solenoid, for the two comparative situations Eqs. (1)–(4). The application of the minimal coupling prescription to go from the hamiltonian in the absence of any fields, Eq. (5), to the one in the presence of a magnetic induction inside the solenoid and the vector potential around it, Eq. (6). The explicit consideration of the time variation of the magnetic induction inside the solenoid and its consequences: the induced electro-motive force around the solenoid, Eq. (10), and the associated induced electric field, Eq. (12), the successive time and line integrals of the latter Eqs. (13)–(15), and their physical meanings; including the connections with the vector potential of Eqs. (12) and (13) which are physically behind the minimal coupling prescription. On the other hand, the quantum elements leading to the A-B effect are the quantization of angular momentum Eqs. (7)–(9) and the connection between action and phase Eq. (16). It is instructive to point out that having recognized the presence of the induced electric intensity field as the source of the force on the charge around the solenoid, its contribution to the change in the action is via the line integral of the vector potential Eq. (13) or the time integral of the electromotive force Eq. (14).

Some comments in response to statements in Refs. 13 and 14 are made in the following, under the light provided by the analysis of Sec. 2. In the stationary situation there are no forces on the charge around the solenoid, but the analysis of the situation when the magnetic induction field is changing inside the solenoid leads to recognize the electromagnetically induced force. This may lift the veil of mystery that has been associated with the A-B effect. More important, the time integrated effect of such a force leads to the change in the vector potential reinforcing the physical interpretation of the latter as a momentum per unit charge, Eq. (13). This is precisely the key idea discussed and explained in Refs. 8–10. Out point of view, concerning the alternative descriptions of electromagnetism in terms of electromagnetic fields and electromagnetic potentials, is that they are complementary, and one does not exclude the other; the potentials and their use are common to both classical and quantum mechanics, while the fields are useful in newtonian mechanics. In this paper the identification of the force and its contributions to the vector potential and action allow a better understanding of the classical and quantum elements participating the A-B effect.

Finally, the issue of the locality or non-locality of the interaction responsible for the A-B effect is examined. Aharonov and Bohm argued in favor of the local interaction of the charge and the vector potential in the exterior of the solenoid. Some authors have not accepted this interpretation as illustrated in the Introduction by the quotation from [13]. Our identification of the electromagnetically induced electric force $q\vec{E}(\vec{r},t)$ outside the solenoid is complemented by recognizing it also as a local interaction. Additionally, its time integrated effect, Eq. (13), leads to the vector potential making contact with and supporting the position of Ref. 1, and also answering the questions of Ref. 13. The issue of non-locality appears because the magnetic induction is present inside the solenoid and the electron is outside. Of course, classical electromagnetism recognizes that $\vec{B}(\vec{r},t)$ of Eq. (2) has the associated vector potential $\vec{A}(\vec{r},t)$ of Eq. (4) and electric intensity field $\vec{E}(\vec{r},t)$ of Eq. (12), both present outside the solenoid and able to interact locally with the electron. The interested readers are referred to the article "On the origin of the A-B effect" [15] for another point of view of the locality *vs.* non-locality issue.

Appendix A

Newton's and Hamilton's formulations of classical mechanics

Newton's second law of motion establishes that the force acting on a particle is equivalent to the time rate of change of the particle's momentum:

$$\vec{F} = \frac{d\vec{p}}{dt}. \tag{17}$$

The impulse of a force describes the integrated effect of the force throughout the time of its application:

$$\vec{I} = \int_{t_i}^{t_f} \vec{F}\, dt. \tag{18}$$

The work done by a force acting on a particle that follows a certain trajectory describes the integrated effect of the force along the trajectory:

$$W = \int_C \vec{F}\cdot d\vec{r}. \tag{19}$$

Substitution of the expression for the force from Eq. (17) in Eqs. (18) and (19) leads to recognize that the effect of the impulse of the force is the change in the particle's momentum,

$$\vec{I} = \vec{p}\,(t_f) - \vec{p}\,(t_i), \tag{20}$$

and that the effect of the work is the change in the kinetic energy of the particle:

$$W = \frac{[p(t_f)]^2}{2m} - \frac{[p(t_i)]^2}{2m}, \tag{21}$$

where

$$\vec{p} = m\frac{d\vec{r}}{dt}. \tag{22}$$

The forces for which the work of Eq. (19) does not depend on the trajectory but only on the initial and final positions,

$$W = \int_{\vec{r}_i}^{\vec{r}_f} \vec{F}\cdot d\vec{r} = -U(\vec{r}_f) + U(\vec{r}_i) \tag{23}$$

are called conservative forces, allowing the identification of a potential energy function such that

$$\vec{F}\cdot d\vec{r} = -dU, \tag{24}$$

or equivalently

$$\vec{F} = -\nabla U \tag{25}$$

Then the combination of Eqs. (21) and (23) leads to the conservation of the total mechanical energy given by the sum of the kinetic and potential energies:

$$\frac{p_f^2}{2m} + V(\vec{r}_f) = \frac{p_i^2}{2m} + U(\vec{r}_i). \tag{26}$$

The total energy as a function of position and momentum of the particle is identified as the hamiltonian function,

$$H(\vec{r},\vec{p}) = \frac{p^2}{2m} + U(\vec{r}). \tag{27}$$

Hamilton's canonical equations

$$\dot{x}_i = \frac{\partial H}{\partial p_i}, \qquad \dot{p}_i = -\frac{\partial H}{\partial x_i} \tag{28}$$

are equivalent to the velocity components, Eq. (22), and Newton's second law of motion, Eq. (17), respectively.

The equivalence between Newton's and Hamilton's formulations of classical mechanics is well established. The use of one or the other is a matter of convenience for the analysis of each specific problem.

Appendix B

Descriptions of the electromagnetic field in terms of forces and potentials

The Lorentz force describes the electromagnetic force acting on a particle with an electric charge q and velocity $\vec{u}$, at the position $\vec{r}$ at time t,

$$\vec{F} = q\vec{E} + \frac{q}{c}\vec{u}\times\vec{B}, \tag{29}$$

in terms of the electric intensity field $\vec{E}(\vec{r},t)$ and the magnetic induction field $\vec{B}(\vec{r},t)$, where c is the speed of light in vacuum.

The relations between the fields and their sources, the electric charge density $\rho(\vec{r},t)$ and electric current density $\vec{J}(\vec{r},t)$, are given by Maxwell's equations:

$$\begin{aligned}
\nabla\cdot\vec{E} &= 4\pi\rho,\\
\nabla\times\vec{B} &= \frac{4\pi}{c}\vec{J} + \frac{1}{c}\frac{\partial\vec{E}}{\partial t},\\
\nabla\times\vec{E} &= -\frac{1}{c}\frac{\partial\vec{B}}{\partial t},\\
\nabla\times\vec{B} &= 0,
\end{aligned} \tag{30}$$

corresponding to the electric Gauss' law, the Ampére-Maxwell law, the Faraday-Lenz-Henry law, and the magnetic Gauss' law, respectively.

The last two laws, which do not depend on the sources, make it possible to introduce the electromagnetic potentials. Indeed, the solenoidal character of the magnetic induction field allows to write the latter as the curl of the vector potential $\vec{A}(\vec{r},t)$:

$$\vec{B} = \nabla \times \vec{A} \tag{31}$$

Then the substitution of this expression in the Faraday-Lenz-Henry law equation leads to the expression for the electric intensity field

$$\vec{E} = -\nabla\phi - \frac{1}{c}\frac{\partial\vec{A}}{\partial t} \tag{32}$$

in terms of the gradient of the scalar potential $\phi(\vec{r},t)$ and the partial time derivative of $\vec{A}$.

The physical meaning of the scalar potential is quite familiar since the study of electrostatics and corresponds to the energy per unit charge. The vector potential also has a physical meaning, although it is not so familiar as in the case of the scalar potential and it is ignored too often. In order to identify both meanings in general it is sufficient to substitute Eqs. (31) and (32) in Eq. (29), and to rewrite the Lorentz force in terms of the potentials in the form

$$\vec{F} = -\nabla\left[q\phi - \frac{q}{c}\vec{u}\cdot\vec{A}\right] - \frac{d}{dt}\left[\frac{q}{c}\vec{A}\right]. \tag{33}$$

The identification of the energy associated with the interaction between the charge and the scalar potential $q\phi$ coincides with the familiar situation of electrostatics and extends it to the time dependent situation. The second term inside the brackets corresponds to the interaction between the moving charge and the vector potential; then the vector potential is the energy of interaction per unit charge and per unit velocity. In addition, since the force is the time rate of change of the particle's momentum according to Eq. (17), then the quantity inside the parenthesis in the last term of Eq. (33) allows the identification of the energy and momentum of interaction between the charge and the electromagnetic field described by the potentials:

$$\begin{aligned} U_{\text{int}} &= q\phi - \frac{q}{c}\vec{u}\cdot\vec{A} \quad , \\ \vec{p}_{\text{int}} &= \frac{q}{c}\vec{A} \end{aligned} \tag{34}$$

The vector potential is a potential of momentum per unit charge, which physically justifies the minimal coupling prescription, $\vec{p} \to \vec{p} - (q/c)\vec{A}$, to incorporate the effects of the electromagnetic field in situations in which the latter was not present originally.

1. Y. Aharonov and D. Bohm, *Phys. Rev. D* **115** (1989) 485.
2. R.G. Chambers, *Phys. Rev. Lett.* **5** (1960) 3.
3. M. Peshkin and A. Tonomura, *The Aharonov-Bohm Effect* (Springer-Verlag, Berlin Heidelberg, 1989), p. 10.
4. D. Kouznetsov, E. Ley-Koo, and G. Villa-Torres, , *Rev. Mex. Fís.* **45** (1999) 485.
5. E. Ley-Koo, G. Villa-Torres y D. Kouznetsov, "Efecto Aharonov-Bohm en estados de Landau en cajas cilíndricas anulares," Programa del XLII Congreso Nacional de Física, 6 SE 3 (1999).
6. E. Castaño, N. Aquino y E.Ley-Koo, "Efecto Aharonov-Bohm en estados de Landau de antipuntos cuánticos", Programa del XLII Congreso Nacional de Física, 4SC1 (1999).
7. E. Ley-Koo, *Topics in Contemporary Physics*, edited by J.A. Heras and R.V. Jiménez (Instituto Politécnico Nacional, México, 2000), p. 17.
8. R.P. Feynman, R. B. Leighton, and M. Sands, *The Feynman Lectures in Physics* (Addison-Wesley, Reading, Mass., 1964), Vol. II., Chap. 15.
9. E.J. Konopinski, *Am. J. Phys.* **46** (1978) 499.
10. E.J. Konopinski,*Electromagnetic Fields and Relativistic Particles* (McGraw-Hill, New York, 1981).
11. T.H. Boyer, *Phys. Rev. D* **8** (1973) 1667.
12. T.H. Boyer, *Phys. Rev. D* **8** (1973) 1680
13. T.H. Boyer, *Nuovo Cimento B* **100** (1987) 685.
14. H. Rubio, J. M. Getino, and O. Rojo, *Nuovo Cimento B* **106** (1991) 407.
15. L. O'Raifertaigh, N. Straumann, and A. Wipf, *Comments Nucl. Part. Phys.* **20** (1991) 15.

Aharonov-Bohm Effect on Landau States in Annular Cylindrical Boxes

E. Ley-Koo[1]*, G. Villa-Torres[1]*, and D. Kouznetsov[2]
[1]Instituto de Fiśica-UNAM., Apartado Postal 20-364, 01000 México, D. F. México
[2]Mathematical Building, Box 87, University of Arizona, Tucson, AZ 85721, USA
(Received September 24, 2001)

The Schrödinger equation for an electron inside an annular cylindrical box and in the presence of an axial uniform magnetic field is solved in two comparative situations: i) when the magnetic induction $\vec{B}_0 = \hat{k}B_0$ is the same in the central perforation and in the box, and ii) when its values in the perforation $\vec{B}_i = \hat{k}B_i$ and in the box $\vec{B}_0 = \hat{k}B_0$ are different. The Aharonov-Bohm effect on the Landau states of the confined electron is exhibited through the analysis of the dependence of the energy eigenvalues and eigenfunctions on the difference of the magnetic flux in the perforation as $B_i - B_0$ changes.

PACS. 03.65.–w – Quantum mechanics.
PACS. 03.65.Bz – Aharonov-Bohm effect.

I. Introduction

This paper deals with the problem of an electron moving under the action of uniform magnetic fields combining the situations of the Landau problem [1-3] and of the Aharonov-Bohm (A-B) effect [4-6]. The first situation corresponds to a uniform magnetic induction at all points of space and to an electron allowed to be at any of those points. The Landau problem has been solved in both the linear gauge and the symmetric gauge, and the connections between the respective eigenstates have been exhibited in [3]. The second situation involves a uniform magnetic induction in a limited region of space from which the electron is excluded. Aharonov and Bohm predicted that the fringe pattern in an electron interference experiment should be shifted by altering the amount of magnetic flux passing between two beams, even though the beams themselves pass only through field-free regions [4]. The experiments performed by Chambers using magnetic whiskers confirmed this prediction [5]. The A-B effect on the bound states of an electron inside an annular cylindrical box was analyzed in [6].

The A-B effect on the Landau states of an electron inside an annular cylindrical box is investigated by comparing two new situations. In Sec. II, the same uniform magnetic induction $\vec{B}(0 \le \rho \le b, \varphi, z) = \hat{k}B_0$ is present in the central perforation $(0 \le \rho \le a)$ and in the box $(a \le \rho \le b)$. In Sec. III, the magnetic induction in the perforation $\vec{B}(0 \le \rho \le b, \varphi, z) = \hat{k}B_i$ is different from the one in the box $B(a \le \rho \le b, \varphi, z) = \hat{k}B_0$. The analysis of both situations involves identifying the respective vector potentials in the perforation and in the box, constructing the Hamiltonians via the minimal-coupling prescription, and solving the corresponding Schrödinger equations. The box is assumed to be impenetrable, which translates into the boundary condition that the eigenfunctions must vanish at the positions of the walls of the box. Sec. IV presents numerical and graphical results illustrating the A-B effect through the changes of the energy eigenvalues and eigenfunction parameters as the magnetic flux difference in the perforation $(B_i - B_0)\pi a^2$ changes, including a discussion of these results. For completeness sake the explicit forms of the Kummer confluent hypergeometric functions are included in the Appendix.

II. Landau states in an annular cylindrical box

This section presents the formulation and solution of the quantum problem of an electron, of mass m_e and electric charge $-e$, confined inside an annular cylindrical box ($a \leq \rho \leq b, 0 \leq \varphi \leq 2\pi, 0 \leq z \leq L$), and under the action of an axial uniform magnetic field,

$$\vec{B}(0 \leq \rho \leq b, \varphi, z) = \hat{k} B_0, \tag{1}$$

which has the same magnitude in both the perforation and the box. The associated magnetic vector potential is chosen as the one in the symmetric gauge,

$$\vec{A}(0 \leq \rho \leq b, \varphi, z) = \hat{\varphi} \frac{B_0 \rho}{2}, \tag{2}$$

congruent with the geometry of the box. The Hamiltonian for the system is constructed by using the minimal-coupling prescription [2],

$$\hat{H} = \frac{(\vec{p} + \frac{e}{c}\vec{A})^2}{2m_e} = \frac{p_\rho^2}{2m_e} + \frac{(\frac{\hat{l}_z}{\rho} + \frac{eB_0\rho}{2c})}{2m_e} + \frac{p_z^2}{2m_e}, \tag{3}$$

involving the radial p_ρ, azimuthal l_z/ρ, and axial p_z components of the canonical momentum; l_z is the canonical angular momentum. Then the corresponding time-independent Schrödinger equation becomes

$$\left\{ -\frac{\hbar^2}{2m_e} \frac{1}{\rho} \frac{\partial}{\partial \rho} \rho \frac{\partial}{\partial \rho} + \frac{\hat{l}_z^2}{2m_e \rho^2} + \frac{eB_0}{2m_e c} \hat{l}_z + \frac{e^2 B_0^2}{8 m_e c^2} \rho^2 - \frac{\hbar^2}{2m_e} \frac{\partial^2}{\partial z^2} \right\} \psi(\rho, \varphi, z) \\ = E\psi(\rho, \varphi, z). \tag{4}$$

The three terms coming from the square of the binomial in Eq. (3) are identified as the rotational kinetic energy, the diamagnetic energy, and the harmonic oscillator potential energy with a frequency $\omega = eB_0/2m_e c$.

Equation (4) admits separable solutions

$$\psi(\rho, \varphi, z) = R(\rho)\Phi(\varphi)Z(z). \tag{5}$$

Each factor satisfies the respective ordinary differential equation in the longitudinal, azimuthal and radial coordinate:

$$-\frac{\hbar^2}{2m_e} \frac{d^2 Z}{dz^2} = E^L Z, \tag{6}$$

$$-i\hbar \frac{d\Phi}{d\varphi} = m\hbar\Phi, \tag{7}$$

$$\left\{-\frac{\hbar^2}{2m_e}\left[\frac{1}{\rho}\frac{d}{d\rho}\rho\frac{d}{d\rho}-\frac{m^2}{\rho^2}\right]+\frac{1}{2}m_e\omega^2\rho^2+m\hbar\omega\right\}R=E^TR. \tag{8}$$

Here the longitudinal and transverse contributions to the energy add up to the total energy,

$$E^L+E^T=E. \tag{9}$$

The eigensolutions of Eq. (6) are determined by the boundary conditions that they must vanish at the lower $z=0$ and upper $z=L$ walls of the box. Their explicit form is

$$Z_n(z)=\sqrt{\frac{2}{L}}\sin\frac{n\pi z}{L},\quad n=1,2,3,\dots. \tag{10}$$

The corresponding longitudinal eigenenergy becomes

$$E_n^L=\frac{\hbar^2n^2\pi^2}{2m_eL^2}. \tag{11}$$

Equation (7) is the eigenvalue equation for the z-component of the angular momentum, with eigensolutions

$$\Phi_m(\varphi)=\frac{e^{im\varphi}}{\sqrt{2\pi}} \tag{12}$$

and integer eigenvalues

$$m=0,\pm1,\pm2,\dots \tag{13}$$

arising from the periodicity condition $\Phi(\varphi+2\pi)=\Phi(\varphi)$.

Apart from the diamagnetic energy term, Eq. (8) is identified as the radial Schrödinger equation for a two-dimensional isotropic harmonic oscillator. Its solutions are well-known; for the electron inside the annular cylindrical box they must vanish at the inner $\rho=a$ and outer $\rho=b$ walls. The general solution is

$$\begin{aligned}R(\rho)=\rho^{|m|}e^{-m_e\omega\rho^2/2\hbar}\Bigg\{&CM\left(-\nu,|m|+1;\frac{m_e\omega\rho^2}{\hbar}\right)\\&+DU\left(-\nu,|m|+1;\frac{m_e\omega\rho^2}{\hbar}\right)\Bigg\},\end{aligned} \tag{14}$$

in terms of the confluent hypergeometric functions M and U [7], where the transverse eigenenergy contribution has the form

$$E_{sm}^T=\hbar\omega[2\nu_s+|m|+1+m]. \tag{15}$$

The radial boundary conditions become:

$$CM\left(-\nu,|m|+1;\frac{m_e\omega a^2}{\hbar}\right)+DU\left(-\nu,|m|+1;\frac{m_e\omega a^2}{\hbar}\right)=0, \tag{16}$$

$$CM\left(-\nu,|m|+1;\frac{m_e\omega b^2}{\hbar}\right)+DU\left(-\nu,|m|+1;\frac{m_e\omega b^2}{\hbar}\right)=0. \tag{17}$$

The value of the transverse eigenenergy parameter ν is determined by the condition that the determinant of the two linear homogeneous algebraic Eqs. (16) and (17) in C and D vanishes,

$$\begin{aligned}&M\left(-\nu,|m|+1;\frac{m_e\omega a^2}{\hbar}\right)U\left(-\nu,|m|+1;\frac{m_e\omega b^2}{\hbar}\right)\\&-U\left(-\nu,|m|+1;\frac{m_e\omega a^2}{\hbar}\right)M\left(-\nu,|m|+1;\frac{m_e\omega b^2}{\hbar}\right)=0.\end{aligned} \tag{18}$$

For an electron confined in an annular cylindrical box with inner and outer radii a and b, under the action of the uniform magnetic induction field defined by Eq. (1), and in an eigenstate with a chosen value of m, Eq. (13), the zeros of Eq. (18) for ν_s, $s=1,2,3,\ldots$ determine the corresponding radial eigenfunctions $R_{sm}(\rho)$, Eq. (14), and transverse eigenenergies E^T_{sm}, Eq. (15). Such zeros are computed numerically using the appropriate representations of the functions M and U [7], Eqs. (A.1), (A.4) with $\alpha=-\nu$ and $n=|m|$.

The normal Landau problem in which the electron may be at any point in the range $0\leq\rho<\infty$ corresponds to the particular case of $a=0$ and $b=\infty$. By recalling that U is singular at $\rho=0$ its presence in Eq. (14) must be eliminated by taking $D=0$. On the other hand, M diverges as exp $(m_e\omega\rho^2/\hbar)$ as $\rho\to\infty$, Eq. (A.5), and the only way to make Eq. (14) still useful is to take ν as a non-negative integer N for which M becomes a polynomial of degree $2N$. Correspondingly, the Landau energy levels of Eq. (15) become the spectrum of odd integers in units $\hbar\omega$, each level being infinitely degenerate on account of the cancellation of the rotation and diamagnetic contributions $|m|+m$ for $m=-|m|$.

The zeros of ν_s in Eq. (18) depend on the values of the other parameters of M and U, namely $|m|$, $(m_e\omega a^2/\hbar)$, and $(m_e\omega b^2/\hbar)$ and in general are not integers. The dimensionless parameter $m_e\omega b^2/\hbar$ can be rewritten in terms of the magnetic induction field as $B_0\pi b^2/(hc/e)$, which can be identified as the magnetic flux in the circular cross-section of radius b expressed in the fluxon unit, $hc/e=4.135\times10^{-7}$ gauss-cm^2. The result of the confinement of the electron inside the annular cylindrical box is to remove the infinite degeneracy of the normal Landau energy levels described in the previous paragraph. Explicit numerical illustrations of these results are shown in Sec. IV.

III. Aharonov-Bohm effect on the landau states in an annular cylindrical box.

In this section we analyze the changes in the eigenenergies and eigenfunctions of the Landau states when the magnetic induction field has a value in the perforation different form its value in the box. Let the respective values be

$$\vec{B}(0\leq\rho\leq a,\varphi,z)=\hat{k}B_i \tag{19}$$

and

$$\vec{B}(a\leq\rho\leq b,\varphi,z)=\hat{k}B_0. \tag{20}$$

The corresponding magnetic vector potential is

$$\begin{aligned}\vec{A}(0 \le \rho \le a, \varphi, z) &= \hat{\varphi}\frac{B_i \rho}{2},\\ \vec{A}(a \le \rho \le b, \varphi, z) &= \hat{\varphi}\left[\frac{B_0\rho}{2} + \frac{(B_i - B_0)a^2}{2\rho}\right].\end{aligned} \tag{21}$$

This potential is continuous at the boundary $\rho = a$, and its curl reproduces the magnetic induction fields in the perforation and in the box. The Hamiltonian for the electron in the box becomes

$$\hat{H} = \frac{\hat{p}_\rho^2}{2m_e} + \frac{\left[\left(\frac{\hat{l}_z}{\rho} + \frac{e(B_i - B_0)a^2}{2c\rho}\right) + \frac{eB_0\rho}{2c}\right]^2}{2m_e} + \frac{\hat{p}_z^2}{2m_e}. \tag{22}$$

The difference of the magnetic induction in the perforation, Eq. (19), compared to the one in the box, Eq. (20), is translated into the difference of the magnetic vector potential of Eq. (21) compared to that of Eq. (2) and correspondingly to the difference between the Hamiltonian of Eq. (22) compared to that of Eq. (3). The latter consists in the replacement

$$\hat{l}_z \to \hat{l}_z + \frac{e(B_i - B_0)a^2}{2c} \tag{23}$$

in going from Eq. (3) to Eq. (22), in the terms inversely proportional to the radial coordinate ρ. Then the new time-independent Schrodinger equation is

$$\begin{aligned}&\left\{-\frac{\hbar^2}{2m_e}\frac{1}{\rho}\frac{\partial}{\partial\rho}\rho\frac{\partial}{\partial\rho} + \frac{[\hat{l}_z + \frac{e(B_i - B_0)a^2}{2c}]^2}{2m_e\rho^2} + \frac{eB_0}{2m_e c}\left[\hat{l}_z + \frac{e(B_i - B_0)a^2}{2c}\right]\right.\\ &\left. + \frac{e^2B_0^2}{8m_e c^2}\rho^2 - \frac{\hbar^2}{2m_e}\frac{\partial^2}{\partial z^2}\right\}\psi(\rho, \varphi, z) = E\psi(\rho, \varphi, z),\end{aligned} \tag{24}$$

instead of Eq. (4). It also admits separable solutions of the same type of Eq. (5), with the same longitudinal and azimuthal eigenfunctions and eigenvalues of Eqs. (10)-(13) satisfying the corresponding differential Eqs. (6) and (7). The radial differential equation becomes

$$\left\{-\frac{\hbar^2}{2m_e}\left[\frac{1}{\rho}\frac{d}{d\rho}\rho\frac{d}{d\rho} - \frac{(m+\mu)^2}{\rho^2}\right] + \frac{1}{2}m_e\omega^2\rho^2 + \hbar\omega(m+\mu)\right\}R = E^T R, \tag{25}$$

where

$$\mu = \frac{e(B_i - B_0)a^2}{2\hbar c} = \frac{(B_i - B_0)\pi a^2}{(hc/e)} \tag{26}$$

is the change in the magnetic flux in the perforation in the fluxon unit when the magnetic induction changes from its value of Eq. (1) to that of Eq. (19). The difference in going from the radial Eq. (8) to that of Eq. (25) is the replacement

$$m \to m + \mu, \tag{27}$$

which follows from that of Eq. (22).

The solutions of the radial Eq. (25) are of the same type as those of Eq. (8) with the replacement of Eq. (27). Their explicit forms are

$$\begin{aligned} R_{sm}(\rho,\mu) =& \rho^{|m+\mu|}e^{-m_e\omega\rho^2/2\hbar}\Big\{CM\Big(-\nu,|m+\mu|+1;\frac{m_e\omega\rho^2}{\hbar}\Big) \\ &+DU\Big(-\nu,|m+\mu|+1;\frac{m_e\omega\rho^2}{\hbar}\Big)\Big\} \end{aligned} \tag{28}$$

instead of Eq. (14), with the new transverse eigenenergy

$$E^T_{sm}(\mu) = \hbar\omega[2\nu_s + |m+\mu| + 1 + m + \mu], \tag{29}$$

instead of Eq. (15), and the ratio of the C and D coefficients and the parameter ν being determined by

$$\frac{C}{D} = -\frac{U(-\nu,|m+\mu|+1,\frac{m_e\omega a^2}{\hbar})}{M(-\nu,|m+\mu|+1,\frac{m_e\omega a^2}{\hbar})} = -\frac{U(-\nu,|m+\mu|+1,\frac{m_e\omega b^2}{\hbar})}{M(-\nu,|m+\mu|+1,\frac{m_e\omega b^2}{\hbar})} \tag{30}$$

instead of Eqs. (16)-(18). Of course, for the case in which $B_i = B_0$ the value of μ vanishes, Eq. (26), and the results of Sec. II are recovered. For the general case of interest here $B_i \neq B_0$, and the A-B effect on the Landau states in the annular cylindrical box is associated with the μ dependence of the radial eigenfunctions, Eq. (28), and the transverse eigenenergies, Eq. (29), determined by the values of ν_s solutions of Eq. (30), with $s = 1, 2, 3, \ldots$. Here the Eq. (A.3) for U must be used for non integer values of μ. Numerically computed values of ν_s and $E^T_{sm}(\mu)$ for different chosen values of μ are presented in the following section.

IV. Numerical results and discussion ,

This section contains some numerical and graphical results illustrating the confinement effect of the annular box on the Landau states, and the A-B effect on the same states, from the analysis in Section II and III, respectively. For the first one, the zeros of Eq. (18) in ν are based on the logarithmic form of the U function, Eq. (A.4). For the second one, Eq. (30) requires the use of the form of U of Eq. (A.3) for non-integer values of μ. Table I and Fig. 1 illustrate the confinement effect, and Table II and Fig. 2 the A-B effect on the Landau states, as explained and discussed next.

Table I presents the transverse energy eigenvalues E^T_{sm} for the Landau states with s = 1, 2, and 3, and $m = 0, \pm1, \pm2, \ldots$ obtained from Eqs. (15) and (18), for the electron confined in boxes with $b = 2a$, $5a$ and $10a$, in different magnetic induction fields producing magnetic fluxes of 1 and 15 fluxons in the circular cross sections of radius b. The values of ν_s from the numerical solution of Eq. (18), when doubled and increased by one unit, give the energy eigenvalues for the zero and negative m states; for the positive m states the further addition of $2m$ is required.

The confinement effect of the box on the electron Landau states is obviously manifested by the departure of the energy levels from the equally spaced and infinitely degenerate $(2N+1)\hbar\omega$ spectra with integer values of N. The data in Table I indicate that such an effect is dominant

TABLE I. Radial s and angular momentum m quantum numbers and transverse energy eigenvalues E^T_{sm} in units $\hbar\omega$, for an electron confined in boxes with $b = 2a$, $5a$ and $10a$, in magnetic induction fields defined by the dimensionless magnetic flux parameter $m_e\omega b^2/\hbar$.

$m_e\omega b^2/\hbar$		1	1	1	15	15	15
$m_e\omega a^2/\hbar$		0.25	0.04	0.01	3.75	0.6	0.15
s	m	E^T_{sm}	E^T_{sm}	E^T_{sm}	E^T_{sm}	E^T_{sm}	E^T_{sm}
1	0	19.79178	7.46920	5.65108	5.33410	2.46994	1.91268
	∓ 1	19.72188	8.16592	6.94048	4.40352	1.76000	1.23668
		21.72188	10.16592	8.94048	6.40352	3.76000	3.23668
	∓ 2	21.50142	11.84566	11.42684	3.61104	1.29718	1.03460
		25.50142	15.84566	15.42684	7.61104	5.29718	5.03460
	∓ 3	25.09870	17.67902	17.58700	2.95458	1.09156	1.00632
		31.09870	23.67902	23.58700	8.95458	7.09156	7.00632
	∓ 4	30.46266	25.06046	25.04484			
		38.46266	33.06046	33.04484			
	∓ 5	37.52606	33.74222	33.73996			
		47.52606	43.74222	43.73996			
2	0	79.00098	30.51030	23.69370	9.06064	5.06776	4.16546
	∓ 1	78.98152	31.64624	26.04792	8.72414	4.21142	3.41790
		80.98152	33.64624	28.04792	10.72414	6.21142	5.41790
	∓ 2	80.92192	36.95496	33.94736	7.91474	3.63896	3.11796
		84.92192	40.95496	37.94736	11.91474	7.63896	7.11796
	∓ 3	84.82974	45.94932	44.86382	7.23292	3.33512	3.09164
		90.82974	51.94932	50.86382	13.23292	9.33512	9.09164
3	0	177.69628	69.02626	54.02880	16.23734	7.82040	6.05602
	∓ 1	177.78674	70.32580	56.94516	15.30200	6.95948	5.74480
		179.78674	72.32580	58.94516	17.30200	8.95948	7.74480
	∓ 2	179.66006	76.24628	67.07614	14.49612	6.38078	5.44980
		183.66006	80.24628	71.07614	18.49612	10.38078	9.44980
	∓ 3	183.62184	86.71936	82.07110	13.82010	6.09200	5.53434
		189.62184	92.71936	88.07110	19.82010	12.09200	11.53434

TABLE II. Transverse energy eigenvalues E^T_{1m} as a function of the parameter $m+\mu$, Eq. (29), for electron confined in boxes with $m_e\omega b^2/\hbar = 1$ and the indicated values of $m_e\omega a^2/\hbar$ and signs of $m+\mu$.

$m_e\omega a^2/\hbar$	0.25		0.04		0.01	
$m+\mu$	$-$	$+$	$-$	$+$	$-$	$+$
$\|m+\mu\|$	E^T_{1m}	E^T_{1m}	E^T_{1m}	E^T_{1m}	E^T_{1m}	E^T_{1m}
0	19.79178	19.79178	7.46920	7.46920	5.65108	5.65108
0.2	19.62901	20.02901	7.33859	7.73859	5.54960	5.94960
0.4	19.54074	20.34074	7.34598	8.14598	5.64130	6.44130
0.6	19.52680	20.72680	7.48904	8.68904	5.91518	7.11518
0.8	19.58724	21.18724	7.76399	9.36399	6.35476	7.95476
1	19.72188	21.72188	8.16592	10.16592	6.94048	8.94048
1.2	19.93154	22.33154	8.68844	11.08844	7.65207	10.05207
1.4	20.21310	23.01310	9.32507	12.12507	8.47078	11.27078
1.6	20.56924	23.76924	10.06840	13.26840	9.38064	12.58064
1.8	20.99979	24.59979	10.91102	14.51102	10.36910	13.96910
2	21.50142	25.50142	11.84566	15.84566	11.42684	15.42684
2.2	22.09683	26.49683	12.86538	17.26538	12.54727	16.94727
2.4	22.72467	27.52467	13.96385	18.76385	13.72597	18.52597
2.6	23.44452	28.64452	15.13541	20.33541	14.95999	20.15999
2.8	24.23603	29.83603	16.37518	21.97518	16.24742	21.84742
3	25.09870	31.09870	17.67902	23.67902	17.58700	23.58700
3.2	26.03209	32.43209	19.04350	25.44350	18.97790	25.37790
3.4	27.03570	33.83570	20.46588	27.26588	20.41952	27.21952
3.6	28.10905	35.30905	21.94392	29.14392	21.91144	29.11144
3.8	29.25156	36.85156	23.47590	31.07590	23.45330	31.05330
4	30.46266	38.46266	25.06046	33.06046	25.04484	33.04484
4.2	31.74178	40.14178	26.69655	35.09655	26.76582	35.16582
4.4	33.08831	41.88831	28.38334	37.18334	28.37600	37.17600
4.6	34.50163	43.70163	30.12020	39.32020	30.11521	39.31521
4.8	35.98110	45.58110	31.90662	41.50662	31.90325	41.50325
5	37.52606	47.52606	33.74222	43.74222	33.73996	43.73996

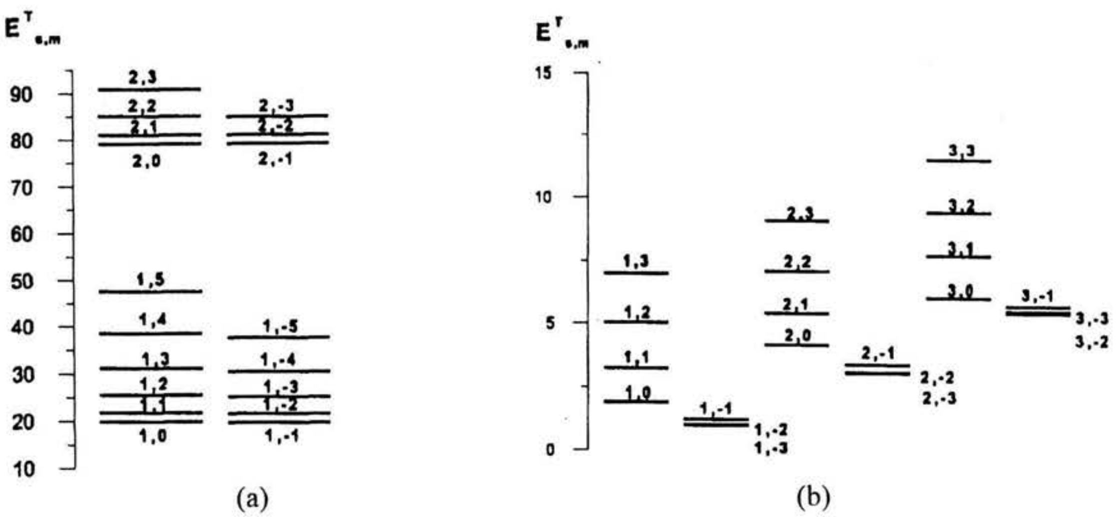

FIG. 1. Lower Landau energy levels E^T_{sm} for an electron confined in boxes with (a) $m_e\omega b^2/\hbar = 1$ and $m_e\omega a^2/\hbar = 0.25$ and (b) $m_e\omega b^2/\hbar = 15$ and $m_e\omega a^2/\hbar = 0.15$.

for the first set of three small boxes and decreases for the set of larger boxes; additionally, within each set, the effect is more noticeable for the boxes with larger perforations.

Figures 1a and 1b illustrate the change of the confinement effect as well as the magnetic field effects in the energy spectra of the electron for the boxes of the first and last columns, respectively. For the small box with $b = 1$ in the unit of length $(\hbar/m_e\omega)^{1/2}$ and large perforation $a = 0.5$, the confinement effect is large as illustrated by numerical values for the eigenergies of the $m = 0$ states in the box expressed in terms of the corresponding normal Landau eigenergies $E^T_{10} = 19.79178E^L_{10}$, $E^T_{20} = 26.33333E^L_{20}$, $E^T_{30} = 35.53925E^L_{30}$, a situation extensive to the other E^T_{sm} states. The reader should notice the different regions in the energy scale in Fig. 1a for the $s = 1$ and 2 energy levels due to the large size of the confinement effect; the inclusion of the $s = 3$ energy levels would require jumping to the region with $E^T_{sm} \geq 170$. The quasi-degeneracy of the energy levels $(s, m \geq 0)$ and $(s, -m-1)$ is readily noticeable, and can be understood as the result of the combination of the confinement effect and the magnetic effects associated with the Landau states, including the distinct behaviour of the $m > 0$ and $m < 0$ states due to the diamagnetic energy. On the other hand, Fig. 1b for a larger box with $b = \sqrt{15}$ and a small perforation $a = \sqrt{15/10}$, the energy scale is the same as for the normal Landau states because the confinement effect is appreciably reduced. Nevertheless it is still definitely present as the comparison $E^T_{10} = 1.91268E^L_{10}$, $E^T_{20} = 1.38849E^L_{20}$, $E^T_{30} = 1.21120E^L_{30}$ indicates. In this case all the energy levels with $s = 1$, 2, and 3 can be drawn together. The spacing of the energy levels for each value of s and the successive positive values of m is not far from 2, the normal Landau energy level spacing. On the other hand, the tendency to degeneracy of the energy levels, for each value of s and the successive negative values of $m = -1, -2, -3, \dots$, at the normal Landau energy level positions $1, 3, 5, \dots$ is explicitly apparent. The energy spectra for the electron in the boxes of columns 2-5 in Table I illustrate their intermediate behavior between the two situations explicitly discussed in connection with Figs. 1(a), 1(b).

Table II presents the transverse energy eigenvalues E^T_{sm} for the Landau states with s = 1 and m = 0, $\mp$ 1, $\mp$ 2, ... for an electron in boxes with b = 1 and a = 0.5, 0.2 and 0.1, when the magnetic induction fields in the perforation and in the box are different according to Eqs. (26) and (29). The values of ν_s are the numerical solutions of Eq. (30) and depend on the value of $|m+\mu|$. The energy eigenvalues themselves also depend on the value and sign of $m+\mu$, as distinguished in the corresponding columns. The first column gives the values of $|m+\mu|$ interpolating between the integer values of m already considered in Table I. Again the values for ν_s, when doubled and increased by one unit give the entries for the energies in the first, third and fifth columns for the states with $(m+\mu) < 0$, in which the rotational and diamagnetic energies cancel each other (see Eq. (29)). The energies for the following columns are obtained by the further addition of $2|m+\mu|$ and correspond to the states with $(m+\mu) > 0$, Eq. (29).

It is important to understand that the entries in each pair of columns of Table II are valid for the energies $E^T_{sm}(\mu)$ for the different combinations of the values of m of the chosen states, and of the differences μ of the magnetic induction field in the perforation with respect to the one in the box. For the sake of illustration let us consider the specific value $|m+\mu|$ = 0.2, common to $m+\mu$ = -0.2 and $m+\mu$ = 0.2. The negative value can be obtained from the following combinations (m,μ) : (0, -0.2), (-1, 0.8), (1, -1.2), (-2, 1.8), (2, -2.2)...; and the positive value from: (0, 0.2), (-1, 1.2), (1, -0.8), (-2, 2.2), (2, -1.8), ... All of them have the common value of ν_s obtained from Eq. (30) with $(m+\mu)$ = 0.2, and, as already stated, the energies for the states with the negative value of $(m+\mu)$ is the entry in the odd column, and the energy for the states with positive values of $(m+\mu)$ is twice this value above. The generalization of this result is

$$E^T_{sm}(m+\mu) = E^T_{sm+N}((m+N)+(\mu-N)), \tag{31}$$

with $N = 0, \pm1, \pm2, \ldots$ expressing the periodic repetition of the Landau energy levels of the electron in the annular box when the magnetic flux in the perforation changes by one fluxon, accompanied by a compensating shift of one unit in the angular momentum quantum number. This behaviour is graphically illustrated in Figs. 2(a) and 2(b) for the boxes with larger and smaller perforations.

For $\mu = 0$, the energy levels coincide with those of Fig. 1(a) and the third column of Table I. As μ increases from its initial value, the states with zero and positive values of m increase their energies, while the states with negative values of m decrease their energies; the state s = 1, m = -1 energy reaches its minimum value for $\mu \approx 0.5$ in Fig. 2(a) and $\mu \approx 0.8$ in Fig. 2(b). When μ reaches the value of 1, the first periodic repetition of Eq. (31) with N = 1 is realized, and continues as μ keeps on increasing. On the other hand, as μ decreases from zero, the states with zero and positive values of m decrease their energies, and the states with negative values of μ increase their energies; the state s = 1, m = 0 reaches its minimum value for $\mu \approx -0.5$ in Fig. 2(a) and $\mu \approx -0.2$ in Fig. 2(b). When μ reaches the value of -1, the first periodic repetition of Eq. (31) with $N = -1$ is realized, and continues as μ keeps on decreasing moving to the left in the graph. By drawing the energy curve $E_{10}(\mu)$ from the data of Table II, the other curves for E^T_{1m} are obtained from horizontal translations of that curve by m units, to the right for negative m and to the left for positive m. Here we have illustrated the A-B effect on the Landau states for the energy levels with s = 1, but it holds in general for any sm states, as expressed by Eq. (31).

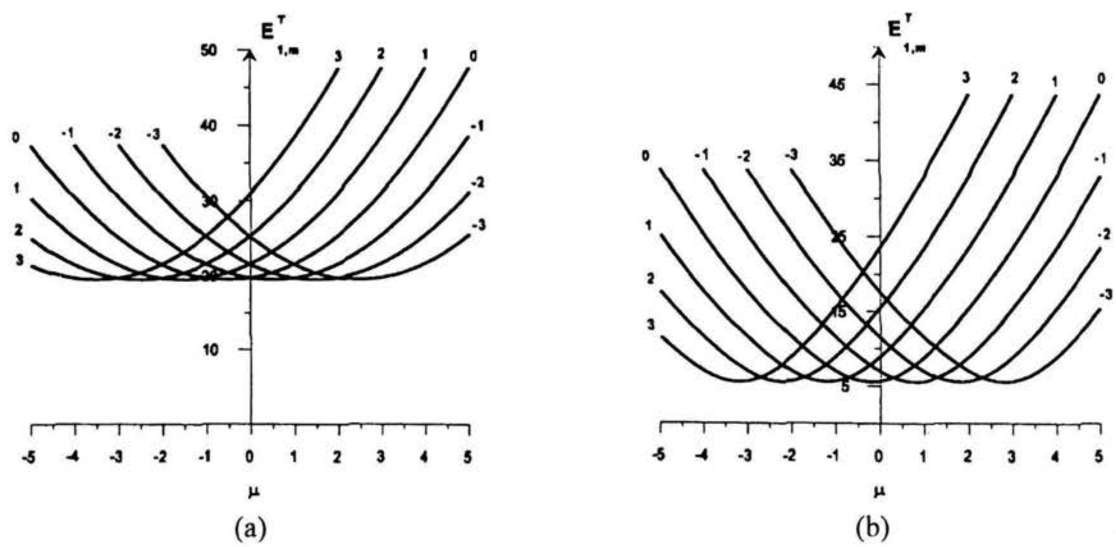

FIG. 2. Aharonov-Bohm effect on Landau energy levels $E^T_{sm}(\mu)$, as illustrated through their periodic dependence on the change of magnetic flux μ in the perforation of annular cylindrical boxes with $m_e\omega b^2/\hbar = 1$, and a) $m\omega_e\omega a^2/\hbar$ = 0.25 and b) $m_e\omega a^2/\hbar$ = 0.01.

In conclusion, this paper has presented an analysis of the confinement effect in annular cylindrical boxes on the Landau states, and of the A-B effect on such states. The signature of the Landau states in the first system is manifested through the higher energies of the positive m states and lower energies of the negative m states, including the evolution of their degeneracy as the boxes get larger. The A-B effect is manifested through the periodic repetition of the energy spectrum as a function of the variation of the magnetic flux in the perforation of the box with the corresponding shifts in the angular quantum number of the Landau states, and with a period of one fluxon.

APPENDIX A

The Kummer confluent hypergeometric functions M and U are defined by

$$M(\alpha,\beta,z) = \sum_{s=0}^{\infty} \frac{(\alpha)_s z^s}{(\beta)_s s!} \tag{A.1}$$

in terms of the Pochhammer symbol,

$$(\alpha)_0 = 1, \quad (\alpha)_s = \alpha(\alpha+1)\ldots(\alpha+s-1) = \frac{\Gamma(\alpha+s)}{\Gamma(\alpha)}; \tag{A.2}$$

and

$$U(\alpha,\beta,z) = \frac{\pi}{\sin\pi\beta}\left\{\frac{M(\alpha,\beta,z)}{\Gamma(1+\alpha-\beta)\Gamma(\beta)} - z^{1-\beta}\frac{M(1+\alpha-\beta,2-\beta,z)}{\Gamma(\alpha)\Gamma(2-\beta)}\right\}. \tag{A.3}$$

The series of Eq. (A.1) is convergent for all values of z and all values of α and β which are not negative integers. It becomes a polynomial of degree N when $\alpha = -N$ is a negative integer.

When β is a positive integer, Eq. (A.3) leads to the logarithmic form

$$\begin{aligned} U(\alpha, n+1, z) = \frac{(-)^{n+1}}{n!\Gamma(\alpha - n)} [&M(\alpha, n+1, z) \ln z \\ &+ \sum_{r=0}^{\infty} \frac{(\alpha)_r z^r}{(n+1)_r r!} \{\psi(\alpha + r) \\ &-\psi(1+r) - \psi(1+n+r)\}] \\ &+ \frac{(n-1)!}{\Gamma(\alpha)} z^{-n} M(\alpha - n, 1-n, z)_n, \end{aligned} \tag{A.4}$$

for $n = 0, 1, 2, \ldots$, where $\psi(x) = \Gamma'(x)/\Gamma(x)$ and the last factor is the sum of n terms with the value zero for $n = 0$. Their asymptotic forms for $z \to \infty$ are

$$M(\alpha, \beta, z) = \frac{\Gamma(\beta)}{\Gamma(\alpha)} e^z z^{\alpha - \beta} [1 + 0(|z|^{-1})], \tag{A.5}$$

$$U(\alpha, \beta, z) = z^{-\alpha} [1 + 0(|z|^{-1})]. \tag{A.6}$$

References

[1] L. D. Landau, Z. Phys. **64**, 629 (1930).
[2] L. D. Landau and I. M. Lifshitz, *Quantum Mechanics*. (Pergamon Press, Oxford, 1977).
[3] M. K. Fung and Y. F. Wang, Chin J. Phys. **37**, 435 (1999).
[4] Y. Aharonov and D. Bohm, Phys. Rev. **115**, 485 (1959).
[5] R. G. Chambers, Phys. Rev. Lett. **5**, 3 (1960).
[6] D. Kouznetsov, E. Ley-Koo and G. Villa-Torres, Rev. Mex. F´s **45**, 485 (1999).
[7] M. Abramowitz and I. Stegun, *Handbook of Mathematical Functions*, (Dover, New York, 1965) Chap. 13.

Aharonov-Bohm effect on the bound states of an electron inside an annular cylindrical box

D. Kouznetsov
Hopelchen 353 L13, Colonia Torres de Padierna, 14200 México, D.F. México

E. Ley-Koo and G. Villa-Torres
Instituto de Física, Universidad Nacional Autónoma de México
Apartado postal 20-364, 01000 México, D.F., Mexico

Recibido el 16 de marzo de 1999; aceptado el 1 de julio de 1999

We solve the Schröedinger equation for an electron inside an annular cylindrical box in two situations: *i)* in the absence of any fields, and *ii)* in the presence of a uniform, axial magnetic induction field confined and centered in the perforation. The Aharonov-Bohm effect on the bound states of the electron is exhibited through the analysis of the dependence of the energy eigenvalues and eigenfunctions on the enclosed magnetic flux. The results of this study serve to illustrate the roles of the magnetic vector potential and the gauge transformations in quantum mechanics.

Keywords: Magnetic vector potential in quantum mechanics

Se resuelve la ecuación de Schröedinger para un electrón en el interior de una caja anular cilíndrica en dos situaciones; *i)* en ausencia de cualquier campo, y *ii)* en presencia de un campo de inducción magnética axial y uniforme confinado y centrado en la perforación. Se exhibe el efecto Aharonov-Bohm sobre los estados ligados del electrón a través del análisis de la dependencia de los eigenvalores de la energía y las eigenfunciones con respecto al flujo magnético encerrado. Los resultados de este estudio sirven para ilustrar los papeles del potencial vectorial magnético y las transformaciones de norma en mecánica cuántica.

Descriptores: Potencial vectorial magnético en mecánica cuántica

PACS: 03.65

1. Introduction

It is almost forty years since Aharonov and Bohm analyzed the significance of the electromagnetic vector potential in quantum theory, and suggested an experiment to test for the effect of the potential in regions where there are no magnetic fields [1]. They predicted that the fringe pattern in an electron interference experiment should be shifted by altering the amount of magnetic flux passing between two beams, even though the beams themselves pass only through field-free regions. Specifically, a shift of ν fringes is associated with an enclosed flux of $\nu hc/e$, where the natural unit of flux or fluxon, $hc/e = 4.135 \times 10^{-7}$ gauss $\cdot$ cm^2, is determined by the Planck constant h, the velocity of light c, and the electron's electric charge e. Within a year, Chambers performed such an experiment reporting the expected shifts of an electron interference pattern by the corresponding magnetic fluxes, including situations in which the pattern appears unchanged due to their association with magnetic fluxes of an integer number of fluxons [2].

It is also twenty years since two didactic articles on related topics were published [3, 4]. In the first one, Konopinski discussed the explicit physical meaning and direct measurability of the electromagnetic vector potential in the classical context. And in the second one, Kobe deduced Maxwell's equations from the gauge invariance of quantum mechanics. Konopinski's book on electromagnetism [5] and Sakurai's books on quantum mechanics [6, 7] contain more detailed treatments of these topics.

Bound state versions of the Aharonov-Bohm effect have also been discussed in the literature [8, 9]. In the specialized book of Peshkin and Tonomura [8], the first author illustrated the effect for the charged rotator in a plane, and pointed out that there are no important changes if the motion is allowed to be three-dimensional inside a torus. In Ballentine's book [9] the charged particle confined to the interior of a torus of rectangular cross-section is also used to recognize that the energy of the stationary states must depend on the magnetic flux in the perforation. In both references the respective authors considered that the detailed quantitative analysis of the problem was not necessary for their purposes.

This paper presents a bound state version of the Aharonov-Bohm effect through the study of the energy spectra and eigenfunctions of an electron inside an annular cylindrical box in two comparative situations: *i)* in the absence of any fields, and *ii)* in the presence of a uniform, axial magnetic induction field confined and centered in the perforation with its associated magnetic vector potential in the interior of the box. In Sect. 2, the reference problem of situation *i)* is formulated and solved for the electron inside a box defined in cylindrical coordinates ($a \leq \rho \leq b$, φ, $0 \leq z \leq L$). Section 3 contains the formulation and solution of the Aharonov-

Bohm problem involving a magnetic induction field $\vec{B} = \hat{k}B$ confined in $(0 < \rho < \rho_0 \leq a,\ \varphi,\ z)$ and the magnetic vector potential $\vec{A} = \hat{\varphi}B\rho_0^2/2\rho$ inside the box. Section 4 presents illustrative numerical and graphical results of the solutions for the energy eigenvalues and eigenfunctions as the magnetic flux enclosed inside the perforation, $\nu = (B\pi\rho_0^2)/(hc/e)$, is changed. Section 5 contains a discussion of the Aharonov-Bohm effect on the bound states with emphasis on the symmetry and periodicity of the energy spectra as functions of ν, including the degeneracies for integer and half-integer values.

2. The electron inside an annular cylindrical box

The Schröedinger equation for the electron inside an annular cylindrical box in cylindrical coordinates,

$$-\frac{\hbar^2}{2m_e}\left[\frac{1}{\rho}\frac{\partial}{\partial\rho}\rho\frac{\partial}{\partial\rho} + \frac{1}{\rho^2}\frac{\partial^2}{\partial\varphi^2} + \frac{\partial^2}{\partial z^2}\right]\psi(\rho,\varphi,z) = E\psi(\rho,\varphi,z), \quad (1)$$

must be solved subject to the boundary condition that the wavefunction vanishes at the positions of the walls of the box:

$$\psi(\rho = a,\varphi,z) = \psi(\rho = b,\varphi,z) = 0, \quad (2a)$$

$$\psi(\rho,\varphi,z) = \psi(\rho,\varphi + 2\pi,z), \quad (2b)$$

$$\psi(\rho,\varphi,z = 0) = \psi(\rho,\varphi,z = L) = 0. \quad (2c)$$

Equation (1) is known to admit the separable solution

$$\psi(\rho,\varphi,z) = R(\rho)\Phi(\varphi)Z(z), \quad (3)$$

in which the respective factors satisfy the ordinary differential equations

$$\frac{\mathrm{d}^2 Z(z)}{\mathrm{d}z^2} = -k_L^2 Z(z), \quad (4a)$$

$$\frac{\mathrm{d}^2\Phi(\varphi)}{\mathrm{d}\varphi^2} = -m^2\Phi(\varphi), \quad (4b)$$

$$\left[\frac{1}{\rho}\frac{\mathrm{d}}{\mathrm{d}\rho}\rho\frac{\mathrm{d}}{\mathrm{d}\rho} - \frac{m^2}{\rho^2}\right]R(\rho) = -k_T^2 R(\rho), \quad (4c)$$

and the energy eigenvalue is the sum of the transverse and longitudinal contributions,

$$E = \frac{\hbar^2}{2m_e}(k_T^2 + k_L^2). \quad (5)$$

The solutions of Eq. (4a) subject to the boundary conditions of Eq. (2c) are

$$Z(z) = \sqrt{\frac{2}{L}}\sin\frac{n\pi z}{L}, \qquad n = 1,2,3,\ldots \quad (6)$$

The solutions of Eq. (4b) are the eigenfuctions of the z-component of the orbital angular momentum,

$$\Phi(\varphi) = \frac{e^{im\varphi}}{\sqrt{2\pi}}, \qquad m = 0,\pm1,\pm2,\ldots \quad (7)$$

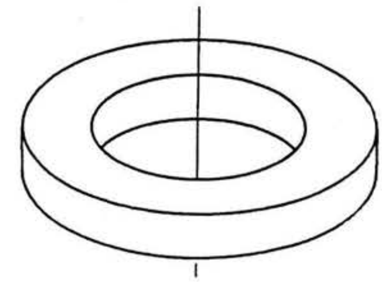

FIGURE 1. Annular cylindrical box with inner radius a, outer radius b and height L. A uniform axial magnetic induction field is applied and centered in the perforation.

Equation (4c) is recognized as the Bessel equation and its general solution is the linear combination of the ordinary Bessel function and the Neumann function [10],

$$R(\rho) = \mathcal{A}_m J_m(k_T\,\rho) + \mathcal{B}_m Y_m(k_T\,\rho), \quad (8)$$

since m is an integer, Eq. (7). The boundary conditions of Eqs. (2a) on this solution are expressed by

$$\mathcal{A}_m J_m(k_T a) + \mathcal{B}_m Y_m(k_T a) = 0, \quad (9a)$$

$$\mathcal{A}_m J_m(k_T b) + \mathcal{B}_m Y_m(k_T b) = 0. \quad (9b)$$

This is a set of two algebraic homogeneous linear equations for the unknown coefficients $\mathcal{A}_m$ and $\mathcal{B}_m$, which admits non-trivial zero solutions only if its determinant vanishes, *i.e.*,

$$J_m(k_T a)Y_m(k_T b) - J_m(k_T b)Y_m(k_T a) = 0. \quad (10)$$

This transcendental equation has to be solved numerically to obtain the transverse wave number k_T. The task is accomplished by using numerical recipes in C [11]. Let $k_T a = x_{ms}$ be the successive solutions $s = 1,2,3,\ldots$, for given values of a and b. The energy eigenvalues of Eq. (5) with the explicit values of the wavenumbers from Eqs. (5) and (10) are given by

$$E_{msn} = \frac{\hbar^2}{2m_e}\left(\frac{x_{ms}^2}{a^2} + \frac{n^2\pi^2}{L^2}\right), \quad (11)$$

in terms of the azimuthal m, radial s and axial n quantum numbers.

The ratio of the coefficients $\mathcal{A}_m$ and $\mathcal{B}_m$ follows from Eq. (9a) or Eq. (9b), and it allows to write the normalized radial eigenfuction, Eq. (8), as

$$R_{ms}(\rho) = \frac{1}{\sqrt{\mathcal{N}_{ms}}}\left[Y_m\left(\frac{x_{ms}b}{a}\right)J_m\left(\frac{x_{ms}\rho}{a}\right) - J_m\left(\frac{x_{ms}b}{a}\right)Y_m\left(\frac{x_{ms}\rho}{a}\right)\right], \quad (12)$$

where the normalization constant is

$$\mathcal{N}_{ms} = \int_a^b \left[Y_m\left(\frac{x_{ms}b}{a}\right)J_m\left(\frac{x_{ms}\rho}{a}\right) - J_m\left(\frac{x_{ms}b}{a}\right)Y_m\left(\frac{x_{ms}\rho}{a}\right)\right]^2 \rho\,\mathrm{d}\rho. \quad (13)$$

The problem of this section has also been studied in the specialized research literature [12].

3. Aharonov-Bohm effect on the bound states of the electron

In this section we formulate and solve the problem with the magnetic induction field confined in the perforation of the annular box and its associated magnetic vector potential inside the box. The Hamiltonian for the system is given by the minimal coupling prescription

$$\hat{H} = \frac{(\hat{\vec{p}} + \frac{e}{c}\vec{A})^2}{2m_e}, \tag{14}$$

in which $\hat{\vec{p}} = -i\hbar\nabla$ is the "conjugate" momentum and the second term is the negative of the "potential momentum" of the electron in the magnetic vector potential [3, 5]. Then the Schödinger equation can be written as

$$\left\{ -\frac{\hbar^2}{2m_e}\frac{1}{\rho}\frac{\partial}{\partial\rho}\rho\frac{\partial}{\partial\rho} + \frac{\left(\ell_z + \frac{eB\rho_0^2}{2c}\right)^2}{2m_e\rho^2} - \frac{\hbar^2}{2m_e}\frac{\partial^2}{\partial z^2}\right\}\psi(\rho,\varphi,z) = E\psi(\rho,\varphi,z). \tag{15}$$

Comparison of Eqs. (1) and (15) shows that they share the same radial and longitudinal contributions to the kinetic energy, and their difference resides in the extra term arising from the magnetic vector potential and added to the z-component of the angular momentum

$$\frac{eB\pi\rho_0^2}{2\pi c} = \hbar\nu, \tag{16}$$

where ν is the magnitude of the magnetic flux in the perforation in the units hc/e. Equation (15) also admits a separable solution of the same form as Eq. (3). Equations (4a) and (6) for the longitudinal eigenfunctions continue to be valid. The eigenfunctions of the z-component of the angular momentum of Eq. (7) are also eigenfunctions of the angular operator of Eq. (15):

$$(\hat{\ell}_z + \hbar\nu)\Phi_m(\varphi) = \hbar(m+\nu)\Phi_m(\varphi). \tag{17}$$

Then the radial part of Eq. (15) becomes

$$\left[\frac{1}{\rho}\frac{\mathrm{d}}{\mathrm{d}\rho}\rho\frac{\mathrm{d}}{\mathrm{d}\rho} - \frac{(m+\nu)^2}{\rho^2}\right]R(\rho) = -k_{\mathrm{T}}^2\, R(\rho). \tag{18}$$

Comparison of the radial Eqs. (4c) and (18) shows that they are of the same type with the difference in their parameters,

$$m \longrightarrow M = m + \nu. \tag{19}$$

While the values of m are restricted to be integers, Eq. (7), the values of M can vary continuously following the corresponding variations of the magnetic flux ν. The solution of the radial Eq. (18) follows the same steps of Eqs. (8)–(13) with the substitution of m by M of Eq. (19).

It is also important to recognize that while the eigenstates of Eq. (4c) given by Eq. (12) are doubly degenerate for $m = \pm1, \pm2, \ldots$, such a degeneracy is removed when there is magnetic flux in the perforation, since the corresponding parameters from Eq. (19), $M = |m| + \nu$ and $M = -|m| + \nu$ are different. On the other hand, starting from given values of m and ν there are an infinite number of combinations of successive values of such parameters,

$$M = m + \nu = (m - N) + (\nu + N), \qquad N = 0, \pm1, \pm2, \pm3, \ldots \tag{20}$$

consistent with the same value of M. The different states for the different magnetic fluxes have the same energies, which translates into a periodic repetition of the energy spectrum as the magnetic flux increases by one unit. In particular, the energy spectra for $\nu = 1, 2, 3, \ldots$ are the same as for $\nu = 0$ including ground states with $m = -1, -2, -3, \ldots$ and excited doubly degenerate states with $m = 0$ and -2, 1 and -3, 2 and $-4, \ldots$; -1 and -3, 0 and -4, 1 and $-5, \ldots$; -2 and -4, -1 and -5, 0 and $-6, \ldots; \ldots$; respectively. By considering the interval $0 < \nu < 1$, and the states with $m = |m|$ and $-|m| - 1$, we identify the common value of

$$M = |m| + \nu \quad \text{and} \quad -M = -(|m|+1) + (1-\nu), \tag{21}$$

leading to the same values of the transverse energies. Notice that the states involved are neighbour states in the angular momentum quantum number and have the same energy for complementary values of the magnetic flux, ν and $1-\nu$. The net result is that the energy of the $|m|$-state increases monotonically as ν changes between 0 and 1, while the energy of the $(-|m|-1)$-state also increases monotonically in the same way as $1-\nu$ changes between 0 and 1. In other words, the latter decreases monotonically as ν changes between 0 and 1. For $\nu = 0.5$ both states have the same energy for the common value of the magnetic flux, producing another situation of double degeneracy. The respective energy curves are symmetric relative to the line $\nu = 0.5$.

4. Illustrative numerical and graphical results

In this section we present some quantitative results illustrating the solutions of the eigenvalue problems formulated in Sects. 2 and 3. The emphasis is on the transverse contribution to the energy eigenvalues and the associated radial eigenfunctions. The numerical results are contained in tables and figures for both cases $\nu = 0$ and $\nu \neq 0$ together.

Figure 2 is a graph of the determinant appearing in Eq. (10)

$$D_M(x) = J_M(x)Y_M\left(\frac{bx}{a}\right) - Y_M(x)J_M\left(\frac{bx}{a}\right), \tag{22}$$

as a function of $x = k_{\mathrm{T}}a$ for different values of the parameter M, Eq. (19), and for the specific case of $b = 2a$. Its zeros x_{Ms}, determined through the corresponding program of [11], are contained in Table I.

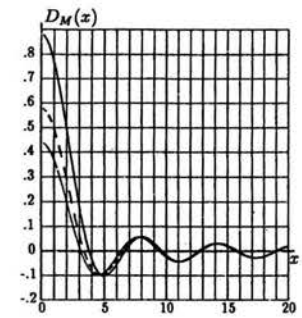

FIGURE 2. Graph of the determinant $D_M(x)$ of Eq. (22) for $M = 0$ (thin line), 1.9 (dashed line) and 3.14 (solid line), and $b = 2a$. Its zeros determine the transverse wave number and the energy eigenvalues according to Eqs. (10) and (11).

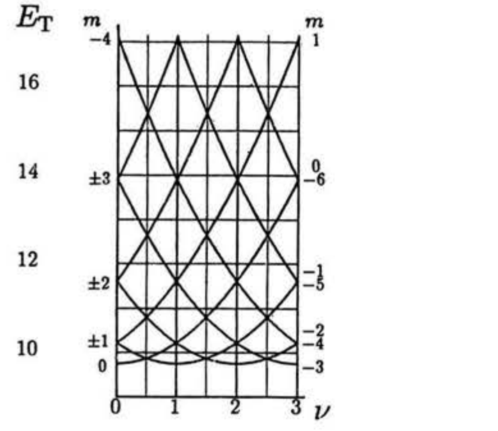

FIGURE 3. Transverse energy eigenvalues E_T in units $\hbar^2/2m_e a^2$ as functions of the magnetic flux ν in units ch/e, for states with the lowest angular excitations $m = 0, \pm 1, \pm 2, \ldots$ and no radial excitation $s = 1$, and $b = 2a$.

TABLE I. Zeros of Eq. (22) x_{Ms} for different values of M and s, and $b = 2a$. Their squares correspond to the transverse energy eigenvalues, Eq. (11).

M \ s	1	2	3	4
0.0	3.12303	6.27344	9.41821	12.56142
0.2	3.12601	6.27500	9.41926	12.56221
0.4	3.13492	6.27968	9.42241	12.56459
0.6	3.14972	6.28747	9.42767	12.56855
0.8	3.17031	6.29837	9.43502	12.57408
1.0	3.19658	6.31235	9.44447	12.58120
1.2	3.22836	6.32940	9.45600	12.58990
1.4	3.26550	6.34950	9.46961	12.60017
1.6	3.30778	6.37261	9.48530	12.61201
1.8	3.35500	6.39871	9.50305	12.62541
2.0	3.40692	6.42777	9.52285	12.64038
2.2	3.46332	6.45974	9.54470	12.65691
2.4	3.52396	6.49458	9.56857	12.67499
2.6	3.58859	6.53226	9.59447	12.69461
2.8	3.65697	6.57272	9.62236	12.71578
3.0	3.72887	6.61592	9.65225	12.73848
3.2	3.80406	6.66181	9.68410	12.76271
3.4	3.88231	6.71033	9.71791	12.78846
3.6	3.96342	6.76144	9.75365	12.81572
3.8	4.04716	6.81507	9.79131	12.84449
4.0	4.13337	6.87116	9.83086	12.87474
4.2	4.22183	6.92967	9.87230	12.90649
4.4	4.31239	6.99054	9.91559	12.93971
4.6	4.40488	7.05369	9.96072	12.97440
4.8	4.49914	7.11908	10.00766	13.01055
5.0	4.59502	7.18665	10.05639	13.04814

TABLA II. Transverse wavenumbers $k_T = x_{Ms}/a$ and coefficients of normalized radial eigenfunction $\mathcal{A}_{Ms}$ and $\mathcal{B}_{Ms}$, Eqs. (8) and (12), for different values of M and s, and $b = 2a$.

M	s	x_{Ms}	$\mathcal{A}_M$	$\mathcal{B}_M$
0	1	3.123039	1.18538	1.37124
	2	6.273439	1.73003	1.89366
	3	9.418211	2.14125	2.29878
	4	12.561424	2.48549	2.64229
	5	15.704000	2.78759	2.94595
	6	18.846249	3.06003	3.22109
1.9	1	3.380384	−1.80494	0.17472
	2	6.412872	−2.48722	−0.60375
	3	9.512694	−2.93332	−1.11832
	4	12.632701	−3.29758	−1.50910
	5	15.761176	−3.61801	−1.83150
	6	18.893965	−3.90917	−2.11052
3.14	1	3.781170	−1.42795	−1.10560
	2	6.647763	−0.21997	−2.55717
	3	9.674336	0.79896	−3.03178
	4	12.755284	1.54066	−3.28064
	5	15.859745	2.11991	−3.45593
	6	18.976334	2.59959	−3.60214

Figure 3 shows the energy levels of the states with lowest angular excitations $m = 0, \pm 1, \pm 2, \ldots$ and no radial excitation $s = 1$, as functions of the magnetic flux ν in the perforation. According to Eq. (11) and its extension for the case $\nu \neq 0$, the energy levels correspond to the squares of the zeros of Table I, x^2_{Ms}, in units of $\hbar^2/(2m_e a^2)$. The reader may appreciate the periodicity of the energy spectra as ν changes by one unit, the double degeneracy of the states for integer and half-integer values of ν, and the symmetry of the energy curves within each unit interval of ν under reflection with respect to the line with the corresponding half-integer value of ν.

Table II presents a sample of the coefficients $\mathcal{A}_M$ and $\mathcal{B}_M$ of the radial function of Eq. (8) and its extensions for $\nu \neq 0$, normalized according to Eqs. (12) and (13).

5. Discussion

The comparative analysis of the formulations and results of the problems of Sects. 2 and 3 serves to exhibit the effects of the magnetic vector potential on the energy eigenvalues and eigenstates of the electron inside the annular box, in which there is no magnetic force field. From the analysis at the end of Sect. 3 and the results of Sect. 4 some general statements about the Aharonov-Bohm effect on the electron's energy eigenvalues, as functions of the magnitude of the magnetic flux in the perforation, can be made. These statements are valid for any chosen values of the radial and longitudinal quantum numbers s and n.

1) The energy eigenvalues of the states with $m = 0, 1, 2, \ldots$ increase monotonically with ν, in such a way that

$$E_m(\nu + 1) = E_{m+1}(\nu), \tag{23a}$$

and the corresponding iterative extension

$$E_m(\nu + N) = E_{m+N}(\nu) \quad \text{for} \quad N = 1, 2, 3, \ldots \tag{23b}$$

2) The energy eigenvalues with $m = -1, -2, \ldots$ decrease monotonically at first, in such a way that they follow Eqs. (23a) and (23b) with the negative values of m, until the magnetic flux takes the values $\nu = -m$. From this value on, each one increases following the same Eqs. (23a) and (23b).

3) Equations (23a) and (23b) describe the periodic nature of the energy spectra as functions of the magnetic flux ν with period one.

A. For $\nu = 0$, the ground state $m = 0$ is nondegenerate and the excited states $m = \pm 1, \pm 2, \ldots$ are doubly degenerate. For $\nu = N$, the ground state is the $m = -N$ state and the doubly degenerate excited states correspond to $m = -N - K$ and $-N + K$, with $K = 1, 2, 3, \ldots$

B. For $\nu = 0.5$ the ground and excited states are all doubly degenerate corresponding to $m = 0$ and -1, and K and $-K - 1$, with $K = 1, 2, 3, \ldots$ respectively. For $\nu = N + 0.5$, the corresponding states have $m = -N$ and $-N - 1$, and $-N + K$ and $-N - 1 - K$.

C. The symmetry of the energy curves in the interval $0 \leq \nu \leq 1$ with respect to reflection in the line $\nu = 0.5$, is repeated in each interval $N \leq \nu \leq N + 1$ with respect to reflection in the line $\nu = N + 0.5$.

It is also instructive to evaluate the energy of the radiative transitions between two transverse states, which follows from the counterpart of Eq. (11) with the substitution $m \to M$ and for the same longitudinal quantum number $n' = n$ with the result

$$\Delta E(Msn \to M's'n) = \frac{\hbar^2}{2m_e a^2}\left(x_{Ms}^2 - x_{M's'}^2\right) \quad \text{for} \quad m' = m \pm 1. \tag{24}$$

The selection rule for the angular momentum quantum number m is the usual standard one for electric dipole transitions [6, 7]. The size of the annular box determines the region of the spectrum for the corresponding radiations. In practice, they could be detected in microscopic conducting rings [13], mesoscopic semiconducting devices [14] and nanometric quantum dots [15], corresponding to microwave, far infrared and near infrared radiations, respectively. While the enclosed magnetic flux is not always quantized, the Aharonov-Bohm effect should open new possibilities in the construction of ultra-sensitive detectors.

As a conclusion of this discussion it is also enlightening to compare the Aharonov-Bohm effect in the standard version of the interference pattern of the electrons and of the electron bound-states version of this paper. The common feature of both versions is their periodicity with period $\nu = 1$, of the interference pattern and of the energy spectrum, respectively. Both versions are solutions of the same physical problem described by the common Schröedinger equation, and their difference consists in their correspondence with scattering states and bound states, respectively.

1. Y. Aharonov and D. Bohm, *Phys. Rev.* **115** (1959) 485.
2. R.G. Chambers, *Phys. Rev. Lett.* **5** (1960) 3.
3. E.J. Konopinski, *Am. J. Phys.* **46** (1978) 499.
4. D.H. Kobe, *Am. J. Phys.* **46** (1978) 342.
5. E.J. Konopinski, *Electromagnetic Fields and Relativistic Particles*, (McGraw-Hill, New York, 1981) p. 158.
6. J.J. Sakurai, *Advanced Quantum Mechanics*, (Addison-Wesley, Reading MA, 1967) p. 11, p. 14, and p. 41.
7. J. J. Sakurai and S.F. Tuan, *Modern Quantum Mechanics*, (Addison-Wesley, Reading, MA, 1994) p. 130 and p. 338.
8. M. Peshkin and A. Tonomura, *The Aharonov-Bohm Effect*, (Springer-Verlag, Berlin Heidelberg, 1989) p. 10.
9. L. Ballentine, *Quantum Mechanics*, (Prentice Hall, Englewood Cliff, N.J., 1990) p. 222.
10. M. Abramowitz and I. Stegun, *Handbook of Mathematical Functions*, (Dover, New York, 1965) Chapt. 9.
11. W.H. Press, S.A. Teukolsky, W.T. Vitterling, and B.P. Flannery, *Numerical Recipes in C. The Art of Scientific Computing*, (U.P. Cambridge New York, U.S.A., 1992) Chapt. 9.
12. M. Kumagai and T. Ohno, *Solid State Commun.* **83** (1992) 837.
13. R.A. Webb, S. Washburn, C.P. Umbach, and R.B. Leibowitz, *Phys. Rev. Lett.* **54** (1985) 2696.
14. G. Timp *et al.*, *Phys. Rev. Lett.* **58** (1987) 2814.
15. C.J.B. Ford *et al.*, *Phys. Rev.* **B43** (1991) 7339.

ENSEÑANZA REVISTA MEXICANA DE FÍSICA 47 (6) 576–581 DICIEMBRE 2001

Classical analysis of the Aharonov-Bohm effect

E. Ley-Koo[1] and G. Villa-Torres
Instituto de Física, Universidad Nacional Autónoma de México
Apartado postal 20-364, 01000 México, D.F., México
e-mail: [1] eleykoo@fisica.unam.mx

Recibido el 30 de marzo de 2001; aceptado el 14 de septiembre 2001

This work presents an analysis of the Aharonov-Bohm effect taking into account both regions where the electron is present and where it is excluded, and also the time variations of the magnetic vector potential and the magnetic induction field as they change between two of their stationary values. This analysis allows the identification of the electrical force field induced in the region where the electron is present by the time variation of the magnetic flux in the region where the electron is excluded, thus providing a classical explanation of the changes in the stationary properties of the electron when the magnetic potential and field change from one set of stationary values to another. Some apparent contradictions in attempts to interpret the A-B effect are also discussed and clarified.

Keywords: Magnetic vector potential in quantum mechanics; particles in electromagnetic fields

En este trabajo se presenta un análisis del efecto Aharonov-Bohm, tomando en cuenta las regiones donde el elelectrón está presente y donde está excluido, y también las variaciones en el tiempo del potencial vectorial y el campo de inducción magnética cuando cambian entre dos de sus valores estacionarios. Este análisis permite la identificación del campo de fuerza eléctrica inducido en la región donde está el electrón por la variación en el tiempo del flujo magnético en la región donde el electrón está excluido, proporcionando así una explicación clásica de los cambios en las propiedades estacionarias del electrón cuando el potencial y el campo magńeticos cambian de un conjunto de valores estacionarios a otro. También se discuten y aclaran algunas contradiccciones aparentes en intentos de interpretar el efecto A-B.

Descriptores: Potencial vectorial magnético en mecánica cuántica; partículas en campos electromagnéticos

PACS: 03.65; 41.70

1. Introduction

The original Aharonov-Bohm (A-B) effect is manifested as the change in the fringe pattern in an electron interference experiment due to the change in the magnetic flux in a region between two electron beams, even though the two beams themselves pass only through a field-free region [1]. The authors were interested in the significance of the electromagnetic vector potential in quantum theory, and came up with this effect testing the potential in a region where the magnetic induction field is absent. Chambers carried out the electron interference experiments around a magnetized whisker confirming the effect predicted by Aharonov and Bohm [2].

Bound state versions of the A-B effect have also been analyzed [3, 4]. Peshkin illustrated the changes in the energy spectrum of a charged rotator in a plane and around an infinite solenoid perpendicular to the plane, due to the change in the magnetic flux inside the solenoid [3]. The A-B effect on the energy eigenvalues and eigenfunctions of the bound states of an electron inside an annular cylindrical box was quantitatively evaluated and illustrated in Ref. 4. In this work, it was also recognized that the electron bound-state and interference versions of the A-B effect are described by the same Schrödinger equation, differing their solutions by the corresponding boundary conditions, but sharing the common feature of energy spectra and interference patterns that are periodic in the magnetic flux in the region where the electrons are excluded. The period is one fluxon $hc/e = 4.135 \times 10^{-7}$ gauss cm^2, the natural unit of flux determined by Planck's constant, the speed of light and the charge of the electron. Our group has also investigated the A-B effect on Landau states of electrons in annular cylindrical boxes and in quantum antidots [5–7].

The Schrödinger equation describes the time evolution of the wave-function of a quantum system. The hamiltonian operator appearing in the equation includes the kinetic and potential energy terms. When the quantum system participates in electromagnetic interactions, the latter are incorporated via the minimal coupling prescription $\vec{p} \to \vec{p} - q/c\vec{A}$, where $\vec{p}$ is the conjugate momentum, q is the electric charge of the particle and $\vec{A}$ is the vector potential. It was in this context that Aharonov and Bohm analyzed the significance of $\vec{A}$ in quantum mechanics [1].

On the other hand, classical mechanics in the newtonian version formulates the time evolution of the system in terms of forces. Of course, in hamiltonian classical mechanics the time evolution of a system is formulated in terms of the hamiltonian function. In any case the equivalence of the newtonian and hamiltonian formulations of classical mechanics are well established. Appendix A contains some of their basic equations and connections.

Classical electrodynamics has also been formulated in terms of the force fields, electric intensity $\vec{E}(\vec{r}, t)$ and magnetic induction $\vec{B}(\vec{r}, t)$, and in terms of the potential fields, the scalar potential $\phi(\vec{r}, t)$ and the vector potential $\vec{A}(\vec{r}, t)$. Feynman [8] and Konopinski [9, 10] have explained the physical meaning of the latter in the classical context, and their works serve as a bridge to understand the quantum A-B effect. Appendix B contains the basic equations of the alternative descriptions of the electromagnetic field, and most important the connections between them.

There are several features of the A-B effect that are worth emphasizing since they contribute to make it interesting, and even mysterious, and are also at the root of some apparent contradictions in attempts to interpret it. First, the distinction between the region where the electron is present and there is no magnetic induction field, and the region where the electron is excluded and the magnetic induction field may change. Second, in both regions there is a magnetic vector potential with a different space dependence in each region, and a magnitude proportional to the magnetic induction. Third, the electron is not subject to any force as it follows from the vanishing of the fields in Eq. (29), but shares the interaction momentum with the vector potential as stated by Eq. (34). Fourth, the electron interference and bound state versions of the A-B effect correspond to stationary situations.

Different interpretations of the A-B effect have been proposed and here some of them are illustrated in order to appreciate the issues that they have raised and addressed. The original authors attributed the change in the electron interference pattern to the local physical effects of the electromagnetic vector potential [1]. Since the primary source of the effect is the change in the magnetic flux in the region where the electron is excluded, the latter's action takes place non-locally or through the local vector potential in the region where the electron is present. Boyer has investigated alternative explanations in terms of classical local electromagnetic fields [11–13]. His position is illustrated through a couple of paragraphs from Ref. 13:

> "The solenoid Aharonov-Bohm effect has attracted considerable attention, partly because the experimental effects are said to be produced without electromagnetic fields being present. Aharonov and Bohm have provided the presently accepted view that indeed electromagnetic fields are not present outside the solenoid, and the observed effects are due to local physical effects of the electromagnetic vector potential. However, this view may be wrong. We suspect that the experimental effects are actually due to electromagnetic fields acting locally and that the only new physics involves an unrecognized classical-electromagnetic-lag effect arising from electromagnetic fields of the multiparticle soleinod system."

He also questioned the work of Feynman

> "..., and a new physical role for the electromagnetic vector potential has now passed into the physics textbook literature," referring to Ref. 8.

Rubio, Getino, and Rojo, in their work "The Aharonov-Bohm effect as a classical Electromagnetic Effect Using Electromagnetic Potentials" [14], start out by recognizing the dispute about whether the force fields or the potentials are the "fundamental" quantities in electromagnetism, and conclude "we agree with Boyer in this interpretation of the AB and AC effects as due to classical lag effects, but instead of rejecting the electromagnetic potentials as something unphysical, we consider them as the fundamental entities of electromagnetism, both quantum and classical." The question of the locality or non-locality of the interaction responsible for the A-B effect, is discussed in Ref. 15.

The literature about the prediction, experimental observation and interpretations of the A-B effect is predominantly in the research area. The present contribution is written from a didactical perspective, recognizing from the outset that there are two complementary, rather than opposing, classical descriptions of the dynamical and electromagnetic phenomena, as summarized in Appendices A and B. Both descriptions are taken into account in Sec. 2 in order to analyze the A-B effect, considering

i) Both regions where the electron is present and excluded.

ii) The magnetic potential and magnetic induction in both regions.

iii) Including their time variations between two sets of their stationary values.

iv) Identifying the presence of the induced electric intensity field and evaluating its time and space integrated effects on the motions of the electron around the region where it is excluded.

The analysis based on *i*) and *ii*) is the standard one to obtain the hamiltonian of the electron. The analysis based additionally on *iii*) and *iv*) is a new one, leading to the same results as the previous one. The equivalence of both analysis, one starting from the magnetic vector potential and the other from the electric intensity field, allows a better understanding of the A-B effect and some of its interpretations as discussed in Sec. 3.

2. Analysis of the Aharonov-Bohm effect in terms of the time changes of the potential and force fields

The idealized experimental situation, on which the analysis of the A-B effect is based, involves and infinite straight solenoid with a circular cross-section of radius a. The electron moves around the solenoid, so that we can recognize the interior of the latter as the region where the electron is excluded and its exterior as the region where the electron is present. Circular cylindrical coordinates (ρ, φ, z) are appropriate for the chosen geometry. The situations to be compared are those in which

1) There is no magnetic induction field anywhere,

$$\vec{B}(0 \leq \rho < \infty, \varphi, z) = 0. \tag{1}$$

2) There is an axial uniform magnetic induction field only in the interior of the solenoid,

$$\vec{B}(0 \leq \rho \leq a, \varphi, z) = \hat{k}B_0. \tag{2}$$

Then the magnetic vector potential for the respective situations can be chosen as

$$\vec{B}(a \leq \rho < \infty, \varphi, z) = 0, \tag{3}$$

and

$$\vec{A}(0 \leq \rho \leq a, \varphi, z) = \frac{1}{2}\hat{\varphi}B_0\rho,$$
$$\vec{A}(a \leq \rho \leq \infty, \varphi, z) = \frac{1}{2}\hat{\varphi}\frac{B_0 a^2}{\rho}, \tag{4}$$

corresponding to the circular or symmetric gauge for the latter. The reader can check that the curls of the magnetic vector potentials of Eqs. (3) and (4) lead to the respective magnetic induction fields of Eqs. (1) and (2), in agreement with Eq. (31).

Then the hamiltonian for the first situation is simply the kinetic energy term,

$$\hat{H}(\vec{r}, \vec{p}) = \frac{p^2}{2m_q} = \frac{p_\rho^2}{2m_q} + \frac{l_z^2}{2m_q\rho^2} + \frac{p_z^2}{2m_q}, \tag{5}$$

in which the radial, rotational and axial contributions to the kinetic energy can be recognized. A particle with an electric charge q and mass m_q is assumed and l_z is the axial component of the orbital angular momentum. The hamiltonian for the second situation is constructed from the minimal coupling prescription described at the end of Appendix B, by using Eqs. (5) and (4):

$$H(\vec{r}, \vec{p}) = \frac{\left(\vec{p} - \frac{q}{c}\vec{A}\right)^2}{2m_q}$$
$$= \frac{p_\rho^2}{2m_q} + \frac{\left(l_z - \frac{qBa^2}{2c}\right)^2}{2m_q\rho^2} + \frac{p_z^2}{2m_q}. \tag{6}$$

Notice that the hamiltonians of Eqs. (5) and (6) have in common the radial and axial terms and differ in the numerator of the rotational term. This difference is associated with the interaction momentum of the charge q and the magnetic vector potential given by Eqs. (34) and (4).

The analysis so far has been classical, and before continuing it through the incorporation of the time variations of the magnetic induction and vector potential, it is appropriate to examine at this moment the quantum implications in the stationary situation. Actually this has been done in detail in Refs. 1 and 4, so it will be sufficient to say here that the angular momentum is quantized:

$$l_z = m\hbar = \frac{mh}{2\pi}, \qquad m = 0, \pm 1, \pm 2, \ldots \tag{7}$$

and the difference of the rotational energy contributions in Eqs. (5) and (6) corresponds for a negatively charged electron with $q = -e$ to the change

$$m \to m + \nu, \tag{8}$$

where

$$\nu = \frac{eB_0a^2}{2c\hbar} = \frac{B_0\pi a^2}{(ch/e)} \tag{9}$$

is the number of fluxons in the interior of the solenoid. At the level of the solutions of the Schrödinger equation the eigenfunctions of the hamiltonian operators of Eqs. (5) and (6) have in common the angular and axial functions; their radial functions, which are Bessel functions, differ in their orders m and $m+\nu$, respectively. This leads to the changes in the electron interference pattern analyzed in Ref. 1 and to the changes in the energy spectra and eigenfunctions analyzed in Ref. 4 as the magnetic flux inside the solenoid, Eq. (9) changes.

Now we continue the classical analysis by considering the time variations of the magnetic induction inside the solenoid. It is important to recognize that the space configuration is maintained, so that the space dependencies of the magnetic induction and vector potential remain the same as given by Eqs. (2) and (4). Therefore, the changes of B_0 are followed by proportional changes in $\vec{A}$ and ν. On the other hand, according to the Faraday-Lenz-Henry law of electromagnetic induction, the time rate of change of the magnetic flux inside the solenoid induces an electromotive force around it:

$$\mathcal{E} = -\frac{d\Phi_m}{c\,dt}. \tag{10}$$

For any circle coaxial with the solenoid and with a radius $\rho > a$, the evaluation of both sides of this equation is immediate:

$$2\pi\rho E = -\frac{dB_0}{c\,dt}\pi a^2, \tag{11}$$

since the electric field intensity $\vec{E}$ has circular lines. Consequently, the induced electric field has the explicit form

$$\vec{E} = -\hat{\varphi}\frac{a^2}{2\rho}\frac{dB_0}{c\,dt}. \tag{12}$$

From Eq. (4), it is recognized that this field is the partial time derivative of the vector potential around the solenoid, which could have been obtained directly by applying Eq. (32) to the situation under study. In any case, it is the electromagnetic induction phenomenon which accounts for the identification of the electric force $q\vec{E}$ in the region where the charge is present during the interval in which the magnetic induction field is changing.

Next, we proceed to evaluate the time and space integrated effects of such a force when the magnetic field changes from one stationary value to another. Without any loss of generality the initial value can be taken as zero and the final one as B_0. The time integration of q times Eq. (12) gives the impulse imparted to the charge,

$$\int q\vec{E}\,dt = -\frac{\hat{\varphi}qB_0a^2}{2c\rho} = -\frac{q}{c}\vec{A}, \qquad (13)$$

which, again through Eq. (4), is identified as minus q/c times the vector potential or the negative of the interaction momentum, [Eq. (34)]. The integration of q times Eq. (12) along a circle around the solenoid gives

$$\oint q\vec{E}\cdot d\vec{r} = -\frac{q}{c}\pi a^2\frac{dB_0}{dt}, \qquad (14)$$

the work done by the force on the charge, which is q times Eq. (10).

Additionally, the line integral of Eq. (13) around the circle or the time integral of Eq. (14) give the change in action due to the change in the magnetic induction:

$$S = -\frac{qB_0\pi a^2}{c} = -\frac{q}{c}\Phi_m. \qquad (15)$$

In quantum mechanics, this change in action divided by $\hbar$ gives the relative phase difference for charged particles which pass around opposite sides of the solenoid due to the change in the magnetic induction inside the solenoid:

$$\frac{S}{\hbar} = -\left.\frac{q\Phi_m}{c\hbar}\right|_{q=-e} = 2\pi\nu. \qquad (16)$$

This result was obtained in Refs. 1 and 12–14 from different assumptions and approximations.

3. Discussion

This section includes a general and brief discussion of the alternative formulations of classical mechanics and electromagnetism and their connections, and also discussions of specific issues related to the analysis and interpretations of the A-B effect. Some of the latter are motivated by specific statements in the works of Refs. 11–15 about the roles of the electromagnetic fields and potentials in classical and quantum mechanics.

We have intentionally included Appendices A and B, making reference to them since the introduction, in recognition that there exist alternative and complementary formulations of mechanics and electromagnetism. Their equivalences in mechanics are well established: integration of the force leads to the potential energy Eq. (23) and the conservation of energy Eq. (26), and differentiation of the potential energy Eq. (25) and of the hamiltonian Eq. (28) lead to the force. Similar relations hold in electromagnetism: the integration of the Maxwell equations independent of the sources, Eqs. (30), lead to the potentials, whose derivatives give the force fields, Eqs. (31) and (32); the Lorentz force may be written in terms of the fields Eq. (29), or in terms of the potentials Eq. (33); the latter allows the identification of the interaction potential energy and interaction potential momentum Eq. (34); also Eqs. (30) correspond to the Maxwell equation in differential form, but they can also be cast into their integral forms or described phenomenologically, like for example Eqs. (14) and (10) for the electromagnetic induction.

Several elements have been used in the classical analysis of Sec. 2. The explicit expressions for the magnetic induction and vector potential inside and outside the solenoid, for the two comparative situations Eqs. (1)–(4). The application of the minimal coupling prescription to go from the hamiltonian in the absence of any fields, Eq. (5), to the one in the presence of a magnetic induction inside the solenoid and the vector potential around it, Eq. (6). The explicit consideration of the time variation of the magnetic induction inside the solenoid and its consequences: the induced electro-motive force around the solenoid, Eq. (10), and the associated induced electric field, Eq. (12), the successive time and line integrals of the latter Eqs. (13)–(15), and their physical meanings; including the connections with the vector potential of Eqs. (12) and (13) which are physically behind the minimal coupling prescription. On the other hand, the quantum elements leading to the A-B effect are the quantization of angular momentum Eqs. (7)–(9) and the connection between action and phase Eq. (16). It is instructive to point out that having recognized the presence of the induced electric intensity field as the source of the force on the charge around the solenoid, its contribution to the change in the action is via the line integral of the vector potential Eq. (13) or the time integral of the electromotive force Eq. (14).

Some comments in response to statements in Refs. 13 and 14 are made in the following, under the light provided by the analysis of Sec. 2. In the stationary situation there are no forces on the charge around the solenoid, but the analysis of the situation when the magnetic induction field is changing inside the solenoid leads to recognize the electromagnetically induced force. This may lift the veil of mystery that has been associated with the A-B effect. More important, the time integrated effect of such a force leads to the change in the vector potential reinforcing the physical interpretation of the latter as a momentum per unit charge, Eq. (13). This is precisely the key idea discussed and explained in Refs. 8–10. Out point of view, concerning the alternative descriptions of electromagnetism in terms of electromagnetic fields and electromagnetic potentials, is that they are complementary, and one does not exclude the other; the potentials and their use are common to both classical and quantum mechanics, while the fields are useful in newtonian mechanics. In this paper the identification of the force and its contributions to the vector potential and action allow a better understanding of the classical and quantum elements participating the A-B effect.

Finally, the issue of the locality or non-locality of the interaction responsible for the A-B effect is examined. Aharonov and Bohm argued in favor of the local interaction of the charge and the vector potential in the exterior of the solenoid. Some authors have not accepted this interpretation as illustrated in the Introduction by the quotation from [13]. Our identification of the electromagnetically induced electric force $q\vec{E}(\vec{r},t)$ outside the solenoid is complemented by recognizing it also as a local interaction. Additionally, its time integrated effect, Eq. (13), leads to the vector potential making contact with and supporting the position of Ref. 1, and also answering the questions of Ref. 13. The issue of nonlocality appears because the magnetic induction is present inside the solenoid and the electron is outside. Of course, classical electromagnetism recognizes that $\vec{B}(\vec{r},t)$ of Eq. (2) has the associated vector potential $\vec{A}(\vec{r},t)$ of Eq. (4) and electric intensity field $\vec{E}(\vec{r},t)$ of Eq. (12), both present outside the solenoid and able to interact locally with the electron. The interested readers are referred to the article "On the origin of the A-B effect" [15] for another point of view of the locality *vs.* non-locality issue.

Appendix A

Newton's and Hamilton's formulations of classical mechanics

Newton's second law of motion establishes that the force acting on a particle is equivalent to the time rate of change of the particle's momentum:

$$\vec{F} = \frac{d\vec{p}}{dt}. \tag{17}$$

The impulse of a force describes the integrated effect of the force throughout the time of its application:

$$\vec{I} = \int_{t_i}^{t_f} \vec{F}\, dt. \tag{18}$$

The work done by a force acting on a particle that follows a certain trajectory describes the integrated effect of the force along the trajectory:

$$W = \int_C \vec{F}\cdot d\vec{r}. \tag{19}$$

Substitution of the expression for the force from Eq. (17) in Eqs. (18) and (19) leads to recognize that the effect of the impulse of the force is the change in the particle's momentum,

$$\vec{I} = \vec{p}\,(t_f) - \vec{p}\,(t_i), \tag{20}$$

and that the effect of the work is the change in the kinetic energy of the particle:

$$W = \frac{[p(t_f)]^2}{2m} - \frac{[p(t_i)]^2}{2m}, \tag{21}$$

where

$$\vec{p} = m\frac{d\vec{r}}{dt}. \tag{22}$$

The forces for which the work of Eq. (19) does not depend on the trajectory but only on the initial and final positions,

$$W = \int_{\vec{r}_i}^{\vec{r}_f} \vec{F}\cdot d\vec{r} = -U(\vec{r}_f) + U(\vec{r}_i) \tag{23}$$

are called conservative forces, allowing the identification of a potential energy function such that

$$\vec{F}\cdot d\vec{r} = -dU, \tag{24}$$

or equivalently

$$\vec{F} = -\nabla U \tag{25}$$

Then the combination of Eqs. (21) and (23) leads to the conservation of the total mechanical energy given by the sum of the kinetic and potential energies:

$$\frac{p_f^2}{2m} + V(\vec{r}_f) = \frac{p_i^2}{2m} + U(\vec{r}_i). \tag{26}$$

The total energy as a function of position and momentum of the particle is identified as the hamiltonian function,

$$H(\vec{r},\vec{p}) = \frac{p^2}{2m} + U(\vec{r}). \tag{27}$$

Hamilton's canonical equations

$$\dot{x}_i = \frac{\partial H}{\partial p_i}, \qquad \dot{p}_i = -\frac{\partial H}{\partial x_i} \tag{28}$$

are equivalent to the velocity components, Eq. (22), and Newton's second law of motion, Eq. (17), respectively.

The equivalence between Newton's and Hamilton's formulations of classical mechanics is well established. The use of one or the other is a matter of convenience for the analysis of each specific problem.

Appendix B

Descriptions of the electromagnetic field in terms of forces and potentials

The Lorentz force describes the electromagnetic force acting on a particle with an electric charge q and velocity $\vec{u}$, at the position $\vec{r}$ at time t,

$$\vec{F} = q\vec{E} + \frac{q}{c}\vec{u}\times\vec{B}, \tag{29}$$

in terms of the electric intensity field $\vec{E}(\vec{r},t)$ and the magnetic induction field $\vec{B}(\vec{r},t)$, where c is the speed of light in vacuum.

The relations between the fields and their sources, the electric charge density $\rho(\vec{r},t)$ and electric current density $\vec{J}(\vec{r},t)$, are given by Maxwell's equations:

$$\begin{aligned}
\nabla\cdot\vec{E} &= 4\pi\rho,\\
\nabla\times\vec{B} &= \frac{4\pi}{c}\vec{J} + \frac{1}{c}\frac{\partial\vec{E}}{\partial t},\\
\nabla\times\vec{E} &= -\frac{1}{c}\frac{\partial\vec{B}}{\partial t},\\
\nabla\times\vec{B} &= 0,
\end{aligned} \tag{30}$$

corresponding to the electric Gauss' law, the Ampére-Maxwell law, the Faraday-Lenz-Henry law, and the magnetic Gauss' law, respectively.

The last two laws, which do not depend on the sources, make it possible to introduce the electromagnetic potentials. Indeed, the solenoidal character of the magnetic induction field allows to write the latter as the curl of the vector potential $\vec{A}(\vec{r},t)$:

$$\vec{B} = \nabla \times \vec{A} \tag{31}$$

Then the substitution of this expression in the Faraday-Lenz-Henry law equation leads to the expression for the electric intensity field

$$\vec{E} = -\nabla\phi - \frac{1}{c}\frac{\partial \vec{A}}{\partial t} \tag{32}$$

in terms of the gradient of the scalar potential $\phi(\vec{r},t)$ and the partial time derivative of $\vec{A}$.

The physical meaning of the scalar potential is quite familiar since the study of electrostatics and corresponds to the energy per unit charge. The vector potential also has a physical meaning, although it is not so familiar as in the case of the scalar potential and it is ignored too often. In order to identify both meanings in general it is sufficient to substitute Eqs. (31) and (32) in Eq. (29), and to rewrite the Lorentz force in terms of the potentials in the form

$$\vec{F} = -\nabla\left[q\phi - \frac{q}{c}\vec{u}\cdot\vec{A}\right] - \frac{d}{dt}\left[\frac{q}{c}\vec{A}\right]. \tag{33}$$

The identification of the energy associated with the interaction between the charge and the scalar potential $q\phi$ coincides with the familiar situation of electrostatics and extends it to the time dependent situation. The second term inside the brackets corresponds to the interaction between the moving charge and the vector potential; then the vector potential is the energy of interaction per unit charge and per unit velocity. In addition, since the force is the time rate of change of the particle's momentum according to Eq. (17), then the quantity inside the parenthesis in the last term of Eq. (33) allows the identification of the energy and momentum of interaction between the charge and the electromagnetic field described by the potentials:

$$\begin{aligned} U_{\text{int}} &= q\phi - \frac{q}{c}\vec{u}\cdot\vec{A} \quad , \\ \vec{p}_{\text{int}} &= \frac{q}{c}\vec{A} \end{aligned} \tag{34}$$

The vector potential is a potential of momentum per unit charge, which physically justifies the minimal coupling prescription, $\vec{p} \to \vec{p} - (q/c)\vec{A}$, to incorporate the effects of the electromagnetic field in situations in which the latter was not present originally.

1. Y. Aharonov and D. Bohm, *Phys. Rev. D* **115** (1989) 485.
2. R.G. Chambers, *Phys. Rev. Lett.* **5** (1960) 3.
3. M. Peshkin and A. Tonomura, *The Aharonov-Bohm Effect* (Springer-Verlag, Berlin Heidelberg, 1989), p. 10.
4. D. Kouznetsov, E. Ley-Koo, and G. Villa-Torres, , *Rev. Mex. Fís.* **45** (1999) 485.
5. E. Ley-Koo, G. Villa-Torres y D. Kouznetsov, "Efecto Aharonov-Bohm en estados de Landau en cajas cilíndricas anulares," Programa del XLII Congreso Nacional de Física, 6 SE 3 (1999).
6. E. Castaño, N. Aquino y E.Ley-Koo, "Efecto Aharonov-Bohm en estados de Landau de antipuntos cuánticos", Programa del XLII Congreso Nacional de Física, 4SC1 (1999).
7. E. Ley-Koo, *Topics in Contemporary Physics*, edited by J.A. Heras and R.V. Jiménez (Instituto Politécnico Nacional, México, 2000), p. 17.
8. R.P. Feynman, R. B. Leighton, and M. Sands, *The Feynman Lectures in Physics* (Addison-Wesley, Reading, Mass., 1964), Vol. II., Chap. 15.
9. E.J. Konopinski, *Am. J. Phys.* **46** (1978) 499.
10. E.J. Konopinski,*Electromagnetic Fields and Relativistic Particles* (McGraw-Hill, New York, 1981).
11. T.H. Boyer, *Phys. Rev. D* **8** (1973) 1667.
12. T.H. Boyer, *Phys. Rev. D* **8** (1973) 1680
13. T.H. Boyer, *Nuovo Cimento B* **100** (1987) 685.
14. H. Rubio, J. M. Getino, and O. Rojo, *Nuovo Cimento B* **106** (1991) 407.
15. L. O'Raifertaigh, N. Straumann, and A. Wipf, *Comments Nucl. Part. Phys.* **20** (1991) 15.

CHINESE JOURNAL OF PHYSICS VOL. 40, NO. 2 APRIL 2002

Aharonov-Bohm Effect on Landau States in Annular Cylindrical Boxes

E. Ley-Koo[1*], G. Villa-Torres[1*], and D. Kouznetsov[2]
[1] *Instituto de Fisica-UNAM., Apartado Postal 20-364, 01000 México, D. F. México*
[2] *Mathematical Building, Box 87, University of Arizona, Tucson, AZ 85721, USA*

(Received September 24, 2001)

The Schrödinger equation for an electron inside an annular cylindrical box and in the presence of an axial uniform magnetic field is solved in two comparative situations: i) when the magnetic induction $\vec{B}_0 = \hat{k}B_0$ is the same in the central perforation and in the box, and ii) when its values in the perforation $\vec{B}_i = \hat{k}B_i$ and in the box $\vec{B}_0 = \hat{k}B_0$ are different. The Aharonov-Bohm effect on the Landau states of the confined electron is exhibited through the analysis of the dependence of the energy eigenvalues and eigenfunctions on the difference of the magnetic flux in the perforation as $B_i - B_0$ changes.

PACS. 03.65.–w – Quantum mechanics.
PACS. 03.65.Bz – Aharonov-Bohm effect.

I. Introduction

This paper deals with the problem of an electron moving under the action of uniform magnetic fields combining the situations of the Landau problem [1-3] and of the Aharonov-Bohm (A-B) effect [4-6]. The first situation corresponds to a uniform magnetic induction at all points of space and to an electron allowed to be at any of those points. The Landau problem has been solved in both the linear gauge and the symmetric gauge, and the connections between the respective eigenstates have been exhibited in [3]. The second situation involves a uniform magnetic induction in a limited region of space from which the electron is excluded. Aharonov and Bohm predicted that the fringe pattern in an electron interference experiment should be shifted by altering the amount of magnetic flux passing between two beams, even though the beams themselves pass only through field-free regions [4]. The experiments performed by Chambers using magnetic whiskers confirmed this prediction [5]. The A-B effect on the bound states of an electron inside an annular cylindrical box was analyzed in [6].

The A-B effect on the Landau states of an electron inside an annular cylindrical box is investigated by comparing two new situations. In Sec. II, the same uniform magnetic induction $\vec{B}(0 \le \rho \le b, \varphi, z) = \hat{k}B_0$ is present in the central perforation $(0 \le \rho \le a)$ and in the box $(a \le \rho \le b)$. In Sec. III, the magnetic induction in the perforation $\vec{B}(0 \le \rho \le b, \varphi, z) = \hat{k}B_i$ is different from the one in the box $B(a \le \rho \le b, \varphi, z) = \hat{k}B_0$. The analysis of both situations involves identifying the respective vector potentials in the perforation and in the box, constructing the Hamiltonians via the minimal-coupling prescription, and solving the corresponding Schrödinger equations. The box is assumed to be impenetrable, which translates into the boundary condition that the eigenfunctions must vanish at the positions of the walls of the box. Sec. IV presents numerical and graphical results illustrating the A-B effect through the changes of the energy eigenvalues and eigenfunction parameters as the magnetic flux difference in the perforation $(B_i - B_0)\pi a^2$ changes, including a discussion of these results. For completeness sake the explicit forms of the Kummer confluent hypergeometric functions are included in the Appendix.

II. Landau states in an annular cylindrical box

This section presents the formulation and solution of the quantum problem of an electron, of mass m_e and electric charge $-e$, confined inside an annular cylindrical box $(a \le \rho \le b, 0 \le \varphi \le 2\pi, 0 \le z \le L)$, and under the action of an axial uniform magnetic field,

$$\vec{B}(0 \le \rho \le b, \varphi, z) = \hat{k}B_0, \tag{1}$$

which has the same magnitude in both the perforation and the box. The associated magnetic vector potential is chosen as the one in the symmetric gauge,

$$\vec{A}(0 \le \rho \le b, \varphi, z) = \hat{\varphi}\frac{B_0\rho}{2}, \tag{2}$$

congruent with the geometry of the box. The Hamiltonian for the system is constructed by using the minimal-coupling prescription [2],

$$\hat{H} = \frac{(\vec{p} + \frac{e}{c}\vec{A})^2}{2m_e} = \frac{p_\rho^2}{2m_e} + \frac{(\frac{\hat{l}_z}{\rho} + \frac{eB_0\rho}{2c})}{2m_e} + \frac{p_z^2}{2m_e}, \tag{3}$$

involving the radial p_ρ, azimuthal l_z/ρ, and axial p_z components of the canonical momentum; l_z is the canonical angular momentum. Then the corresponding time-independent Schrödinger equation becomes

$$\begin{aligned}&\left\{-\frac{\hbar^2}{2m_e}\frac{1}{\rho}\frac{\partial}{\partial\rho}\rho\frac{\partial}{\partial\rho} + \frac{\hat{l}_z^2}{2m_e\rho^2} + \frac{eB_0}{2m_ec}\hat{l}_z + \frac{e^2B_0^2}{8m_ec^2}\rho^2 - \frac{\hbar^2}{2m_e}\frac{\partial^2}{\partial z^2}\right\}\psi(\rho,\varphi,z)\\ &= E\psi(\rho,\varphi,z).\end{aligned} \tag{4}$$

The three terms coming from the square of the binomial in Eq. (3) are identified as the rotational kinetic energy, the diamagnetic energy, and the harmonic oscillator potential energy with a frequency $\omega = eB_0/2m_ec$.

Equation (4) admits separable solutions

$$\psi(\rho,\varphi,z) = R(\rho)\Phi(\varphi)Z(z). \tag{5}$$

Each factor satisfies the respective ordinary differential equation in the longitudinal, azimuthal and radial coordinate:

$$-\frac{\hbar^2}{2m_e}\frac{d^2Z}{dz^2} = E^L Z, \tag{6}$$

$$-i\hbar\frac{d\Phi}{d\varphi} = m\hbar\Phi, \tag{7}$$

$$\left\{-\frac{\hbar^2}{2m_e}\left[\frac{1}{\rho}\frac{d}{d\rho}\rho\frac{d}{d\rho}-\frac{m^2}{\rho^2}\right]+\frac{1}{2}m_e\omega^2\rho^2+m\hbar\omega\right\}R=E^TR. \tag{8}$$

Here the longitudinal and transverse contributions to the energy add up to the total energy,

$$E^L+E^T=E. \tag{9}$$

The eigensolutions of Eq. (6) are determined by the boundary conditions that they must vanish at the lower $z=0$ and upper $z=L$ walls of the box. Their explicit form is

$$Z_n(z)=\sqrt{\frac{2}{L}}\sin\frac{n\pi z}{L},\quad n=1,2,3,\dots. \tag{10}$$

The corresponding longitudinal eigenenergy becomes

$$E_n^L=\frac{\hbar^2n^2\pi^2}{2m_eL^2}. \tag{11}$$

Equation (7) is the eigenvalue equation for the z-component of the angular momentum, with eigensolutions

$$\Phi_m(\varphi)=\frac{e^{im\varphi}}{\sqrt{2\pi}} \tag{12}$$

and integer eigenvalues

$$m=0,\pm1,\pm2,\dots \tag{13}$$

arising from the periodicity condition $\Phi(\varphi+2\pi)=\Phi(\varphi)$.

Apart from the diamagnetic energy term, Eq. (8) is identified as the radial Schrödinger equation for a two-dimensional isotropic harmonic oscillator. Its solutions are well-known; for the electron inside the annular cylindrical box they must vanish at the inner $\rho=a$ and outer $\rho=b$ walls. The general solution is

$$\begin{aligned}R(\rho)=&\rho^{|m|}e^{-m_e\omega\rho^2/2\hbar}\left\{CM\left(-\nu,|m|+1;\frac{m_e\omega\rho^2}{\hbar}\right)\right.\\&\left.+DU\left(-\nu,|m|+1;\frac{m_e\omega\rho^2}{\hbar}\right)\right\},\end{aligned} \tag{14}$$

in terms of the confluent hypergeometric functions M and U [7], where the transverse eigenenergy contribution has the form

$$E_{sm}^T=\hbar\omega[2\nu_s+|m|+1+m]. \tag{15}$$

The radial boundary conditions become:

$$CM\left(-\nu,|m|+1;\frac{m_e\omega a^2}{\hbar}\right)+DU\left(-\nu,|m|+1;\frac{m_e\omega a^2}{\hbar}\right)=0, \tag{16}$$

$$CM\left(-\nu,|m|+1;\frac{m_e\omega b^2}{\hbar}\right)+DU\left(-\nu,|m|+1;\frac{m_e\omega b^2}{\hbar}\right)=0. \tag{17}$$

The value of the transverse eigenenergy parameter ν is determined by the condition that the determinant of the two linear homogeneous algebraic Eqs. (16) and (17) in C and D vanishes,

$$\begin{aligned}&M\left(-\nu,|m|+1;\frac{m_e\omega a^2}{\hbar}\right)U\left(-\nu,|m|+1;\frac{m_e\omega b^2}{\hbar}\right)\\&-U\left(-\nu,|m|+1;\frac{m_e\omega a^2}{\hbar}\right)M\left(-\nu,|m|+1;\frac{m_e\omega b^2}{\hbar}\right)=0.\end{aligned} \tag{18}$$

For an electron confined in an annular cylindrical box with inner and outer radii a and b, under the action of the uniform magnetic induction field defined by Eq. (1), and in an eigenstate with a chosen value of m, Eq. (13), the zeros of Eq. (18) for ν_s, $s=1,2,3,\ldots$ determine the corresponding radial eigenfunctions $R_{sm}(\rho)$, Eq. (14), and transverse eigenenergies E^T_{sm}, Eq. (15). Such zeros are computed numerically using the appropriate representations of the functions M and U [7], Eqs. (A.1), (A.4) with $\alpha=-\nu$ and $n=|m|$.

The normal Landau problem in which the electron may be at any point in the range $0\leq\rho<\infty$ corresponds to the particular case of $a=0$ and $b=\infty$. By recalling that U is singular at $\rho=0$ its presence in Eq. (14) must be eliminated by taking $D=0$. On the other hand, M diverges as exp $(m_e\omega\rho^2/\hbar)$ as $\rho\to\infty$, Eq. (A.5), and the only way to make Eq. (14) still useful is to take ν as a non-negative integer N for which M becomes a polynomial of degree $2N$. Correspondingly, the Landau energy levels of Eq. (15) become the spectrum of odd integers in units $\hbar\omega$, each level being infinitely degenerate on account of the cancellation of the rotation and diamagnetic contributions $|m|+m$ for $m=-|m|$.

The zeros of ν_s in Eq. (18) depend on the values of the other parameters of M and U, namely $|m|$, $(m_e\omega a^2/\hbar)$, and $(m_e\omega b^2/\hbar)$ and in general are not integers. The dimensionless parameter $m_e\omega b^2/\hbar$ can be rewritten in terms of the magnetic induction field as $B_0\pi b^2/(hc/e)$, which can be identified as the magnetic flux in the circular cross-section of radius b expressed in the fluxon unit, $hc/e=4.135\times10^{-7}$ gauss-cm^2. The result of the confinement of the electron inside the annular cylindrical box is to remove the infinite degeneracy of the normal Landau energy levels described in the previous paragraph. Explicit numerical illustrations of these results are shown in Sec. IV.

III. Aharonov-Bohm effect on the landau states in an annular cylindrical box.

In this section we analyze the changes in the eigenenergies and eigenfunctions of the Landau states when the magnetic induction field has a value in the perforation different form its value in the box. Let the respective values be

$$\vec{B}(0\leq\rho\leq a,\varphi,z)=\hat{k}B_i \tag{19}$$

and

$$\vec{B}(a\leq\rho\leq b,\varphi,z)=\hat{k}B_0. \tag{20}$$

The corresponding magnetic vector potential is

$$\vec{A}(0 \leq \rho \leq a, \varphi, z) = \hat{\varphi}\frac{B_i \rho}{2},$$
$$\vec{A}(a \leq \rho \leq b, \varphi, z) = \hat{\varphi}\left[\frac{B_0 \rho}{2} + \frac{(B_i - B_0)a^2}{2\rho}\right]. \tag{21}$$

This potential is continuous at the boundary $\rho = a$, and its curl reproduces the magnetic induction fields in the perforation and in the box. The Hamiltonian for the electron in the box becomes

$$\hat{H} = \frac{\hat{p}_\rho^2}{2m_e} + \frac{\left[\left(\frac{\hat{l}_z}{\rho} + \frac{e(B_i - B_0)a^2}{2c\rho}\right) + \frac{eB_0\rho}{2c}\right]^2}{2m_e} + \frac{\hat{p}_z^2}{2m_e}. \tag{22}$$

The difference of the magnetic induction in the perforation, Eq. (19), compared to the one in the box, Eq. (20), is translated into the difference of the magnetic vector potential of Eq. (21) compared to that of Eq. (2) and correspondingly to the difference between the Hamiltonian of Eq. (22) compared to that of Eq. (3). The latter consists in the replacement

$$\hat{l}_z \to \hat{l}_z + \frac{e(B_i - B_0)a^2}{2c} \tag{23}$$

in going from Eq. (3) to Eq. (22), in the terms inversely proportional to the radial coordinate ρ. Then the new time-independent Schrodinger equation is

$$\left\{-\frac{\hbar^2}{2m_e}\frac{1}{\rho}\frac{\partial}{\partial\rho}\rho\frac{\partial}{\partial\rho} + \frac{[\hat{l}_z + \frac{e(B_i - B_0)a^2}{2c}]^2}{2m_e\rho^2} + \frac{eB_0}{2m_e c}\left[\hat{l}_z + \frac{e(B_i - B_0)a^2}{2c}\right]\right.$$
$$\left. + \frac{e^2B_0^2}{8m_e c^2}\rho^2 - \frac{\hbar^2}{2m_e}\frac{\partial^2}{\partial z^2}\right\}\psi(\rho, \varphi, z) = E\psi(\rho, \varphi, z), \tag{24}$$

instead of Eq. (4). It also admits separable solutions of the same type of Eq. (5), with the same longitudinal and azimuthal eigenfunctions and eigenvalues of Eqs. (10)-(13) satisfying the corresponding differential Eqs. (6) and (7). The radial differential equation becomes

$$\left\{-\frac{\hbar^2}{2m_e}\left[\frac{1}{\rho}\frac{d}{d\rho}\rho\frac{d}{d\rho} - \frac{(m+\mu)^2}{\rho^2}\right] + \frac{1}{2}m_e\omega^2\rho^2 + \hbar\omega(m+\mu)\right\}R = E^T R, \tag{25}$$

where

$$\mu = \frac{e(B_i - B_0)a^2}{2\hbar c} = \frac{(B_i - B_0)\pi a^2}{(hc/e)} \tag{26}$$

is the change in the magnetic flux in the perforation in the fluxon unit when the magnetic induction changes from its value of Eq. (1) to that of Eq. (19). The difference in going from the radial Eq. (8) to that of Eq. (25) is the replacement

$$m \to m + \mu, \tag{27}$$

which follows from that of Eq. (22).

The solutions of the radial Eq. (25) are of the same type as those of Eq. (8) with the replacement of Eq. (27). Their explicit forms are

$$R_{sm}(\rho,\mu) = \rho^{|m+\mu|} e^{-m_e\omega\rho^2/2\hbar}\left\{ CM\left(-\nu, |m+\mu|+1; \frac{m_e\omega\rho^2}{\hbar}\right) + DU\left(-\nu, |m+\mu|+1; \frac{m_e\omega\rho^2}{\hbar}\right)\right\} \tag{28}$$

instead of Eq. (14), with the new transverse eigenenergy

$$E^T_{sm}(\mu) = \hbar\omega[2\nu_s + |m+\mu| + 1 + m + \mu], \tag{29}$$

instead of Eq. (15), and the ratio of the C and D coefficients and the parameter ν being determined by

$$\frac{C}{D} = -\frac{U(-\nu, |m+\mu|+1, \frac{m_e\omega a^2}{\hbar})}{M(-\nu, |m+\mu|+1, \frac{m_e\omega a^2}{\hbar})} = -\frac{U(-\nu, |m+\mu|+1, \frac{m_e\omega b^2}{\hbar})}{M(-\nu, |m+\mu|+1, \frac{m_e\omega b^2}{\hbar})} \tag{30}$$

instead of Eqs. (16)-(18). Of course, for the case in which $B_i = B_0$ the value of μ vanishes, Eq. (26), and the results of Sec. II are recovered. For the general case of interest here $B_i \neq B_0$, and the A-B effect on the Landau states in the annular cylindrical box is associated with the μ dependence of the radial eigenfunctions, Eq. (28), and the transverse eigenenergies, Eq. (29), determined by the values of ν_s solutions of Eq. (30), with $s = 1, 2, 3, \ldots$. Here the Eq. (A.3) for U must be used for non integer values of μ. Numerically computed values of ν_s and $E^T_{sm}(\mu)$ for different chosen values of μ are presented in the following section.

IV. Numerical results and discussion .

This section contains some numerical and graphical results illustrating the confinement effect of the annular box on the Landau states, and the A-B effect on the same states, from the analysis in Section II and III, respectively. For the first one, the zeros of Eq. (18) in ν are based on the logarithmic form of the U function, Eq. (A.4). For the second one, Eq. (30) requires the use of the form of U of Eq. (A.3) for non-integer values of μ. Table I and Fig. 1 illustrate the confinement effect, and Table II and Fig. 2 the A-B effect on the Landau states, as explained and discussed next.

Table I presents the transverse energy eigenvalues E^T_{sm} for the Landau states with s = 1, 2, and 3, and $m = 0, \pm 1, \pm 2, \ldots$ obtained from Eqs. (15) and (18), for the electron confined in boxes with $b = 2a$, $5a$ and $10a$, in different magnetic induction fields producing magnetic fluxes of 1 and 15 fluxons in the circular cross sections of radius b. The values of ν_s from the numerical solution of Eq. (18), when doubled and increased by one unit, give the energy eigenvalues for the zero and negative m states; for the positive m states the further addition of $2m$ is required.

The confinement effect of the box on the electron Landau states is obviously manifested by the departure of the energy levels from the equally spaced and infinitely degenerate $(2N+1)\hbar\omega$ spectra with integer values of N. The data in Table I indicate that such an effect is dominant

TABLE I. Radial s and angular momentum m quantum numbers and transverse energy eigenvalues E^T_{sm} in units $\hbar\omega$, for an electron confined in boxes with $b = 2a$, $5a$ and $10a$, in magnetic induction fields defined by the dimensionless magnetic flux parameter $m_e\omega b^2/\hbar$.

	$m_e\omega b^2/\hbar$	1	1	1	15	15	15
	$m_e\omega a^2/\hbar$	0.25	0.04	0.01	3.75	0.6	0.15
s	m	E^T_{sm}	E^T_{sm}	E^T_{sm}	E^T_{sm}	E^T_{sm}	E^T_{sm}
1	0	19.79178	7.46920	5.65108	5.33410	2.46994	1.91268
	∓ 1	19.72188	8.16592	6.94048	4.40352	1.76000	1.23668
		21.72188	10.16592	8.94048	6.40352	3.76000	3.23668
	∓ 2	21.50142	11.84566	11.42684	3.61104	1.29718	1.03460
		25.50142	15.84566	15.42684	7.61104	5.29718	5.03460
	∓ 3	25.09870	17.67902	17.58700	2.95458	1.09156	1.00632
		31.09870	23.67902	23.58700	8.95458	7.09156	7.00632
	∓ 4	30.46266	25.06046	25.04484			
		38.46266	33.06046	33.04484			
	∓ 5	37.52606	33.74222	33.73996			
		47.52606	43.74222	43.73996			
2	0	79.00098	30.51030	23.69370	9.06064	5.06776	4.16546
	∓ 1	78.98152	31.64624	26.04792	8.72414	4.21142	3.41790
		80.98152	33.64624	28.04792	10.72414	6.21142	5.41790
	∓ 2	80.92192	36.95496	33.94736	7.91474	3.63896	3.11796
		84.92192	40.95496	37.94736	11.91474	7.63896	7.11796
	∓ 3	84.82974	45.94932	44.86382	7.23292	3.33512	3.09164
		90.82974	51.94932	50.86382	13.23292	9.33512	9.09164
3	0	177.69628	69.02626	54.02880	16.23734	7.82040	6.05602
	∓ 1	177.78674	70.32580	56.94516	15.30200	6.95948	5.74480
		179.78674	72.32580	58.94516	17.30200	8.95948	7.74480
	∓ 2	179.66006	76.24628	67.07614	14.49612	6.38078	5.44980
		183.66006	80.24628	71.07614	18.49612	10.38078	9.44980
	∓ 3	183.62184	86.71936	82.07110	13.82010	6.09200	5.53434
		189.62184	92.71936	88.07110	19.82010	12.09200	11.53434

TABLE II. Transverse energy eigenvalues E_{1m}^{T} as a function of the parameter $m+\mu$, Eq. (29), for electron confined in boxes with $m_e\omega b^2/\hbar = 1$ and the indicated values of $m_e\omega a^2/\hbar$ and signs of $m+\mu$.

$m_e\omega a^2/\hbar$	0.25		0.04		0.01	
$m+\mu$	$-$	$+$	$-$	$+$	$-$	$+$
$\|m+\mu\|$	E_{1m}^{T}	E_{1m}^{T}	E_{1m}^{T}	E_{1m}^{T}	E_{1m}^{T}	E_{1m}^{T}
0	19.79178	19.79178	7.46920	7.46920	5.65108	5.65108
0.2	19.62901	20.02901	7.33859	7.73859	5.54960	5.94960
0.4	19.54074	20.34074	7.34598	8.14598	5.64130	6.44130
0.6	19.52680	20.72680	7.48904	8.68904	5.91518	7.11518
0.8	19.58724	21.18724	7.76399	9.36399	6.35476	7.95476
1	19.72188	21.72188	8.16592	10.16592	6.94048	8.94048
1.2	19.93154	22.33154	8.68844	11.08844	7.65207	10.05207
1.4	20.21310	23.01310	9.32507	12.12507	8.47078	11.27078
1.6	20.56924	23.76924	10.06840	13.26840	9.38064	12.58064
1.8	20.99979	24.59979	10.91102	14.51102	10.36910	13.96910
2	21.50142	25.50142	11.84566	15.84566	11.42684	15.42684
2.2	22.09683	26.49683	12.86538	17.26538	12.54727	16.94727
2.4	22.72467	27.52467	13.96385	18.76385	13.72597	18.52597
2.6	23.44452	28.64452	15.13541	20.33541	14.95999	20.15999
2.8	24.23603	29.83603	16.37518	21.97518	16.24742	21.84742
3	25.09870	31.09870	17.67902	23.67902	17.58700	23.58700
3.2	26.03209	32.43209	19.04350	25.44350	18.97790	25.37790
3.4	27.03570	33.83570	20.46588	27.26588	20.41952	27.21952
3.6	28.10905	35.30905	21.94392	29.14392	21.91144	29.11144
3.8	29.25156	36.85156	23.47590	31.07590	23.45330	31.05330
4	30.46266	38.46266	25.06046	33.06046	25.04484	33.04484
4.2	31.74178	40.14178	26.69655	35.09655	26.76582	35.16582
4.4	33.08831	41.88831	28.38334	37.18334	28.37600	37.17600
4.6	34.50163	43.70163	30.12020	39.32020	30.11521	39.31521
4.8	35.98110	45.58110	31.90662	41.50662	31.90325	41.50325
5	37.52606	47.52606	33.74222	43.74222	33.73996	43.73996

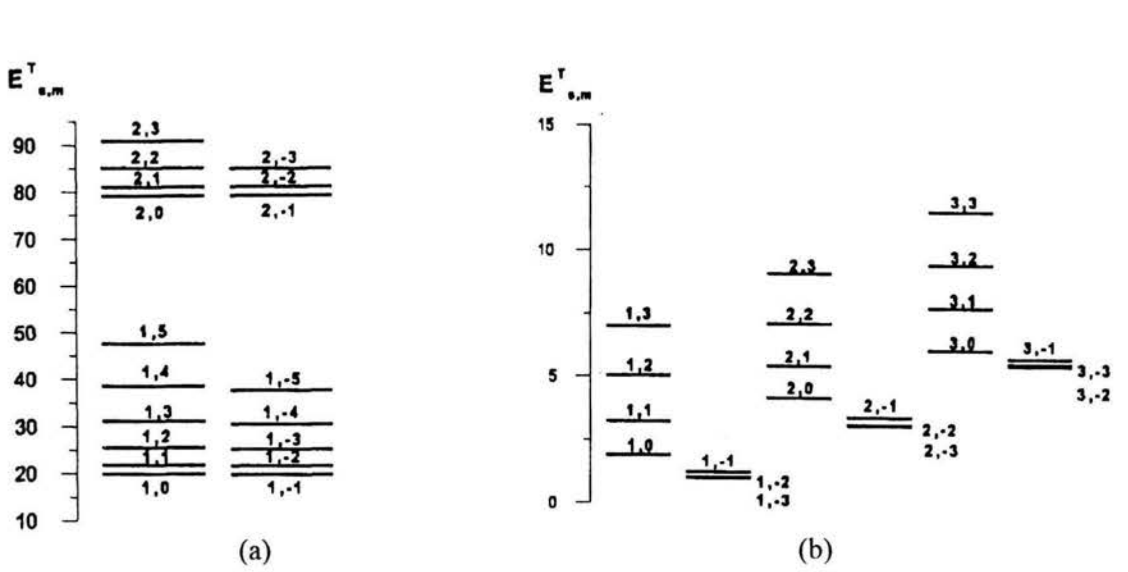

FIG. 1. Lower Landau energy levels E^T_{sm} for an electron confined in boxes with (a) $m_e\omega b^2/\hbar = 1$ and $m_e\omega a^2/\hbar = 0.25$ and (b) $m_e\omega b^2/\hbar = 15$ and $m_e\omega a^2/\hbar = 0.15$.

for the first set of three small boxes and decreases for the set of larger boxes; additionally, within each set, the effect is more noticeable for the boxes with larger perforations.

Figures 1a and 1b illustrate the change of the confinement effect as well as the magnetic field effects in the energy spectra of the electron for the boxes of the first and last columns, respectively. For the small box with $b = 1$ in the unit of length $(\hbar/m_e\omega)^{1/2}$ and large perforation $a = 0.5$, the confinement effect is large as illustrated by numerical values for the eigenergies of the $m = 0$ states in the box expressed in terms of the corresponding normal Landau eigenergies $E^T_{10} = 19.79178E^L_{10}$, $E^T_{20} = 26.33333E^L_{20}$, $E^T_{30} = 35.53925E^L_{30}$, a situation extensive to the other E^T_{sm} states. The reader should notice the different regions in the energy scale in Fig. 1a for the $s = 1$ and 2 energy levels due to the large size of the confinement effect; the inclusion of the $s = 3$ energy levels would require jumping to the region with $E^T_{sm} \geq 170$. The quasi-degeneracy of the energy levels $(s, m \geq 0)$ and $(s, -m-1)$ is readily noticeable, and can be understood as the result of the combination of the confinement effect and the magnetic effects associated with the Landau states, including the distinct behaviour of the $m > 0$ and $m < 0$ states due to the diamagnetic energy. On the other hand, Fig. 1b for a larger box with $b = \sqrt{15}$ and a small perforation $a = \sqrt{15/10}$, the energy scale is the same as for the normal Landau states because the confinement effect is appreciably reduced. Nevertheless it is still definitely present as the comparison $E^T_{10} = 1.91268E^L_{10}$, $E^T_{20} = 1.38849E^L_{20}$, $E^T_{30} = 1.21120E^L_{30}$ indicates. In this case all the energy levels with $s = 1$, 2, and 3 can be drawn together. The spacing of the energy levels for each value of s and the successive positive values of m is not far from 2, the normal Landau energy level spacing. On the other hand, the tendency to degeneracy of the energy levels, for each value of s and the successive negative values of $m = -1, -2, -3, \ldots$, at the normal Landau energy level positions $1, 3, 5, \ldots$ is explicitly apparent. The energy spectra for the electron in the boxes of columns 2-5 in Table I illustrate their intermediate behavior between the two situations explicitly discussed in connection with Figs. 1(a), 1(b).

Table II presents the transverse energy eigenvalues E^T_{sm} for the Landau states with s = 1 and m = 0, $\mp$ 1, $\mp$ 2, ... for an electron in boxes with b = 1 and a = 0.5, 0.2 and 0.1, when the magnetic induction fields in the perforation and in the box are different according to Eqs. (26) and (29). The values of ν_s are the numerical solutions of Eq. (30) and depend on the value of $|m+\mu|$. The energy eigenvalues themselves also depend on the value and sign of $m+\mu$, as distinguished in the corresponding columns. The first column gives the values of $|m+\mu|$ interpolating between the integer values of m already considered in Table I. Again the values for ν_s, when doubled and increased by one unit give the entries for the energies in the first, third and fifth columns for the states with $(m+\mu) < 0$, in which the rotational and diamagnetic energies cancel each other (see Eq. (29)). The energies for the following columns are obtained by the further addition of $2|m+\mu|$ and correspond to the states with $(m+\mu) > 0$, Eq. (29).

It is important to understand that the entries in each pair of columns of Table II are valid for the energies $E^T_{sm}(\mu)$ for the different combinations of the values of m of the chosen states, and of the differences μ of the magnetic induction field in the perforation with respect to the one in the box. For the sake of illustration let us consider the specific value $|m+\mu|$ = 0.2, common to $m+\mu$ = -0.2 and $m+\mu$ = 0.2. The negative value can be obtained from the following combinations (m,μ) : (0, -0.2), (-1, 0.8), (1, -1.2), (-2, 1.8), (2, -2.2)...; and the positive value from: (0, 0.2), (-1, 1.2), (1, -0.8), (-2, 2.2), (2, -1.8), ... All of them have the common value of ν_s obtained from Eq. (30) with $(m+\mu)$ = 0.2, and, as already stated, the energies for the states with the negative value of $(m+\mu)$ is the entry in the odd column, and the energy for the states with positive values of $(m+\mu)$ is twice this value above. The generalization of this result is

$$E^T_{sm}(m+\mu) = E^T_{sm+N}((m+N)+(\mu-N)), \tag{31}$$

with $N = 0, \pm1, \pm2, \ldots$ expressing the periodic repetition of the Landau energy levels of the electron in the annular box when the magnetic flux in the perforation changes by one fluxon, accompanied by a compensating shift of one unit in the angular momentum quantum number. This behaviour is graphically illustrated in Figs. 2(a) and 2(b) for the boxes with larger and smaller perforations.

For $\mu = 0$, the energy levels coincide with those of Fig. 1(a) and the third column of Table I. As μ increases from its initial value, the states with zero and positive values of m increase their energies, while the states with negative values of m decrease their energies; the state s = 1, $m = -1$ energy reaches its minimum value for $\mu \approx 0.5$ in Fig. 2(a) and $\mu \approx 0.8$ in Fig. 2(b). When μ reaches the value of 1, the first periodic repetition of Eq. (31) with N = 1 is realized, and continues as μ keeps on increasing. On the other hand, as μ decreases from zero, the states with zero and positive values of m decrease their energies, and the states with negative values of μ increase their energies; the state s = 1, m = 0 reaches its minimum value for $\mu \approx -0.5$ in Fig. 2(a) and $\mu \approx -0.2$ in Fig. 2(b). When μ reaches the value of -1, the first periodic repetition of Eq. (31) with $N = -1$ is realized, and continues as μ keeps on decreasing moving to the left in the graph. By drawing the energy curve $E_{10}(\mu)$ from the data of Table II, the other curves for E^T_{1m} are obtained from horizontal translations of that curve by m units, to the right for negative m and to the left for positive m. Here we have illustrated the A-B effect on the Landau states for the energy levels with s = 1, but it holds in general for any sm states, as expressed by Eq. (31).

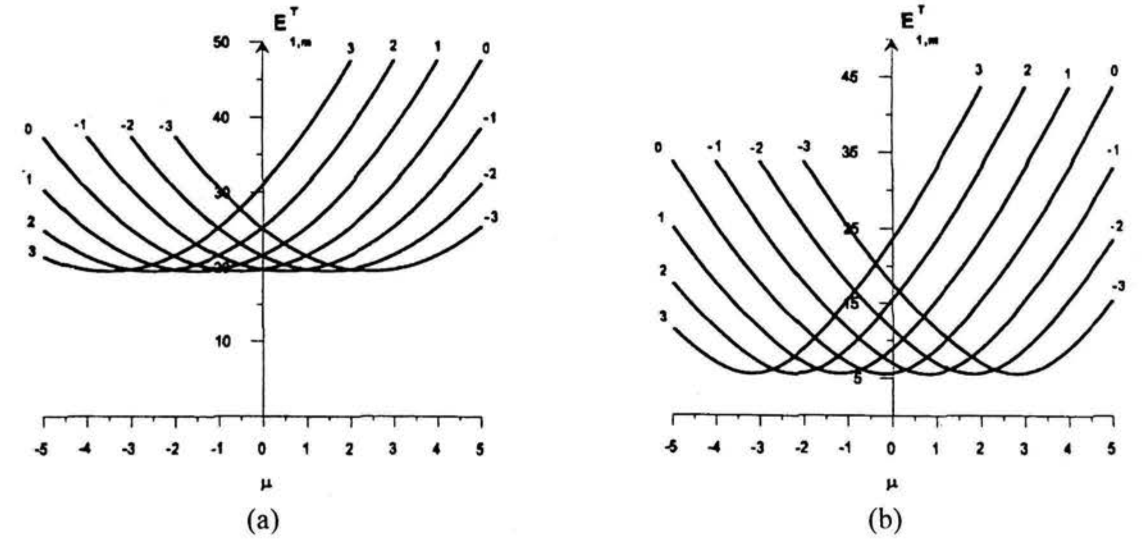

FIG. 2. Aharonov-Bohm effect on Landau energy levels $E^{T}_{sm}(\mu)$, as illustrated through their periodic dependence on the change of magnetic flux μ in the perforation of annular cylindrical boxes with $m_e\omega b^2/\hbar = 1$, and a) $m\omega_e\omega a^2/\hbar = 0.25$ and b) $m_e\omega a^2/\hbar = 0.01$.

In conclusion, this paper has presented an analysis of the confinement effect in annular cylindrical boxes on the Landau states, and of the A-B effect on such states. The signature of the Landau states in the first system is manifested through the higher energies of the positive m states and lower energies of the negative m states, including the evolution of their degeneracy as the boxes get larger. The A-B effect is manifested through the periodic repetition of the energy spectrum as a function of the variation of the magnetic flux in the perforation of the box with the corresponding shifts in the angular quantum number of the Landau states, and with a period of one fluxon.

APPENDIX A

The Kummer confluent hypergeometric functions M and U are defined by

$$M(\alpha,\beta,z) = \sum_{s=0}^{\infty} \frac{(\alpha)_s z^s}{(\beta)_s s!} \tag{A.1}$$

in terms of the Pochhammer symbol,

$$(\alpha)_0 = 1, \quad (\alpha)_s = \alpha(\alpha+1)\ldots(\alpha+s-1) = \frac{\Gamma(\alpha+s)}{\Gamma(\alpha)}; \tag{A.2}$$

and

$$U(\alpha,\beta,z) = \frac{\pi}{\sin \pi\beta}\left\{\frac{M(\alpha,\beta,z)}{\Gamma(1+\alpha-\beta)\Gamma(\beta)} - z^{1-\beta}\frac{M(1+\alpha-\beta,2-\beta,z)}{\Gamma(\alpha)\Gamma(2-\beta)}\right\}. \tag{A.3}$$

The series of Eq. (A.1) is convergent for all values of z and all values of α and β which are not negative integers. It becomes a polynomial of degree N when $\alpha = -N$ is a negative integer.

When β is a positive integer, Eq. (A.3) leads to the logarithmic form

$$\begin{aligned} U(\alpha, n+1, z) = \frac{(-)^{n+1}}{n!\Gamma(\alpha-n)} & \Big[M(\alpha, n+1, z)\ln z \\ & + \sum_{r=0}^{\infty} \frac{(\alpha)_r z^r}{(n+1)_r r!} \{\psi(\alpha+r) \\ & - \psi(1+r) - \psi(1+n+r)\}\Big] \\ & + \frac{(n-1)!}{\Gamma(\alpha)} z^{-n} M(\alpha-n, 1-n, z)_n, \end{aligned} \tag{A.4}$$

for n = 0, 1, 2, . . . , where $\psi(x) = \Gamma'(x)/\Gamma(x)$ and the last factor is the sum of n terms with the value zero for n = 0. Their asymptotic forms for $z \to \infty$ are

$$M(\alpha, \beta, z) = \frac{\Gamma(\beta)}{\Gamma(\alpha)} e^z z^{\alpha-\beta}[1 + 0(|z|^{-1})], \tag{A.5}$$

$$U(\alpha, \beta, z) = z^{-\alpha}[1 + 0(|z|^{-1})]. \tag{A.6}$$

References

[1] L. D. Landau, Z. Phys. **64**, 629 (1930).

[2] L. D. Landau and I. M. Lifshitz, *Quantum Mechanics*. (Pergamon Press, Oxford, 1977).

[3] M. K. Fung and Y. F. Wang, Chin J. Phys. **37**, 435 (1999).

[4] Y. Aharonov and D. Bohm, Phys. Rev. **115**, 485 (1959).

[5] R. G. Chambers, Phys. Rev. Lett. **5**, 3 (1960).

[6] D. Kouznetsov, E. Ley-Koo and G. Villa-Torres, Rev. Mex. F's **45**, 485 (1999).

[7] M. Abramowitz and I. Stegun, *Handbook of Mathematical Functions*, (Dover, New York, 1965) Chap. 13.